Title

Establishment and maintenance of the proper protein folding environment of the endoplasmic reticulum

Permalink

https://escholarship.org/uc/item/3b12h779

Author

Travers, Kevin J.

Publication Date

2001

Peer reviewed|Thesis/dissertation

Establishment and Maintenance of the Proper Protein Folding Environment of the Endoplasmic Reticulum

by

Kevin J. Travers

DISSERTATION

Submitted in partial satisfaction of the requirements for the degree of
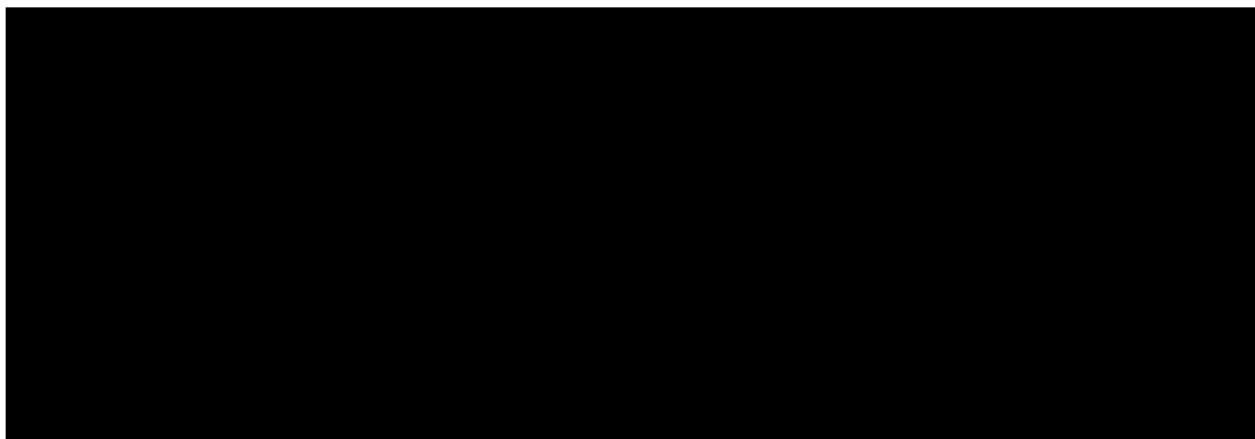
DOCTOR OF PHILOSOPHY

in

Biochemistry

in the

GRADUATE DIVISION

of the

UNIVERSITY OF CALIFORNIA SAN FRANCISCO

. . . .

Date   University Librarian

Degree Conferred: . . . .

Acknowledgments

First and foremost, I must express my thanks to the people whose own efforts have directly contributed to this thesis. I have had the opportunity to collaborate with many fantastic people in the course of this thesis work. In particular, I thank Mike Pollard, who began the disulfide bond formation project as a technician in the Weissman lab, taught me everything I needed to know about yeast, and made everyone else's musical choices seem tame; Benjamin Tu, who had the bravery to try the impossible and put Ero1p in a folding reaction; and Siew Ho-Schleyer, who, in addition to her many scientific contributions, has been a great friend. I also thank Chris Patil, my classmate and collaborator for over two years on the microarray experiments. Chris could always find a way to lighten my mood, which was much appreciated during our mind-numbing days of data collection and the endless revisions of our manuscript.

I owe many thanks to Jonathan Weissman. I thank him for giving me the opportunity to work in his lab and for his guidance of my work, particularly in the slow times that might otherwise have lasted far longer than they did. I would also like to thank Jonathan for teaching me to write clearly and for allowing me ample opportunity to practice this skill. I would also like to thank the other members of my thesis committee, Erin O'Shea and Peter Walter. Erin has been extremely helpful whenever I've needed it – for example, when I gave the worst practice talk ever for a PIBS Journal Club and needed to learn a lot about the cell cycle in a hurry – and I appreciate that dedication to graduate student education. I have

worked somewhat closer with Peter over the last couple of years through a collaboration with his lab, and have learned a great deal from his approach to science.

The environment of the Weissman lab has had as much to do with the completion of this thesis as any scientific contributions from the lab. This is entirely due to the students and post-docs, former and present, that I have had the great fortune to work with over the years. I thank my baymates, Jue Wang, Siew Ho-Schleyer, and Lev Osherovich, for making it enjoyable to come to the bench every day; Peter Chien and Vladimir Denic for numerous coffee and snack breaks and for their terrific enthusiasm in thinking about experiments, regardless of how poorly they might have turned out in practice; Angela DePace for never allowing me to forget the volume of a plate and for making the lab a fun environment; Helmut Sparrer for sharing my enthusiasm for great hikes and high altitudes; and Alex Santoso for being both a great scientist and one of the kindest people I have known.

Most importantly, I thank my family. They have always encouraged me to pursue whatever I wanted and supported me in those endeavors. I also thank Amy for her infinite patience and understanding.

Without the assistance, support, and encouragement of all of these people, none of this work would have been possible.

Establishment and Maintenance of the Proper Protein Folding Environment of the Endoplasmic Reticulum

by

Kevin J. Travers

Abstract

Proteins enter the secretory pathway of eukaryotic cells through the endoplasmic reticulum (ER), which must then ensure that such proteins reach their native state before allowing them to progress to their final destinations. Like other compartments in which folding occurs, the ER contains a number of factors that directly assist folding.

The ER is unique, however, in that protein folding in this compartment is coupled to covalent modifications, including disulfide bond formation. The machinery responsible for maintaining the oxidizing environment favorable to disulfide bond formation is beginning to be elucidated with the identification of a gene, *ERO1*, whose activity is responsible for determining the ER oxidation state. Mutations in *ero1* cause an increased sensitivity to reducing agents, while overexpression of *ERO1* leads to increased resistance. Moreover, mutation of *ERO1* results in a specific defect in the folding of those proteins that are dependent on disulfide bond formation.

Biochemical studies have identified the activity carried out by the Ero1p protein: the FAD-dependent oxidation of protein disulfide isomerase. This system is analogous to that found in the bacterial periplasm for the oxidation of proteins. However, Ero1p is not coupled to the respiratory chain, as depletion of respiratory chain components does not affect the ability of yeast cells to oxidize secretory proteins. Contrary to previous expectations, glutathione is not necessary for Ero1p-dependent oxidation.

In addition to assisting the folding of secretory proteins, the ER also contains a quality control system to recognize misfolded species and then remove them in a process known as ER-associated degradation. In the event that misfolded proteins accumulate, the ER initiates a response known as the unfolded protein response (UPR). Our analysis of transcriptional targets of the UPR has revealed regulation of nearly all aspects of secretory pathway function, suggesting that maintaining an efficient protein folding environment requires more than directly assisting the folding of proteins. This idea was tested for one specific class of UPR targets, those involved in the process of ERAD. This analysis revealed that the UPR and ERAD together perform an essential task for the cell: the removal of misfolded proteins from the secretory pathway.

Jonathan Weissman, Ph.D.
Advisor

Contributions Acknowledgment

Portions of the text and figures presented in this thesis are reproduced with permission from material published previously. Chapter 2, "Ero1p: a Novel and Ubiquitous Protein with an Essential Role in Oxidative Protein Folding in the Endoplasmic Reticulum," was published in January, 1998 in *Molecular Cell*, Vol. 1, pp. 171-82. This paper was the result of a collaboration with Michael Pollard. The cloning of *ERO1* from the bank of cold-sensitive mutant strains, the sequence comparisons of Ero1p homologs, the co-localization, and CPY folding assays, presented in Figures 3, 4, and 5, were performed by Mr. Pollard, under the supervision of Dr. Jonathan Weissman. Dr. Jonathan Weissman assayed the DTT sensitivity of *ero1* mutant strains, shown in Figure 1, and the β-lactamase secretion defect of *ero1* mutant strains, shown in Figure 5.
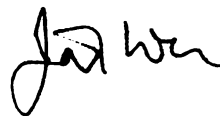
Chapter 3, "Biochemical Basis of Oxidative Protein Folding in the Endoplasmic Reticulum," was published on November 24, 2000 in *Science*, Vol. 290, pp. 1571-4. The previously published version of this work included on-line supplemental material, which has now been incorporated into Chapter 3. This work was the result of a collaboration with Benjamin Tu and Dr. Siew Ho-Schleyer. The depletion experiments presented in Figure 1 and the anaerobic experiments presented in Figures 5 and 6 were performed by Dr. Ho-Schleyer under the supervision of Dr. Weissman. The FAD-binding and *in vitro* folding

experiments presented in Figures 2 through 4 and 8, 9, and 10, were carried out by Mr. Tu, under the supervision of Dr. Weissman.

Chapter 4, "Functional and Genomic Analyses Reveal Essential Coordination Between the Unfolded Protein Response and Endoplasmic Reticulum-associated Degradation," was originally published April 28, 2000 in *Cell*, Vol. 101, pp. 249-58. This work was the result of a collaboration with Chris Patil, supervised by Dr. Peter Walter, and Drs. Lisa Wodicka and David Lockhart, then at Affymetrix, Incorporated. Portions of the data collection and analysis presented in Figure 1, the UPR target classification presented in Table 1, and the ERAD assays presented in Figure 4 were performed by Mr. Patil, under the supervision of Dr. Walter.

With the exceptions of those items listed above, the work presented in this thesis was performed by its author, Kevin J. Travers, under the supervision of Dr. Jonathan Weissman.

Dear Mr Travers

MOLECULAR CELL, Vol 1, No 2, 1998, pp 171-182, MG Pollard et al: "Ero1p: a novel...";
CELL, Vol 101, No 3, 2000, pp 249-258, KJ Travers et al: "Functional and genomic..."

As per your letter dated 15th May 2001, we hereby grant you permission to reprint the aforementioned material at no charge in your thesis subject to the following conditions:

1.   If any part of the material to be used (for example, figures) has appeared in our publication with credit or acknowledgement to another source, permission must also be sought from that source. If such permission is not obtained then that material may not be included in your publication/copies.

2.   Suitable acknowledgment to the source must be made, either as a footnote or in a reference list at the end of your publication, as follows:

        "Reprinted from Journal title, Volume number, Author(s), Title of article, Pages No., Copyright (Year), with permission from Elsevier Science".

3.   Reproduction of this material is confined to the purpose for which permission is hereby given.

4.   This permission is granted for non-exclusive world English rights only. For other languages please reapply separately for each one required. Permission excludes use in an electronic form. Should you have a specific

electronic project in mind please reapply for permission.

5.   This includes permission for UMI to supply single copies, on demand, of the complete thesis. Should your thesis be published commercially, please reapply for permission.

Yours sincerely

Frances Rothwell (Mrs)
Global Rights Manager

The processing of permission requests for all Elsevier Science (including Pergamon imprint) journals has been centralised in Oxford, UK. Your future requests will be handled more quickly if you write directly to: Subsidiary Rights Department, Elsevier Science, PO Box 800, Oxford OX5 1DX, UK. Fax: 44-1865 853333; e-mail: permissions@elsevier.co.uk

.

Permissions Letter

Ref # 01-0984

DATE: Wednesday, May 09, 2001

TO: Kevin Travers
University of California
513 Parnassus Avenue Box 0450
San Francisco, CA 94143-0450

FROM: Karen Lentz, Permissions Assistant
RE: Your request for permission dated 05/07/01

Regarding your request, we are pleased to grant you non-exclusive, non-transferable permission, but limited to print and microform formats only, and provided that you meet the criteria below. Such permission is for one-time use and therefore does not include permission for future editions, revisions, additional printings, updates, ancillaries, customized forms, any electronic forms, braille editions, translations, or promotional pieces. We must be contacted for permission each time such use is planned. This permission does not apply to figures / artwork that are credited to non-AAAS sources. This permission does not include the right to modify AAAS material.

Print the required copyright credit line on the first page that the material appears: "Reprinted (abstracted/excerpted) with permission from [FULL REFERENCE CITATION]. Copyright [YEAR] American Association for the Advancement of Science." Insert the appropriate information in place of the capitalized words.

Permission is limited to the number of copies specified in your request or your first printing.

AAAS must publish the full paper prior to use of any text.

AAAS does not supply photos or artwork. Use of the AAAS material must not imply any endorsement by the American Association for the Advancement of Science. This permission is not valid for the use of the AAAS and/or SCIENCE logos.

Thank you for writing. If you have any questions please call me at (202) 326-6765 or write to me via fax at (202) 682-0816. For international calls, -1 is the country code for the United States.

Headquarters: 1200 New York Avenue NW, Washington, DC 20005 USA

Permission is valid for use of the following AAAS content only:
Tu, et al., Biochemical Basis of Oxidative Protein Folding in the Endoplasmic Reticulum. Science 290, 1571 (2000).

Table of Contents

List of Tables and Figures

Chapter 1

Introduction

Cells contact their external environment via the cell surface, consisting of the plasma membrane and its associated protein and carbohydrate molecules. It is through the cell surface that cells are able to recognize one another; to receive behavioral, developmental, and other cues from the external world; to transmit signals into the external environment; and to modify their environment. Due to the importance of communicating with the external environment, eukaryotic cells have evolved an elaborate network of intracellular organelles, collectively known as the secretory pathway, to handle the production and sorting of molecules to be displayed on the cell surface.

Proteins destined to reside within the various organelles of the secretory pathway or to be secreted from the cell enter the secretory pathway by way of the endoplasmic reticulum (ER) (Zapun et al., 1999). As soon as nascent chains enter the ER they face an environment dramatically different from that within the cytoplasm, but more similar to that present outside the cell. As the primary regulator of cellular Ca^{++} levels (Stevens and Argon, 1999), the ER possesses a significantly higher concentration of free Ca^{++} than found in the cytosol (1 mM in the ER compared with 100 nM in the cytosol; Chapman et al., 1998). Also, the ER is significantly more oxidizing than the cytoplasm (with a redox potential of -230 mV versus -150 mV; Hwang et al., 1992), which in turn means that disulfide bond formation is favored within the ER, whereas disulfide bonds are virtually absent in the cytoplasm (Rietsch and Beckwith, 1998). In fact, a hallmark of secretory proteins is the presence of disulfide bonds that in many cases are

absolutely required for folding and/or activity (Rietsch and Beckwith, 1998). Additionally, many secretory proteins are N-glycosylated in the ER, a modification that is frequently required for proper folding and/or activity (Helenius and Aebi, 2001).

Protein folding in the ER presents specific challenges not faced by the folding of proteins in other cellular compartments. For example, the chemical steps involved in disulfide bond formation and rearrangement are intrinsically slow compared to conformational rearrangements. Moreover, partial native structure can dramatically inhibit access to buried cysteines, further slowing disulfide rearrangement (Weissman and Kim, 1992). Similarly, transmembrane domains must be inserted with correct topology into the ER membrane if a protein is to adopt its native structure. This problem is solved in part through the co-translational insertion of transmembrane domains (Johnson and van Waes, 1999). However, as illustrated by the recently described maturation of aquaporin-1 (Lu et al., 2000), transmembrane domains are not always correctly oriented until after synthesis of nearly the entire polypeptide.

The ER serves both as a protein-folding compartment and as a gatekeeper, guaranteeing the structural integrity of each protein before it is presented extracellularly (Hammond and Helenius, 1995; Hurtley and Helenius, 1989). As such, the ER is highly enriched in the factors that promote efficient protein folding (known as chaperones), as well as factors that prevent improperly

folded proteins from progressing through the ER. To prevent the forward progression of misfolded proteins, the ER contains a quality control system that is able to detect the folded state of a protein. If misfolded proteins accumulate to significant levels, the ER contains a signaling pathway known as the unfolded protein response (UPR) that allows the cell to survive folding stress.

The goal of the research presented in this thesis was to understand how the ER is able to maintain an environment favorable to proper protein folding. As this work led us from thinking specifically about protein folding *in vivo* to the ways in which cells deal with misfolding, each of these aspects of secretory pathway function will be briefly described.

Chaperones in the endoplasmic reticulum

Early protein denaturation/renaturation experiments clearly demonstrated that the information required for the proper folding of a protein is contained within the primary sequence of the protein (reviewed in Anfinsen, 1973). As the field of protein folding developed, however, it became clear that the process of protein folding could be assisted by other cellular factors. By the early 1990s, the basic paradigm that efficient protein folding *in vivo* depends on a set of highly conserved proteins termed molecular chaperones was well established (Cheng et al., 1989; Gething and Sambrook, 1992; Hemmingsen et al., 1988; Ostermann et al., 1989; Pelham, 1986; Rothman, 1989). Four major classes of conserved

chaperones/heat shock proteins emerged from these studies: the chaperonin family (including Hsp60 and the *E. coli* protein GroEL; reviewed in Sigler et al., 1998), which is characterized by the formation of ring-shaped oligomers; Hsp70, which functions together with Hsp40 and (in bacteria) GrpE (reviewed in Bukau and Horwich, 1998); Hsp90 (reviewed in Buchner, 1999; Mayer and Bukau, 1999); and Hsp100, which also forms ring-shaped oligomers and is capable of both recovering previously aggregated protein and of denaturing stably folded proteins (reviewed in Saibil, 2000).

Members of virtually all classes of molecular chaperones are found within the ER, two notable exceptions being members of the Hsp60/GroEL family (Stevens and Argon, 1999) and the Hsp104 family. Given the particular demands on folding in the ER, it is perhaps not surprising that there are in addition several chaperone systems unique to the ER. These include general chaperones, such as calnexin and its soluble homolog calreticulin, and the machinery responsible for the introduction of disulfide bonds into proteins, as well as a number of chaperones dedicated to assisting the maturation of a single or a limited number of proteins.

Perhaps the best characterized chaperones within the secretory pathway are members of the 70 kDa heat shock protein (Hsp70) family, and the central role of the most abundant Hsp70 in the lumen, BiP or Kar2p as it is known in yeast, in protein folding has been well-documented (Gething and Sambrook,

1992; Wei and Hendershot, 1996). Yeast with reduced levels of lumenal Hsp70 activity exhibit protein folding defects (Simons et al., 1995) and synthetic interactions with mutated alleles of genes encoding the lumenal Hsp40 chaperones and components of the oligosaccharyl transferase (Nishikawa and Endo, 1997; Schlenstedt et al., 1995; Szyperski et al., 1994). Kar2p most likely aids folding by preventing off-pathway intermediates from forming. Both Kar2p and another Hsp70 homolog in yeast, Lhs1p/Hsp170, also play an active role in the refolding of heat-damaged secreted proteins in the lumen (Jämsä et al., 1995; Saris et al., 1997).

The activity of Hsp70 family members is facilitated by members of the GrpE and Hsp40 (DnaJ) families. Identified first in bacteria, GrpE stimulates the exchange of ATP for ADP on the bacterial Hsp70 DnaK (Liberek et al., 1991), thus facilitating release of substrate and permitting the commencement of a new binding cycle (Szabo et al., 1994). However, a GrpE-like exchange factor does not appear to be involved in the early secretory pathway. In contrast, Hsp40/DnaJ chaperones, which stimulate the ATPase activity of Hsp70 and thus promote stable substrate binding (McCarty et al., 1995; Schmid et al., 1994), are critical at many steps in the eukaryotic secretory pathway.

Another class of chaperone found in the ER is the Hsp90 class of molecular chaperones. These are abundant, essential proteins that have been studied primarily for their role in kinase and steroid hormone receptor maturation

6

(reviewed in Caplan, 1999). While mammalian cells contain both cytoplasmic and lumenal Hsp90s, yeast lack an ER-lumenal Hsp90 homolog. The involvement of Hsp90 in general protein folding is somewhat controversial. The evidence for their involvement in protein folding includes the observations that Hsp90 can maintain aggregation-prone substrates in a refolding-competent state *in vitro* (Bose et al., 1996; Freeman and Morimoto, 1996) and that it associates with unassembled immunoglobulin chains in the mammalian ER (Melnick et al., 1994; Schiebel and Buchner, 1997). In addition, Hsp90 can enhance the Hsp70- and Hsp40-mediated folding of luciferase *in vitro* and *in vivo* (Grenert et al., 1999; Johnson et al., 1998; Schumacher et al., 1996). However, the folding of most proteins is unaffected in yeast lacking functional Hsp90 (Nathan et al., 1997).

The peptidyl prolyl isomerases (PPIases) comprise another family of chaperones, with members found in virtually all cellular compartments where protein folding occurs. The PPIases catalyze the *cis/trans* isomerization of the peptide bond immediately preceding proline residues, which is kinetically unfavorable when uncatalyzed (Lang et al., 1987). These chaperones can be divided into two structurally distinct classes based on homology: the immunophilin family, whose founding member is the target of the immunosuppressant cyclosporin, and the FK-binding protein (FKBP) family, whose founding member is the target of the compound FK506 (Zapun et al., 1999). PPIases have multiple functions, some of which have little to do with protein folding, which has lead to some controversy regarding the requirement for

PPIases in folding reactions. However, a number of observations support their significance to protein folding in the ER. First, PPIases are induced by the UPR (Chapman et al., 1998; Travers et al., 2000; Chapter 4). Second, the physiological significance of a cyclophilin family member from *Drosophila melanogaster* known as *ninaA* has been well established: this PPIase is necessary for the proper secretion of a subset of rhodopsins in the fly eye (Baker et al., 1994; Colley et al., 1991; Stamnes et al., 1991).

Disulfide bond formation and protein folding

Disulfide bonds are frequently observed in proteins of the secretory pathway. These bonds are unique in protein folding in that they covalently link portions of a peptide through the sulfhydryl groups at the ends of two cysteine side chains. The formation of this bond is the result of a redox reaction, in which a pair of cysteines becomes oxidized, while another molecule is reduced. Disulfide bond formation can be important for stabilizing the native state of a protein. For example, if one of the cysteines involved in the disulfide bond found in β-lactamase is mutated to serine to prevent oxidation of β-lactamase, the thermal stability of the protein is greatly weakened (Schultz et al., 1987). Conversely, introduction of a disulfide bond into a protein can greatly increase its stability, as can be seen by the addition of disulfide bonds into T4 lysozyme (Matsumura et al., 1989) or into the dimer interface of λ repressor (Sauer et al., 1986).

In other cases, disulfide bonds appear to play an important role in the formation of native structure. For example, bovine pancreatic trypsin inhibitor (BPTI) contains three disulfides in its native state. The folding pathway of BPTI involves multiple conformational intermediates with non-native disulfide bonds (Creighton, 1977; Weissman and Kim, 1991; Weissman and Kim, 1992), the rearrangement of which lead to the native fold. An even more dramatic example is that of the P22 tailspike protein, whose native state contains no disulfide bonds, and yet a number of disulfide bonds are formed during the folding reaction (Robinson and King, 1997).

Since the classical protein folding studies performed by Anfinsen, it has been clear that oxidation can proceed spontaneously in an aerobic environment. However, oxidative protein folding occurs much more rapidly *in vivo* than *in vitro*. For example, whereas reduced ribonuclease A recovers activity *in vitro* with a half-life of ~1 hour, immunoglobulins are oxidized *in vivo* with a half-life of ~30 seconds (Gilbert, 1990). This difference between *in vivo* and *in vitro* folding suggests that protein oxidation must be catalyzed within living cells (Anfinsen, 1973). Indeed, it was this observation that led to the initial identification of protein disulfide isomerase (PDI) over 30 years ago as a chaperone that catalyzed the rearrangement of pre-existing disulfide bonds (Goldberger et al., 1963). Subsequent studies examining the role of PDI in oxidative protein folding have also suggested that it is capable of introducing *de novo* disulfide bonds into

substrate proteins, as long as the enzyme is supplied with a suitably oxidizing environment (discussed below; Freedman et al., 1994). Consistent with its significance in the process of oxidative protein folding, PDI is a highly abundant (with a concentration in the ER of ~1-2 mM; Gilbert, 1990), soluble, ER-lumenal protein (Lambert and Freedman, 1985).

The sequence of PDI reveals that it contains two domains with similarity to the thioredoxin family, designated as **a** and **a'**. The two thioredoxin-like domains are separated by two domains with weak homology to each other, designated **b** and **b'** (Edman et al., 1985). Although only the weakest of homology can be detected between either the **b** or **b'** domain and thioredoxin, both domains also appear to exhibit the thioredoxin fold, on the basis of NMR structural studies (Kemmink et al., 1997). PDI contains a final domain at its C-terminus, designated the **c** domain, which is rich in acidic amino acids and is a putative Ca^{++}-binding domain (Freedman et al., 1994). However, this domain appears to not be required for PDI function (Koivunen et al., 1999). The **a** and **a'** domains contain the active site $C-X_a-X_b-C$ residues that are characteristic of the thioredoxin family, and it is these residues that are required for full activity of the PDI protein both *in vivo* and *in vitro* (Holst et al., 1997; Westphal et al., 1999). When a disulfide is present within either of these active sites, the enzyme is capable of introducing disulfide bonds directly into nascent chains (Lyles and Gilbert, 1991). When the active sites are reduced, PDI can either rearrange a

pre-existing disulfide bond within a protein or reduce a protein (Frand et al., 2000).

As alluded to earlier, the ability to introduce disulfide bonds into proteins is dependent on the bulk redox environment, which *in vivo* is thought to be a mixture of the reduced and oxidized forms of the tripeptide glutathione (GSH and GSSG, respectively; Hwang et al., 1992). Studies on the abundance of these small molecules *in vivo* suggest that the ratio of GSH to GSSG varies between the cytoplasm and the secretory pathway. The ratio in the cytoplasm was measured as ~100:1 (Hwang et al., 1992), sufficiently reducing to prevent the formation of disulfide bonds in the cytoplasm. In contrast, the ratio of GSH to GSSG in the secretory pathway is ~3:1 (Hwang et al., 1992). This ratio of reduced to oxidized glutathione corresponds very well with that found to be optimal for protein folding *in vitro* (Hwang et al., 1992; Konishi et al., 1982a; Konishi et al., 1982b).

One might assume from these observations that the presence of the glutathione buffer alone was sufficient to maintain an environment favorable for protein oxidation. However, every disulfide bond that is formed in a nascent chain introduces reducing equivalents into the ER that must be disposed of in order to keep the environment in a net oxidized state. A number of models have been proposed to explain how this happens, including import of oxidizing equivalents from the cytoplasm (Kaderbhai and Austen, 1985; Scheele and

Jacoby, 1983), secretion of reducing equivalents, and a host of different enzymatic activities (Frand et al., 2000; Hwang et al., 1992; Ziegler and Poulsen, 1977), none of which have been entirely satisfactory.

Some clues as to how cells maintain an oxidative protein folding environment have come from analysis of protein folding in another cellular compartment, that of the bacterial periplasm. In many respects, the periplasm is analogous to the secretory pathway of eukaryotic cells, including a coupling of disulfide bond formation with protein folding. The discovery of factors responsible for the oxidation of proteins in the periplasm began with studies of protein translocation across the bacterial inner membrane, in which bacterial strains were isolated on the basis of an inability to properly transport a β-gal/MalF fusion protein across the bacterial inner membrane (Bardwell et al., 1991). Fortuitously, the fusion protein contained a number of cysteines in the periplasmic portion of the protein that could be oxidized. In the absence of a gene later called dsbA, bacteria were unable to oxidize this domain of the fusion protein, the transmembrane domain was destabilized, and the β-gal protein re-entered the cytoplasm. Subsequent analysis of the DsbA protein demonstrated that it was a member of the thioredoxin family and that it is required for the oxidation of periplasmic proteins, including OmpA, alkaline phosphatase, and β-lactamase (Bardwell et al., 1991).

As DsbA must become reduced each time it introduces a disulfide bond into a protein, a mechanism must exist to re-oxidize DsbA. This factor, known as DsbB, was identified by two labs carrying out genetic screens: Beckwith and co-workers identified the gene encoding DsbB in their β-gal/MalF fusion screen (Bardwell et al., 1993), while Raina and co-workers identified it looking for mutations that conferred sensitivity to reducing agents or genes whose overexpression provide resistance to reducing agents (Missiakas et al., 1993). Mutations in *dsbB* result in similar phenotypes as mutations in *dsbA*: accumulation of reduced OmpA and reduced β-lactamase (Bardwell et al., 1993; Missiakas et al., 1993). DsbB was implicated as an oxidant of DsbA by virtue of the fact that mild oxidizing reagents were able to complement a lack of DsbB, while they could not complement a loss of DsbA (Bardwell et al., 1993; Missiakas et al., 1993). Furthermore, in the absence of DsbB, DsbA accumulates in a reduced form (Bardwell et al., 1993; Kishigami et al., 1995a). If an active-site cysteine in DsbA is mutated, a mixed-disulfide complex between DsbB and DsbA can be isolated (Guilhot et al., 1995; Kishigami et al., 1995b).

While the machinery encoded by the *dsbB* and *dsbA* genes is very effective at oxidizing proteins in the periplasm, this only solves part of the problem. Some proteins contain multiple disulfides, in which case it is not enough that the protein is oxidized: the correct pairs of cysteines must be oxidized to generate a native protein. This often requires that pre-existing, but incorrect, disulfides must be re-arranged or isomerized during the folding

13

reaction. This is accomplished through the activities of proteins encoded by the *dsbD* and *dsbC* genes (Missiakas et al., 1994; Rietsch et al., 1996; Shevchik et al., 1994). Whereas *dsbA* or *dsbB* are required for all oxidation, *dsbC* and *dsbD* appear to be required only for the folding of proteins with multiple disulfide bonds (Rietsch et al., 1996; Sone et al., 1997). In order for DsbC to function as an isomerase, its active site cysteines must be in a reduced state, allowing for the formation of a mixed-disulfide intermediate between DsbC and its substrate. The factor found to be responsible for maintaining DsbC in a reduced form is DsbD (Missiakas et al., 1995; Rietsch et al., 1996).

Although the studies on the bacterial periplasm described thus far clearly establish a relay of disulfide bond transfer that ultimately results in the oxidation of substrates, the discovery of the DsbA/DsbB pathway traces the transfer of oxidizing equivalents only as far back as the plasma membrane. Initial clues as to how DsbB remains in its oxidized form came from Ito and co-workers, who guessed that the membrane-localized electron transport chain used in respiration might be involved in periplasmic oxidation (Kobayashi et al., 1997). They disabled components of the respiratory chain by deleting electron carriers such as hemes and ubiquinones and found that the removal of these factors blocked oxidation.

A more detailed understanding of the mechanism used to transfer electrons from DsbB to the electron transport chain came from Bardwell and co-

workers, who established a biochemical assay for DsbB function and isolated a fraction from the bacterial membrane that was necessary and sufficient for oxidation of DsbA in a DsbB-dependent reaction (Bader et al., 1999). It was subsequently found that this fraction contained cytochrome bd oxidase, although cytochrome bo oxidase performs the same reaction. In either case, ubiquinone acts as an intermediary, coupling DsbB to the cytochrome oxidases. Under aerobic growth conditions, the excess electrons are ultimately transferred to molecular oxygen. However, this work also demonstrated that oxidation can occur under anaerobic conditions, in which case electrons are transferred from DsbB to the final acceptor, fumarate, using menaquinone as an intermediary.

Protein Quality Control: Retention

Despite the ER's highly optimized folding environment, an inevitable consequence of the large flux of proteins through the ER is that the folding process will occasionally fail, resulting in the production of unrecoverably misfolded proteins. The ER also has a robust "quality control" system that is responsible for recognizing misfolded proteins and preventing their progress through the secretory pathway (reviewed in Brodsky and McCracken, 1999; Ellgaard et al., 1999; Hurtley and Helenius, 1989). This quality control system provides the dual benefit of keeping folded proteins within the chaperone-rich folding environment of the ER and preventing misfolded proteins from passing to the cell surface where they could potentially be toxic.

The exact mechanism by which the quality control system works remains in many cases unclear, but it seems likely that there are in fact multiple different mechanisms that contribute to quality control. These may act at the level of active retention in the ER by immobilization or aggregation, inhibition of recognition by the ER export machinery, or promotion of continuous retrieval from post-ER compartments (Brodsky and McCracken, 1999; Ellgaard et al., 1999; Nehls et al., 2000).

The primary step in ER quality control is retention of misfolded or misassembled proteins, and the most common mechanism for retaining misfolded proteins is through association with other proteins that are themselves normally retained (Ellgaard et al., 1999). As the exposure of epitopes rendering a protein susceptible to recognition by molecular chaperones is a feature likely to be common to all misfolded or misassembled proteins, chaperones are particularly good candidates for retention molecules. In fact, the calnexin/calreticulin system (Zhang et al., 1997), BiP (Hammond and Helenius, 1994; Hurtley and Helenius, 1989), and PDI (Reddy and Corley, 1998) have been implicated in aspects of quality control (for review, see Ellgaard et al., 1999).

Studies examining the trafficking of the glycoprotein of vesicular stomatitis virus (VSVG) support the notion that association with a chaperone is sufficient for ER-retention. In these studies, the sub-cellular localization of a temperature-

16

sensitive mutant of VSVG was studied through indirect immunofluorescence (Hammond and Helenius, 1994). At the non-permissive temperature, VSVG could be found throughout the ER as well as in ER-Golgi intermediate compartments. The only marker that co-localized with the VSVG protein was BiP. Interestingly, when BiP localization was examined in non-transfected cells or in cells expressing VSVG at the permissive temperature, BiP is only seen in the ER. This suggests that misfolded VSVG is able to pull BiP out of the ER, but that VSVG-BiP complexes are returned to the ER, thus keeping VSVG mutant protein from being secreted.

The processing of the core oligosaccharyl glycan in the ER has perhaps been the best-studied example of a mechanism of retention of a misfolded protein in the ER, although its relevance to the yeast ER is questionable. Initially, a branched chain of sugars of the composition $Glc_3Man_9GlcNAc_2$ is added to asparagines within the sequence motif NX(S/T). Glycoproteins with the attached sugar chain undergo a rapid trimming, in which the three external glucose residues are removed sequentially through the actions of glucosidase I and II (Helenius and Aebi, 2001). A single glucose residue can be added back by UDP-glucose:glycoprotein glucosyltransferase (UGGT; Fernandez et al., 1998; Parodi et al., 1983), but UGGT only recognizes misfolded proteins. The monoglycoslyated glycan is recognized by the lectins calnexin and its soluble homolog calreticulin, which retain the glycoprotein in the ER and facilitate its folding (Helenius and Aebi, 2001). Removal of the terminal glucose triggers

17

dissociation of the calnexin/calreticulin-glycoprotein complex and the correctly folded glycoprotein can then exit the ER (Hebert et al., 1995). However, misfolded proteins are recognized by UGGT and re-glycosylated, leading to re-association with the lectins and permitting another chance at folding (Hammond et al., 1994). Thus, unlike modification of glycosyl groups in the Golgi, which are used for creating diversity (Helenius and Aebi, 2001), modification of the basic glycosylation structure in the ER appears to be primarily a mechanism used by the quality control machinery to distinguish folded and misfolded proteins.

An additional complication in quality control of misfolded proteins is that the ER must distinguish between slowly folding proteins and those that are terminally misfolded. It has recently become clear that competition between enzymes that attach or remove sugar moieties may function as a timer for the folding of individual glycoproteins in the mammalian ER (Ellgaard et al., 1999; Liu et al., 1999). After prolonged retention of a misfolded protein in the ER, the trimming of mannose residues may divert the protein from the calnexin-catalyzed folding pathway and into a quality control pathway (Ayalon-Soffer et al., 1999; Chillaron et al., 2000; Chung et al., 2000; de Virgilio et al., 1999; Liu et al., 1999; Tokunaga et al., 2000; Wilson et al., 2000). Consistent with this model, degradation of a mutated form of the vacuolar-targeted carboxypeptidase Y (CPY*) in yeast depends upon glycosylation and requires the mannosidase I-generated $Man_7GlcNAc_2$ moiety (Jakob et al., 1998; Knop et al., 1996). However, there is limited evidence for a calreticulin or calnexin binding cycle in S.

cerevisiae. Indeed, yeast do not contain the UGGT enzyme (Parodi, 2000). Instead, factors like the recently identified α-mannosidase-like protein, Mnl1p, may identify glycoproteins containing $Man_7GlcNAc_2$ linkages as ERAD substrates (Nakatsukasa et al., 2001).

Protein Quality Control: ER Associated Protein Degradation (ERAD)

Individually, irrevocably misfolded ER proteins are blocked from further progress through the secretory pathway and are retrotranslocated into the cytosol, where they undergo ubiquitin- and proteasome-dependent degradation, a multi-step, constitutively-active process known as ER-associated degradation (ERAD; Hampton and Bhakta, 1997; Hampton et al., 1996; McCracken and Brodsky, 1996; Werner et al., 1996; Wiertz et al., 1996a). The unfolded nature of nascent chains entering the ER and the requirement for ERAD to selectively degrade only misfolded or regulated proteins suggests that this process is complex. However, a combination of biochemical and genetic studies has begun to identify the cellular players and mechanisms involved in this degradation process, which include ER membrane proteins, chaperones, and cytosolic components of the ubiquitination and proteolytic machinery (reviewed in Brodsky and McCracken, 1999).

While still unclear, it seems that many of the same molecular chaperones involved in folding proteins in the ER or retaining misfolded proteins in the ER also play a part in the removal of ERAD substrates. Aberrant secretory proteins

may have exposed structural motifs (Schmitz et al., 1995; Skowronek et al., 1998; Wileman et al., 1990) or hydrophobic patches that could prolong chaperone interactions and trigger their destruction. Consistent with this model, the chaperones Kar2p (Brodsky et al., 1999; Plemper et al., 1997), calnexin (McCracken and Brodsky, 1996), and PDI (Gillece et al., 1999) are required for the degradation of some ERAD substrates in yeast. In addition, two lumenal Hsp40 homologs in yeast, Scj1p and Jem1p, interact with Kar2p (Nishikawa and Endo, 1997; Schlenstedt et al., 1995) and help prevent the aggregation of misfolded proteins prior to their removal (Nishikawa et al., 2001).

The export of soluble ERAD substrates occurs by retrotranslocation through the Sec61p translocation pore. The strongest evidence supporting this hypothesis is the stabilization of yeast ERAD substrates *in vitro* (Pilon et al., 1997) and *in vivo* (Plemper et al., 1997; Zhou and Schekman, 1999) in *sec61* mutant microsomes or cells, respectively. Despite using the same channel and requiring Kar2p, the isolation of ERAD-specific mutations in *KAR2* (Brodsky et al., 1999) and *SEC61* (Wilkinson et al., 2000; Zhou and Schekman, 1999) suggests that translocation and retrotranslocation are mechanistically distinct processes. In addition, because signal sequences are generally cleaved concomitant with translocation, there must be a different mechanism for targeting ERAD substrates to the lumenal face of the Sec61 pore. Several studies suggest that BiP/Kar2p may deliver misfolded proteins to the Sec61 channel (Brodsky et al., 1999; Knittler et al., 1995; Schmitz et al., 1995; Skowronek et al.,

1998) and perhaps gate the pore to regulate opposing traffic (Hamman et al., 1998; Plemper and Wolf, 1999).

Multiple studies indicated that ERAD substrates are degraded in the cytoplasm by the proteasome (Biederer et al., 1996; Hampton et al., 1996; Hiller et al., 1996; Jensen et al., 1995; Oda et al., 1996; Qu et al., 1996; Sommer and Jentsch, 1993; Werner et al., 1996; Wiertz et al., 1996c). This complex proteolytic machine consists of a catalytic 20S cylindrical core particle and 2 copies of the 19S (PA700) regulatory particle that "caps" the 20S subunit (Baumeister et al., 1998). Ubiquitination is necessary for proteasomal processing of most (Biederer et al., 1997; Hampton and Bhakta, 1997; Hiller et al., 1996; Jensen et al., 1995; Loayza and Michaelis, 1998; Ward et al., 1995; Zhou and Schekman, 1999) but not all ERAD substrates (McGee et al., 1996; Werner et al., 1996; Yu et al., 1997). Two ubiquitin-conjugating enzymes, Ubc6p and Ubc7p (Biederer et al., 1996; Biederer et al., 1997; Hiller et al., 1996; Sommer and Jentsch, 1993) and a ubiquitin ligase, Hrd1p/Der3p (Bays et al., 2001; Deak and Wolf, 2001; Gardner et al., 2000) reside at the yeast ER membrane and are required for the degradation of many ERAD substrates. In addition to targeting substrates to the proteasome, ubiquitination is also required for the retrotranslocation of some proteins (Biederer et al., 1996; Bordallo et al., 1998; de Virgilio et al., 1998).

Additional components of the ERAD machinery have been identified in three independent yeast genetic screens. Stabilization of hydroxymethylglutaryl-coenzyme A reductase (HMG-R) in mutant yeast strains (Hampton et al., 1996) led to the discovery of Hrd1p (also known as Der3p, see below) and Hrd3p, which form a stoichiometric complex that spans the ER membrane (Gardner et al., 2000) and preferentially ubiquitinates misfolded proteins (Bays et al., 2001). Also identified in this screen was Hrd2p, a component of the 19S regulatory subunit of the proteasome. A screen by Wolf and coworkers for mutants in which CPY* is stabilized uncovered three *DER* genes (see above; Knop et al., 1996). Der1p is an integral ER membrane protein of unknown function (Knop et al., 1996) and *DER2* and *DER3* encode for Ubc7p and Hrd1p, respectively, factors known to be involved in ERAD (Bordallo et al., 1998; Knop et al., 1996). Finally, mutations that result in the accumulation of a heterologously expressed variant of the mammalian ERAD substrate, alpha-1 protease inhibitor (A1PiZ), have identified seven complementation groups that may represent novel genes involved in ERAD (McCracken et al., 1996).

The Unfolded Protein Response (UPR)

A primary mechanism by which eukaryotic cells counteract the accumulation of misfolded proteins within the lumen of the ER is known as the unfolded protein response (UPR). This response was initially recognized in mammalian cells by the induction of a specific set of proteins in response to

glucose starvation, a growth condition that results in protein misfolding through the under-glycosylation of nascent polypeptides (Chapman et al., 1998). The proteins induced through this treatment were designated GRPs as a consequence of their glucose regulation (e.g., GRP78 was the original name given to BiP), and consisted largely of molecular chaperones. A variety of other treatments were soon discovered that increased the transcription of the same set of genes, including tunicamycin (an inhibitor of N-linked glycosylation), DTT, and calcium-ionophores. However, other general stress conditions, including heat shock, do not induce the expression of the same set of genes. This stereotyped response to ER-specific folding stressors is shared among all eukaryotic cells.

Rapid progress in detailing the mechanism of UPR activation became possible with the discovery that this response existed in S. cerevisiae. A promoter element, termed the UPRE, was found in the upstream regions of UPR targets in S. cerevisiae (Mori et al., 1992). This promoter element was subsequently used to begin genetically defining the signaling pathway between the ER and nucleus that is responsible for activation of UPR target gene expression (Cox et al., 1993; Mori et al., 1993).

The first screens performed resulted in the identification of molecules at the extreme ends of the signaling pathway. The signal originates in the lumen of the endoplasmic reticulum with the activation of the transmembrane serine/threonine kinase Ire1p (Cox et al., 1993; Mori et al., 1993). When

unfolded proteins begin to accumulate in the ER, the Ire1p kinase dimerizes and is autophosphorylated *in trans* (Shamu and Walter, 1996). At the other end of the signaling pathway lies Hac1p, a member of the bZIP family of transcription factors (Cox and Walter, 1996; Mori et al., 1996). Both of these factors are absolutely required for UPR induction, as deletion of either gene results in a strain unable to increase the expression of known UPR targets in response to ER folding stress.

The discovery of the pathway linking Ire1p and Hac1p awaited the convergence of a number of different observations. First, *HAC1* mRNA migrates differently when isolated from UPR-induced or non-induced cells (Cox and Walter, 1996; Mori et al., 1996). Second, Hac1p can only be detected in cells under conditions that induce the UPR (Cox and Walter, 1996; Mori et al., 1996). Finally, another genetic screen implicated *RLG1*, a tRNA ligase, in induction of the UPR (Sidrauski et al., 1996). When combined with the observation that Ire1p contains a domain with homology to nucleases (Cox et al., 1993; Mori et al., 1993), a model emerged in which Ire1p becomes an active nuclease when unfolded proteins accumulate within the ER. Ire1p then cleaves the transcribed *HAC1* message (termed *HAC1^u*) at specific locations near the 3' end, removing a non-conventional intron (Kawahara et al., 1997; Sidrauski and Walter, 1997). The alternative splicing of the *HAC1* mRNA is completed through the action of Rlg1p, which ligates the alternative exon to the *HAC1* message, forming a new message designated *HAC1^i* (Sidrauski et al., 1996; Sidrauski and Walter, 1997).

Only the protein encoded by the alternatively spliced message accumulates to a significant level in cells. This reaction has since been reconstituted *in vitro* using only Ire1p, *HAC1* mRNA, and Rlg1p (Gonzalez et al., 1999).

One model to explain how cells might sense unfolded proteins predicts that BiP binds to the Ire1p lumenal domain during normal growth conditions, preventing the dimerization of Ire1p molecules. As unfolded proteins accumulate in the ER, increasing amounts of BiP are recruited from Ire1p. Eventually, enough free Ire1p accumulates to allow its dimerization, thus initiating the UPR signaling pathway. This model was recently tested by Ron and co-workers (Bertolotti et al., 2000), who were able to detect a physical association between Ire1p and BiP in extracts from a rat pancreas-derived cell line under normal growth conditions; under conditions of UPR induction, a physical interaction between Ire1p and BiP was absent. A similar pathway is also likely to exist in the yeast ER (Okamura et al., 2000).

The pathway leading to UPR activation in mammalian cells is more complex than that in *S. cerevisiae* and, consequently, has been less clearly defined. A number of groups have identified Ire1p homologs in higher eukaryotes, including Ire1α (identified in humans; Tirasophon et al., 1998), Ire1β (identified in mouse cells; Wang et al., 1998), and PERK (Harding et al., 1999; Shi et al., 1998). Whereas both Ire1α and Ire1β show homology to Ire1p throughout their entire lengths, PERK is homologous to Ire1p only in its ER

lumenal domain and has a kinase domain more like that of eIF2α than that of Ire1p. Consistent with these data, Ire1α, Ire1β, and PERK respond to the same inducers, but diverge in the downstream signaling events that they mediate. Whereas Ire1α and Ire1β induce the expression of BiP and CHOP (another UPR target), PERK responds to the accumulation of unfolded proteins by phosphorylating eIF2α, leading to a decrease in translation (Harding et al., 1999).

In contrast to the situation in *S. cerevisiae*, it has been suggested that activation of the mammalian UPR involves a proteolysis step at the level of Ire1 activation. Upon stimulation of the UPR, both Ire1α and Ire1β are cleaved from the membrane, and the newly released, soluble form redistributes to the nucleus (Niwa et al., 1999). This redistribution seems to depend on the activity of presinilin-1 (PS1), as cells lacking PS1 activity are unable to produce the soluble form of Ire1. In addition, in at least some cell lines, lack of PS1 decreases the level of UPR induction as measured by BiP expression (Katayama et al., 1999; Niwa et al., 1999). However, it should be noted that while two groups have observed a role for PS1, a third report finds no effect of PS1 on UPR activation (Sato et al., 2000). As the conditions used in these experiments are not identical, the full significance of PS1 in UPR activation will await future experiments.

Proteolysis has also been implicated in the activation of at least one transcription factor that is responsible for the ER stress response in metazoan cells. ATF6, a Type-II transmembrane protein, is cleaved into two fragments in

response to treatments that lead to the accumulation of misfolded proteins, and the released cytosolic domain translocates into the nucleus and induces the transcription of several chaperones (Brown et al., 2000; Haze et al., 1999). Goldstein and co-workers subsequently demonstrated that S1P and S2P, the proteases responsible for cleavage of the sterol-starvation transcription factors of the SREBP family, are necessary for cleavage of ATF6 and for a normal ER stress response (Ye et al., 2000). However, unlike the SREBP targets of S1P and S2P, sterols do not affect activation of gene expression through ATF6.

At this point, the relationship between the ATF6 and Ire1α/Ire1β pathways is unclear. Data from Kaufman and co-workers suggests that ATF6 activation lies downstream of Ire1α activation and that the response to ER stress begins with activation of Ire1α (Wang et al., 2000). However, ATF6 does not appear to be alternatively spliced under conditions of ER stress (Yoshida et al., 1998). As both Ire1α and Ire1β show homology to the nuclease domain of S. cerevisiae IRE1 (Tirasophon et al., 1998; Wang et al., 1998), it is possible that another transcription factor in mammalian cells, yet to be identified, is activated in the same fashion as HAC1 in S. cerevisiae. Indeed, both Ire1α and Ire1β are capable of cleaving yeast HAC1 mRNA in vitro (Niwa et al., 1999; Tirasophon et al., 1998).

Outline of the Thesis

In the work to be described in this thesis, we took advantage of the combination of genetics and biochemistry that are possible in the budding yeast *Saccharomyces cerevisiae* to study the requirements for protein folding within the secretory pathway of eukaryotic cells. Chapter Two, titled "Ero1p: a Novel and Ubiquitous Protein with an Essential Role in Oxidative Protein Folding in the Endoplasmic Reticulum," was the result of work carried out in conjunction with Mike Pollard that was published in the journal *Molecular Cell* in 1998. In this work, we carried out two genetic screens in *S. cerevisiae* to identify novel factors that are required for the proper formation of disulfide bonds. These screens both resulted in the identification of a gene we named *ERO1*. A variety of secondary assays were employed to confirm the importance of the *ERO1* gene to oxidative protein folding, including measurements of the overall amount of unfolding in the ER as well as a direct assessment of the ability to fold a specific substrate of the secretory pathway, carboxypeptidase Y (CPY), whose folding requires disulfide bond formation.

Subsequent work on *ERO1* and the mechanism by which it affects the oxidative environment of the ER is described in Chapter Three, titled "Biochemical Basis of Oxidative Protein Folding in the Endoplasmic Reticulum." This work resulted from a collaboration with Ben Tu and Dr. Siew Ho-Schleyer, and was published in the journal *Science* in 2000. This work combines genetic

and biochemical analysis to demonstrate that the protein encoded by the *ERO1* gene, Ero1p, depends on the small molecule flavin adenine dinucleotide (FAD) to oxidize the ER. *In vivo*, oxidative folding is exquisitely sensitive to cellular FAD levels, as loss of FAD through depletion of riboflavin completely blocks the ability of cells to fold CPY, while overexpression of Fad1p, the protein that synthesizes FAD, restores the ability of *ero1* mutant cells to grow. This sensitivity can also be seen in a partially purified microsome system. When purified from yeast cells, the Ero1p protein is associated with FAD. Most importantly, an *in vitro* folding assay was developed using purified Ero1p, PDI, and FAD. In this assay, the ability to fold was absolutely dependent on the addition of both PDI and FAD. This was the first ER-lumenal FAD-dependent protein identified.

Chapter Four, titled "Functional and Genomic Analyses Reveal Essential Coordination Between the Unfolded Protein Response and Endoplasmic Reticulum-associated Degradation", was the result of a collaboration with Chris Patil in the laboratory of Dr. Peter Walter and Drs. Lisa Wodicka and David Lockhart at Affymetrix, Inc. This work took a broader view of the requirements for efficient protein folding in the ER, with an effort to establish a complete list of targets of the UPR. We were able to combine the genetics possible in *S. cerevisiae* with the ability to analyze the transcriptional changes of every gene in the genome of *S. cerevisiae* to establish a comprehensive list of such UPR targets. This work greatly expanded not just our view of the UPR, but also of the requirements for efficient protein folding. Targets were identified throughout the

secretory pathway spanning a large range of secretory pathway functions. We chose to focus on one class of targets, that of ERAD, and analyzed the functional significance of the regulatory relationship between the UPR and ERAD. This led to the realization that ERAD and the UPR are intimately coordinated and together carry out the essential function of removing misfolded proteins from the secretory pathway.

The work presented in this thesis is summarized in Chapter 5, which also contains some more speculative comments. Appendix A contains the results of an experiment leading from the work presented in Chapter 4. All references cited in this thesis can be found in Appendix B.

Chapter 2

Ero1p: a Novel and Ubiquitous Protein with an Essential Role in Oxidative Protein Folding in the Endoplasmic Reticulum

Ero1p: a Novel and Ubiquitous Protein with an Essential Role in Oxidative Protein Folding in the Endoplasmic Reticulum

Michael G. Pollard*, Kevin J. Travers*, and Jonathan S. Weissman

Departments of Cellular & Molecular Pharmacology, and Biochemistry & Biophysics, University of California - San Francisco, 513 Parnassus Ave., San Francisco, CA 94143-0450 (email: jsw1@itsa.ucsf.edu)
*These authors contributed equally to this work.

Summary

The structure of many proteins entering the secretory pathway is dependent on stabilization by disulfide bonds. In order to support disulfide-linked folding, the endoplasmic reticulum (ER) must maintain a strongly oxidizing environment compared to the cytosol. We report here the identification and characterization of Ero1p, a novel and essential ER-resident protein. Mutations in Ero1p cause extreme sensitivity to the reducing agent DTT, whereas overexpression confers DTT resistance. Strikingly, compromised Ero1p function results in ER retention of disulfide stabilized proteins in a reduced, nonnative form, while not affecting structural maturation of a disulfide-free protein. We conclude that there exists a specific cellular redox machinery required for disulfide-linked protein folding in the ER and that Ero1p is an essential component of this machinery.

Introduction

The endoplasmic reticulum (ER) is a highly specialized protein folding compartment responsible for the structural maturation of proteins entering the secretory pathway (for review see Helenius et al., 1992). The folding capacity of the ER can be enormous, with some cell types having a daily output greater than their own mass. To accomplish this, the ER provides a milieu highly optimized for efficient folding. For example, the ER contains a rich cocktail of molecular chaperones such as BiP (Hsp70), peptidyl-proline isomerase, and protein disulfide isomerase (PDI). The ER also possesses a constitutive "quality control" system which ensures that proteins do not leave this compartment before they have reached their native state (Hurtley and Helenius, 1989). Finally, in response to the accumulation of an excess of misfolded proteins in the ER, the cell induces an unfolded protein response (UPR) that results in the synthesis of ER-specific chaperones (Cox et al., 1993; Mori et al., 1993). Loss of UPR function, while having only mild effects on growth under nonstress conditions, results in extreme sensitivity to the accumulation of unfolded proteins in the ER.

Protein folding reactions in the ER differ in several fundamental ways from folding in other cellular compartments. First, there are no members of the "chaperonin" family of ring-shaped molecular chaperones in the ER while chaperonins, such as GroEL, play an essential role in assisting folding in almost every other cellular compartment where protein folding occurs (Fenton and Horwich, 1997; Hartl, 1996). Second, folding is often accompanied by

glycosylation which can mediate interactions with the recently described ER-specific chaperones calnexin and calreticulin (Hebert et al., 1995; Ou et al., 1993). Third, folding in the ER often involves the simultaneous insertion of portions of the protein into the membrane.

Perhaps the most distinctive feature of protein folding in the ER is the abundance of disulfide bonds in proteins entering the secretory pathway as compared to their near absence in cytosolic proteins. In order to allow efficient disulfide formation, the ER must closely regulate its redox potential. Under strongly reducing conditions, such as those prevalent in the cytosol, disulfide formation is kinetically and thermodynamically disfavored (Braakman et al., 1992). Likewise, excessively oxidizing conditions result in misfolding due to the formation of incorrect intra- and inter-molecular disulfide bonds (Marquardt et al., 1993). The measured redox potential of the ER in intact cells (Hwang et al., 1992) is similar to that determined independently as being optimal for the PDI-mediated folding of ribonuclease A in vitro (Lyles and Gilbert, 1991). Thus there must exist an oxido-reductase system that maintains the ER at a relatively high oxidation potential even though the ER is embedded in a much larger volume of highly reducing cytosol. The molecular basis of the ER oxido-reductase system is unknown.

Because the requirement to maintain an oxidized ER is shared by all eukaryotic cells, we have taken a genetic approach in *S. cerevisiae* to identify

proteins important for this process. We present here the identification and characterization of a novel protein termed Ero1p (Endoplasmic Reticulum Oxido-reductin). Ero1p is an essential, ER-resident protein with homologs in a variety of eukaryotes including humans and trypanosomes. Loss of Ero1p function results in the accumulation of proteins whose folding is dependent upon disulfide bond formation in a reduced and unfolded form within the ER. These and other observations argue that Ero1p plays a critical role in maintaining an oxidative environment in the ER.

Results

Two Strategies for Identifying Proteins Important for Disulfide-linked Folding

Treatment of eukaryotic cells with the membrane-permeable reducing agent DTT inhibits disulfide bond formation in the ER and leads to cell death (Braakman et al., 1992; Jämsä et al., 1994; Simons et al., 1995). While cells do not normally encounter DTT, this treatment mimics the reducing effect that the normal transit of folding proteins has on the ER environment. Yeast unable to induce the UPR have an elevated DTT sensitivity (Cox et al., 1993; Mori et al., 1993). This implies that upregulation of the ER oxidation machinery is part of the normal physiological response to ER stress and that this machinery helps the cell counter the effects of DTT. These considerations suggest that DTT sensitivity could be exploited to identify genes responsible for maintaining the oxidative environment of the ER. A similar approach has recently proved useful for identifying proteins important for disulfide-linked folding in the bacterial periplasm (for review see Missiakas and Raina, 1997).

Two parallel strategies, both exploiting DTT sensitivity, were employed. The first aimed to find components of the oxidation machinery that are upregulated by the UPR. For these studies, we selected for genes that conferred DTT resistance when overexpressed in yeast with either a functional or nonfunctional UPR. The second strategy was designed to identify components

of the oxidative machinery that function during nonstress conditions. Here we screened banks of mutant libraries to identify genes that caused increased DTT sensitivity when mutated. In addition to mutants defective in oxidative protein folding, this screen could also identify strains defective in induction of the UPR as well as mutations that cause some other cellular process to become DTT sensitive. We therefore examined induction of the UPR in the DTT sensitive strains because mutants accumulating unfolded proteins at low concentrations of DTT are expected to have an exaggerated UPR.

Overexpression of *ERO1* (*YML130c*) Confers Resistance to DTT Both in the Presence and Absence of a Functional Unfolded Protein Response

To identify proteins that confer resistance to DTT when expressed at high levels, *S. cerevisiae* were transformed with a high copy genomic plasmid library (Nasmyth and Reed, 1980). Transformants were then selected for the ability to grow on plates containing normally lethal DTT levels. From a pool of 32,000 transformants, a single plasmid was found that allowed growth on 8 mM DTT (Figure 1A), compared to a limit of 4 mM for untransformed yeast. DNA sequencing revealed that this plasmid contained an insert from the extreme left end of chromosome 13 (Bowman et al., 1997). Systematic deletion of the open reading frames (ORFs) in this insert demonstrated that overexpression of a single gene, termed *ERO1* (Endoplasmic Reticulum Oxidoreductin 1, *YML130c*), is both necessary and sufficient to confer DTT resistance.

If induction of *ERO1* were part of the UPR-mediated tolerance of DTT, we would expect that overexpression of this gene in a UPR defective strain would partially counter its DTT super-sensitivity. A high copy plasmid containing *ERO1* was transformed into a yeast strain (ire1Δ) made defective in the UPR by disruption of *IRE1* (a transmembrane kinase required to transmit the UPR signal from the ER to the nucleus; Cox et al., 1993; Mori et al., 1993). The untransformed ire1Δ strain failed to grow on DTT concentrations greater than 1 mM. By contrast, overexpression of *ERO1* allowed ire1Δ yeast to grow in the presence of 3 mM (Figure 1A), although this strain still showed a somewhat greater sensitivity to DTT than did the parental strain. These data suggest that *ERO1* is a major contributor to the DTT tolerance conferred by the UPR. Consistent with this proposal, we found that *ERO1* is normally induced by the UPR (see below) to a level near that expected from the ire1Δ strain carrying the *ERO1* gene on a high copy plasmid, arguing for the physiological relevance of the restored DTT tolerance in this strain. Nonetheless, it remains possible that other proteins, such as PDI, also contribute to the UPR-mediated DTT tolerance.

Mutation of *ERO1* Results in Extreme Sensitivity to DTT and Exaggerated Induction of the Unfolded Protein Response

We also conducted a screen to identify mutations that cause DTT sensitivity. For these studies, we screened three independent mutant libraries:

insertional mutants generated by us using the method of Snyder and coworkers (Burns et al., 1994), and previously described banks of cold-sensitive (Moir et al., 1982) and heat-sensitive (Hartwell, 1967) mutants. Panels of mutant yeast were replica-plated onto plates containing 0 mM to 4 mM DTT (the limit tolerated by unmutagenized yeast). Approximately 40 different strains were found to have modest to strong sensitivity to DTT (i.e., less than or comparable to that of the ire1Δ strain). Strikingly, a single mutant strain, termed YJW150, showed extreme DTT sensitivity (Figure 1). In liquid culture, the growth of YJW150 was inhibited by the addition of 1 mM DTT (Figure 1B). By contrast, the doubling time of the parental strain was unaffected by this treatment, and YJW150 showed only a very modest (20 percent) decrease in growth rate in the absence of DTT.

Mutants with the strongest DTT sensitivity were then tested for the accumulation of unfolded proteins in the ER, as evidenced by an exaggerated induction of the UPR in the presence of low DTT concentrations. The strength of the UPR as a function of DTT concentration was measured using a reporter construct consisting of either the green fluorescent protein (GFP) or the lacZ gene under transcriptional control of the KAR2 unfolded protein response element (UPRE; Cox et al., 1993; Mori et al., 1992). Reporter levels were determined by fluorescence activated cell sorting (FACS) or enzymatic analysis, accordingly. The mutants fell into three categories with respect to the strength of UPR induction: absent to weak, normal, or exaggerated (examples of each class are shown in Figure 2A). YJW150, however, showed a much stronger induction

of the UPR than did all other mutants tested. At very low DTT concentrations (0.5 mM) YJW150 showed a 20-fold stronger induction of the UPR than did the DBY2063 parental strain (Figure 2A). Even in the absence of DTT, FACS analyses indicated that YJW150 had a modest induction of the UPR (Figure 2B), arguing for a folding defect in YJW150 even under nonstress conditions.

Molecular cloning of the defective gene in YJW150 demonstrated that it is identical to *ERO1*, the gene identified above as conferring DTT resistance. Matings between YJW150 and the parental strain DBY2063 revealed that the defect in YJW150 was recessive and segregated in a simple Mendelian manner through three rounds of backcrossing and sporulation. Although YJW150 was originally identified in a *cs* library, the observed DTT sensitivity did not cosegregate with the *cs* phenotype. The gene responsible for the defect in YJW150 was cloned by selecting for plasmids that complemented the DTT sensitivity. All of the plasmids identified in this manner contained *ERO1*, and systematic deletion of the ORFs on one of the complementing plasmids revealed that *ERO1* is necessary and sufficient to restore DTT tolerance to the YJW150 strain. *ERO1* is located 12 kb from the *PHO84* gene. Consistent with a mutation in *ERO1* being responsible for the YJW150 phenotype, linkage analysis indicated that the defective gene in YJW150 is located ~16 centimorgans (roughly 15 kb) from *PHO84* (data not shown). DNA sequencing of the *ero1* allele derived from YJW150 identified a point mutation resulting in the replacement of a conserved histidine (residue 231) with tyrosine (Figure 3A).

Ero1p is a Conserved and Essential ER-resident Protein that is Induced by the Unfolded Protein Response

Three features of the Ero1p protein are notable (Figure 3). First, it contains a putative signal sequence at its amino-terminus, suggesting that it enters the secretory pathway. Second, it contains nine potential N-linked glycosylation sites (Asn-X-Ser/Thr). Third, Ero1p is cysteine-rich. Examination of the available sequence databases revealed a variety of homologs to Ero1p from a broad set of eukaryotic organisms (Figure 3). These included a full length trypanosome protein that is ~30 percent identical to Ero1p. Fragments of related genes from *S. pombe*, the nematodes *C. elegans* and *B. malayi*, *Arabidopsis*, *P. olivaceus*, and *Drosophila*, as well as mouse and human were also found. By identifying overlapping expressed sequence tags (ESTs), it was possible to string together the nearly full length mouse and human genes. Arguing for the validity of this EST assembly, RT-PCR using primers complementary to the 5' and 3' ends of the putative human gene and northern blot analysis of HeLa cell RNA revealed a gene of the expected length (not shown).

Disruption of the *ERO1* gene demonstrated that it is essential for viability. A heterozygous diploid strain was generated in which one copy of the *ERO1* gene was disrupted with the *TRP1* gene. Tetrad analysis of this strain revealed a 2:2 viable to lethal segregation. Microscopic examination showed that the

inviable spores halted at the single cell stage. In all cases the viable spores were tryptophan auxotrophs, demonstrating that an intact *ERO1* gene is required for viability in haploid cells even in the absence of DTT.

Subcellular localization of Ero1p indicated that it is an ER-resident glycoprotein. To facilitate identification by western blot analysis and immunofluorescence, we constructed a low copy (CEN/ARS) plasmid (pMP008), in which three copies of the HA antigen were fused to the carboxyl-terminus of Ero1p driven by its own promoter. Transformation of YJW150 with pMP008 allowed this strain to grow on plates containing up to 3 mM DTT indicating that the epitope-tagged Ero1p was active, though possibly at a somewhat lower level than the untagged protein. Because N-linked glycosylation occurs in the ER, we examined the glycosylation state of Ero1p to determine if the protein enters the secretory pathway. Western blot analysis revealed that Ero1p is a glycoprotein, as endoglycosidase H treatment (Figure 4A) resulted in a decrease in the apparent molecular weight from 100kD to 80kD as determined by SDS-PAGE. Double immunofluorescence microscopy revealed that Ero1p is contained in a perinuclear compartment that precisely colocalizes with the known ER-resident protein Kar2p/BiP (Figure 4B).

Examination of both the RNA and protein levels indicated that *ERO1* is strongly induced by the UPR. Northern analysis with an *ERO1* probe revealed that upon induction of the UPR by DTT treatment, the RNA level of *ERO1*

increased 8.7-fold relative to actin (Figure 4C). This level of induction is comparable to that seen for known ER chaperones like Kar2p and PDI (Cox et al., 1993; Mori et al., 1993). This transcriptional induction was dependent on an intact UPR pathway as it was not observed in an ire1Δ strain. Similarly, western blot analysis of the HA-tagged version of Ero1p revealed that induction of the UPR by DTT treatment caused a large increase in protein levels (Figure 4A).

Mutations in *ERO1* Result in a Specific Defect in ER-mediated Folding of Disulfide-containing Proteins

By monitoring the structural maturation of the vacuolar protease carboxypeptidase Y (CPY), it was possible to examine directly the effect of the Ero1p mutation on disulfide-linked protein folding in the ER. Three distinct subcellular forms of CPY, differing in their carbohydrate and proteolytic trimming, can be distinguished by reducing SDS-PAGE: a 67kD ER form termed p1CPY, a 69kD Golgi form termed p2CPY, and a 61kD mature vacuolar form termed mCPY (Stevens et al., 1982). The structure of CPY is stabilized by five disulfide bonds. Previous studies have shown that CPY synthesized in the presence of 5 mM DTT accumulates in a reduced, nonnative form that is retained in the ER by the quality control system, and thus migrates as the p1 intermediate (Jämsä et al., 1994; Simons et al., 1995). This block in folding, oxidation and maturation, however, is readily reversible upon removal of DTT.

As expected, we found that in both the parental (DBY2063) and *ero1* (YJW150) strains, only p1CPY accumulated in the presence of 5 mM DTT (Figure 5A). In the parental strain, CPY was efficiently converted to the p2 form and ultimately to the mature protein with a half time of ~15 min upon removal of DTT. In striking contrast, CPY in YJW150 was unable to resume folding after removal of DTT and was instead retained in the ER and degraded over ~60 minutes (Figure 5A). Fully reduced p1CPY (red p1CPY) can be distinguished from the oxidized, native form (ox p1CPY) by nonreducing SDS-PAGE (Simons et al., 1995). We found that the ER-retained p1CPY in YJW150 comigrated with the reduced form (Figure 5B). Similarly, we found that in YJW150 the continuous presence of a low concentration of DTT (1 mM) caused CPY to be retained in the ER and degraded (Figure 5C). By contrast, 1 mM DTT did not inhibit CPY maturation in DBY2063. As with the 5 mM DTT pulse, CPY from YJW150 grown in 1 mM DTT comigrated with the reduced nonnative ER form (Figure 5D). Thus, as suggested by the exaggerated induction of the UPR, loss of function of Ero1p results in the accumulation of at least one unfolded protein in the ER. These results are in excellent agreement with those of Frand and Kaiser (1998) in which it was found that under the nonpermissive conditions for a strain carrying a temperature sensitive allele of *ero1*, CPY remained in a reduced, unfolded form in the ER.

A similar folding defect in YJW150 was observed for an HSP150-β-lactamase fusion protein termed Kpn-bla (Simonen et al., 1994). The

heat inducible *Kpn-bla* gene product is particularly convenient for monitoring folding as it is secreted into the medium, and the activity can be readily monitored by assaying for β-lactamase function. Previously, Makarow and coworkers have shown that folding of Kpn-bla is dependent on correct disulfide formation: the protein accumulates in an inactive ER form when synthesized in the presence of 5 mM DTT (Simonen et al., 1994). We found that YJW150 exhibited only a modest defect in activity when Kpn-bla expression was induced in the absence of DTT (Figure 5E). However, continuous presence of 1 mM DTT almost completely inhibited production of active Kpn-bla in YJW150 while only modestly affecting activity in the parental strain. Similarly, pretreatment of cells with a 20 min pulse of 5 mM DTT prior to induction of Kpn-bla resulted in a large decrease (4-fold) in β-lactamase activity in YJW150.

It is possible that the defect in production of native CPY and Kpn-bla is due to a general defect in function and integrity of the ER. To test this possibility, we examined the folding and secretion of the nondisulfide-containing protein invertase, which previous studies have shown to be insensitive to high concentrations of DTT (Jämsä et al., 1994). To examine the effect of DTT on secretion, we exploited a *sec18* strain (Kaiser and Schekman, 1990) which has a reversible block in ER-Golgi transport at elevated temperatures (≥30°C). Enzymatically active invertase was accumulated in the ER of either a *sec18* strain (H393) or *sec18; ero1* double mutant strain (YJW170) by induction of invertase at 37°C. The time course of invertase secretion following release of the

ER-Golgi block by shifting to 25°C was then determined in the presence or absence of 1 mM DTT. We found that YJW150 has no general defect in secretion: in both strains the rates of export of invertase ($t_{1/2}$~20 min) were identical and unaffected by the presence of DTT (Figure 6A).

We also found that folding of invertase did not show heightened DTT sensitivity in the *ero1* strain (YJW150). Both the YJW150 and parental (DBY2063) strains were subjected to the following treatments: no DTT, continuous 1 mM DTT, or a 20 minute pulse of 5 mM DTT. Invertase expression was induced and the activity assayed as a function of time. Although the total level of invertase activity was modestly lower (~20 percent), none of the DTT treatments caused an exaggerated loss of invertase function in YJW150 as compared to the parental strain (Figure 6B).

Discussion

Ero1p is an Essential Component of the ER Redox Machinery

During the life of a cell, reduced proteins continuously enter the ER and undergo oxidative protein folding. This leads to a steady stream of electrons flowing into the ER. In order to sustain efficient protein folding, the ER must have an oxidation machinery capable of rapidly disposing of these excess electrons. The efficiency and generality of this oxidation system is emphasized by the observation that in organisms as divergent as yeast (Jämsä et al., 1994) and humans (Braakman et al., 1992), the ER is able to reestablish oxidative protein folding minutes after complete reduction of protein thiols by DTT. This oxidation system must assess the redox potential and maintain homeostasis as an overly strong oxidizing potential results in misfolding due to the accumulation of inappropriate inter- and intra-molecular disulfide bonds (Marquardt et al., 1993).

Several observations argue that the ER-resident protein Ero1p is an essential component of this oxidation machinery. First, overexpression of Ero1p increases the ability of the ER to reoxidize itself, as evidenced by the ability to grow in the presence of normally lethal DTT concentrations. Reciprocally, in an independent study, Frand and Kaiser (1998) found that yeast deleted in *ERO1* will grow if diamide, a cell-permeable oxidizing agent, is present. Second, loss of Ero1p function results in the accumulation of unfolded proteins in the ER as

evidenced by a dramatic induction of the unfolded protein response (UPR). Third, Ero1p expression is strongly induced by the UPR. Moreover, even in the absence of a functional UPR, overexpression of Ero1p substantially increases resistance to DTT, suggesting that Ero1p plays a major role in DTT tolerance conferred by the UPR. It does, however, remain possible that other UPR-induced proteins contribute to this tolerance. Fourth, nonlethal mutations in Ero1p result in extreme sensitivity to perturbation of the ER redox potential by DTT.

Direct examination of the folding of several proteins demonstrates that the *ero1* mutation can lead to a specific defect in disulfide-linked folding. In the sustained presence of low DTT (1 mM) or following a 20 minute pulse of 5 mM DTT, the endogenous disulfide-containing protein CPY fails to leave the ER and instead accumulates in an unfolded and reduced form. Similarly, a fusion protein between Hsp150 and β-lactamase whose folding is known to require disulfide formation is inactive under these conditions. These defects are not due to a general loss of ER integrity, since the nondisulfide-containing protein invertase is both efficiently folded and transported out of the ER under identical conditions.

In theory, the folding defects we see could be an indirect result of an effect of DTT on the mutant Ero1p protein itself. However, several observations argue strongly against this possibility and instead indicate that Ero1p function is required for oxidative folding in the ER. First, as mentioned above,

overexpression of wild-type Ero1p allows growth at elevated DTT concentrations. Second, the folding defect in *ero1* mutant strains is specific to disulfide-containing proteins. Finally, in a parallel study, Kaiser and Frand found that in a *ts* allele of *ero1*, incubation at the nonpermissive temperature results in accumulation of reduced CPY in the ER as well as retention of another endogenous disulfide containing protein, Gas1p, even in the absence of DTT treatment (Frand and Kaiser, 1998). Together the two studies show that for three different substrates and two different alleles of *ero1*, loss of Ero1p function results in failure of disulfide-linked protein folding. While these data provide a strong case that Ero1p is an essential component of the ER oxido-reductase system, none of these data preclude the possibility that Ero1p functions as a molecular chaperone that binds newly synthesized proteins.

Comparison with Oxidation Machinery in the Bacterial Periplasm

The periplasm of bacteria is in many ways analogous to the ER of eukaryotes. In both systems, proteins are synthesized in the cytosol and are translocated in an unfolded form across a lipid bilayer (Wolin, 1994). Protein folding in the periplasm is often accompanied by the formation of disulfide bonds (for review see Missiakas and Raina, 1997). Recent biochemical and genetic studies have begun to elucidate the process by which disulfide-linked folding is achieved in the bacterial periplasm (Figure 7; e.g., Bardwell et al., 1991). Two proteins, termed DsbA and DsbC, catalyze oxidation and rearrangement of

disulfide bonds, respectively, in newly synthesized proteins. This activity is analogous to that of the ER protein PDI and its homologs. The functional similarity to PDI is also reflected in a structural and mechanistic similarity, since like PDI, DsbA and DsbC contain an active site vicinal cysteine motif (Cys-X$_2$-Cys) found in proteins with thioredoxin folds. In addition, a pair of transmembrane proteins termed DsbB and DsbD (DipZ) regulate the redox environment of the periplasm by respectively maintaining DsbA in an oxidized state, allowing it to function as a protein oxidant, and DsbC in the reduced state required for disulfide isomerase activity.

A remarkable phenotypic parallel is seen between *ero1* mutants and mutants in the *dsb* genes. First, loss of function of either DsbA or DsbB confers extreme sensitivity to DTT. Second, as with Ero1p, overexpression of DsbB confers resistance to DTT (Missiakas et al., 1993), thus supporting the notion that DsbB acts in a manner similar to that of Ero1p as the main source of oxidizing potential (Figure 7). Third, mutations in DsbA and DsbB result in periplasmic accumulation of disulfide-containing proteins in a reduced and unfolded form. Finally, accumulation of excess misfolded proteins in the periplasm (Missiakas and Raina, 1997) results in the upregulation of periplasmic proteases and chaperones in a response that has parallels to the UPR of eukaryotes. As with Ero1p, mutations in the Dsb proteins result in the induction of this response. Reciprocally, at least one of the Dsb proteins (DsbA) is upregulated by this periplasmic stress response (Danese and Silhavy, 1997).

Despite this phenotypic parallel, we find no primary sequence homology between Ero1p and any of the Dsb proteins. This is perhaps not surprising given the physical differences between the ER and the bacterial periplasm. In particular, glutathione is thought to be the major redox buffer in the ER (Hwang et al., 1992), whereas the periplasm of Gram negative bacteria is separated from the extracellular environment by a porous membrane that allows passive diffusion of small molecules such as glutathione. As a consequence of its exposure to the external environment and the lack of an effective redox buffer, the bacterial periplasm is likely to suffer much greater variations in its oxidative environment and pH than does the ER. Thus the functional requirements for the ER and periplasmic oxido-reductase systems are likely to be dramatically different.

Ero1p: an Iron-Sulfur Protein that Acts as a Sensor and/or Effector of Redox State in the ER?

Comparison of the Ero1p sequence with the public genomic databases reveals that several divergent eukaryotic organisms have homologs to Ero1p. For example, an uncharacterized protein from *T. brucei* is 30 percent identical to Ero1p (Leegwater et al., 1991), and nearly full length homologous human and mouse genes could be pieced together from overlapping entries in expressed sequence tag (EST) libraries. In addition, incomplete DNA fragments encoding

proteins homologous to Ero1p from *S. pombe*, *Drosophila*, *Arabidopsis*, *P. olivaceus*, and the nematodes *C. elegans* and *B. malayi* are available. The trypanosome and mammalian homologs share some sequence similarities to Ero1p throughout the entire length of the protein such as the spacing of many of the cysteine residues (Figure 3). There are several segments of these proteins that show more extensive similarities to Ero1p. Particularly notable is a domain near the carboxyl-terminus comprising approximately residues 340 to 375 of Ero1p, which we term a "TALK-Box" for the conserved Thr-Ala-Leu-Lys sequence (Figure 3B). The TALK-Box shows ~70 percent identity and ~90 percent similarity between human, mouse, and yeast proteins.

Despite the existence of a number of homologs, the sequence analysis offers few immediate insights as to the biochemical activity of Ero1p. A variety of different proteins involved in disulfide bond formation, including the Dsb proteins and PDI (Martin et al., 1993), contain thioredoxin-like folds with an active site Cys-X$_2$-Cys motif. Ero1p does contain the sequence **Cys**-Val-Gln-**Cys**-Asp-Arg-**Cys**. In contrast to other thioredoxin motif proteins, however, a third vicinal cysteine is also observed, and all three cysteines are found in all of the TALK-Box containing proteins (Figure 3B).

A search for homologs of the available TALK-Box domains suggests an alternate explanation for the three conserved cysteines: ligation of an iron-sulfur cluster. In particular, the ferredoxin family of proteins uses a Cys-X$_2$-Cys-X$_2$-Cys

53

+ distal Cys motif to hold an Fe4S4 cluster. The possibility that Ero1p is an iron-sulfur cluster protein is intriguing as the rich chemistry of this prosthetic group could make it well suited to act as a sensor and/or effector of the oxidation potential in the ER (for review see Beinert et al., 1997). Ferredoxin family members are involved in a large number of diverse redox reactions including reduction of NAD+ in photosynthesis II and reduction of thioredoxin during metabolic respiration (Stryer, 1995). The redox potential of an iron-sulfur cluster is strongly modulated by the protein environment in which it is embedded and thus could be tuned to match the requirements for oxidative folding in the ER. In addition to its role in electron transport, there is precedence for iron-sulfur clusters acting as sensors of the oxidative state of a cell. For example, the *E. coli* transcription factor FNR, which regulates the expression of genes required for anaerobic growth, contains an iron-sulfur cluster. Oxidation of this cluster by molecular oxygen inactivates FNR, thereby turning off synthesis of the anaerobic genes. While the role of iron-sulfur chemistry in ER redox control is speculative, the identification of Ero1p should greatly facilitate efforts to understand the biochemical basis of this fundamental cellular process.

Experimental Procedures

General procedures and reagents

All nucleic acid manipulations were performed according to standard laboratory protocols (Ausubel et al., 1995). Yeast transformations were carried out by an optimized lithium acetate procedure (Geitz and Schiestl, 1995). Other yeast manipulations were carried out using standard methods (Sherman, 1991) except that the pH of YPD was lowered to that of SD (5.4) to inhibit oxidation of DTT. All incubations were at 30°C unless otherwise indicated. Anti-BiP/Kar2p antibodies were provided by Dr. Davis Ng. Anti-CPY antibody was provided by the laboratories of Drs. Peter Novick and Tom Stevens. The following oligonucleotides were used in this study: P1, AGTTACTCTTCTCATGTTTTACCTGCACGTTACTGTG; P2, AGTTACTCTTCCCCAGGAACATCT GGGAATTA; P3, AGTTACTCTTCAATGGGAAGCATTTAATAGACAGCATCG; P4, AGTTACTCTTCATGGTCACACCGCATAGGCAAGTGC.

Screen for DTT sensitive strains

DTT sensitive strains were isolated by replica plating banks of mutant yeast onto SD plates containing 0, 1, 2, 3 or 4 mM DTT. ~450 cs (Moir et al., 1982), 400 ts (Hartwell, 1967) and 15,000 insertional (Burns et al., 1994) mutants were screened. Mutants were retested by replica-plating using an inoculation prong. The ire1Δ and JC104 strains were included on all plates as internal controls for DTT sensitive phenotypes. The original ero1-2 mutant was the cs

library strain DBY4033. YJW150 was produced by two rounds of backcrossing and sporulation with the parental strain DBY2063.

Cloning of *ERO1* and construction of HA-tagged Ero1p

YJW150 was transformed with a genomic library (Hardwick and Murray, 1995). Transformants were selected for on SD-ura plates and harvested by washing with 1 ml dH$_2$0. Harvested cells were replated on SD-ura supplemented with 2 mM DTT and plasmids from DTT tolerant cells isolated. Restriction analysis of plasmids isolated from 4 independent transformations indicated that they contained overlapping inserts. DNA sequencing of a rescuing plasmid (pMP001) revealed that it contained three ORFs including *ERO1*. A fragment from 958 bp upstream to 1195 bp downstream of *ERO1*, generated by digestion of pMP001 with BamHI and SacI, was subcloned into pRS316, generating pMP003. In order to construct an HA epitope tagged *ERO1* gene, the stop codon of *ERO1* was replaced with a unique XbaI site by PCR mutagenesis generating pMP007. A DNA fragment encoding 3 copies of the HA antigen (i.e, YPYDVPDYA-G-YPYDVPDYA-GS-YPYDVPDYA-AQC) was then ligated between the XbaI and SacI sites in pMP007, generating pMP008.

High copy DTT resistance screen

The W303-1B strain was transformed with an *S. cerevisiae* 2μ genomic library (ATCC #37323, Nasmyth and Reed, 1980). Transformants were selected on SD-leu plates and harvested by washing with 1 ml TE. Harvested cells were

plated at a density of 8000 cells/plate on SD-leu supplemented with 0 mM to 12 mM DTT. A single colony was found to reproducibly grow on 8 mM DTT. Isolation of the plasmid (YEp13-1) from this colony and partial sequencing of the insert revealed that it contained a 7.2 kb fragment from the left arm of chromosome 13 starting at nucleotide 11024 and ending at ~18208. A fragment containing the *ERO1* gene was generated by BamHI digestion, using a naturally occurring site 800 bp upstream of the start codon and a 3' site 500 bp downstream of the stop codon that was generated by ligation of the Sau3AI genomic fragment with the YEp13 vector backbone. This BamHI fragment was subcloned into pRS426 (Christianson et al., 1992) generating pKT001.

ERO1 disruption

The *ERO1* disruption plasmid pMP011, in which nucleotides 1-1566 of the *ERO1* ORF in pMP003 were replaced with the *TRP1* gene, was constructed using the Seamless Cloning kit (Stratagene). The backbone was generated by PCR using a pMP003 template and primers P1 and P2. The insert was generated by PCR using pRS424 (Christianson et al., 1992) as a template and P3 and P4 primers. The diploid strain heterozygous for *ERO1* disruption (YJW169) was generated by transformation of the diploid strain W303-1AxW303-1B with a BamHI-SacI fragment derived from pMP011 and selection for growth on SD-trp. Correct genomic insertion was confirmed by PCR.

Immunofluorescence and western blot analysis

DBY2063 bearing pMP008 was grown in SD-ura to early log phase (OD_{600} 0.1) and incubated for an additional 3.5-4 hr in the absence or presence of 2 mM DTT to induce Ero1p expression. Identical fluorescence patterns were seen in the induced and uninduced cells. Immunofluorescence was conducted as described (Ausubel et al., 1995) using formaldehyde fixation. For Ero1p and BiP localization, the mouse monoclonal α-HA antibody 16B12 (BAbCo) and a rabbit α-BiP polyclonal antibody were used, respectively. Secondary antibodies were goat α-mouse IgG conjugated to BODIPY® TMR-X, and goat α-rabbit IgG conjugated to BODIPY® FL (Molecular Probes). For western blot analysis, cells were washed with water and disrupted by glassbead lysis and boiling in SDS-PAGE sample buffer. Endoglycosidase H digestion was performed according to the manufacturer's instructions (Boehringer Mannheim). Samples were analyzed by SDS-PAGE and western blot analysis (Ausubel et al., 1995) using the 16B12 antibody and goat α-mouse IgG - HRP conjugate (Bio-Rad).

Northern blot analysis

To generate RNA samples for northern blot analysis, 50 ml cultures of JC103 and CS165 (ire1Δ) were grown in YPD. At early log phase, where indicated, cultures were induced for the UPR by 1 hr incubation in 2 mM DTT. Total RNA was isolated by hot phenol extraction as described (Schmitt et al., 1990). Standard techniques were used for the blot preparation, using 20 μg of total RNA per sample. Probes for both *ACT1* and *ERO1* were prepared by PCR

amplification of the full length genes and ^{32}P-radiolabeling with the Ready-to-Go kit (Pharmacia). Prehybridization and hybridization were performed using 10 ml Church buffer (0.5 M sodium phosphate pH 7.2, 1 mM EDTA, 7% SDS). Quantitation was performed using a Bio-Rad phosphorimaging system.

β-Galactosidase assays

Strains assayed for β-galactosidase activity were transformed with pJC005 (Cox et al., 1993), a 2μ plasmid carrying the *lacZ* gene under the control of the UPRE from *KAR2*. Cells were harvested four hours after addition of the indicated DTT concentration. To prepare cell extracts, cells from a 10 ml culture were washed with Z buffer (120 mM sodium phosphate, pH 7.0, 10 mM KCl, 1 mM MgSO$_4$, 20-40 mM β-mercaptoethanol) and a protease inhibitor cocktail (1 mM PMSF, 2 μg/ml leupeptin, 2 μg/ml pepstatin, 10 μg/ml aprotinin). Cells were then pelleted and disrupted by glassbead lysis in the same buffer. Protein concentrations in extracts were determined by OD$_{595}$ measurement using a Bio-Rad assay. β-galactosidase activity was determined by addition of substrate solution (0.5 mM CPRG in Z buffer). After a defined amount of time, the absorbance at 550 nm was measured. Units of activity were defined as:

$$\text{units} = 2.5 \times 10^4 \times \frac{OD_{550}}{OD_{595} \times \text{min.}} \times \frac{vol._{(OD_{595})}}{vol._{(OD_{550})}}.$$

FACS analysis

The YJW173 and YJW156 strains, which have a GFP reporter driven by 4 repeats of the *KAR2* UPRE integrated into the *URA3* locus, were generated by transformation of YJW150 and W303-1B, respectively, with the vector pKT007, linearized by EcoRV. pKT007 was derived from pJCl86 (J. Cox, unpublished result) by replacement of Ser65 of GFP with Thr yielding GFP*. Cultures for FACS analysis were grown in YPD media to early log phase, and induced for the UPR by 2 hour growth in the indicated DTT concentration. FACS analysis was performed on a FACScan instrument (Becton-Dickinson).

CPY folding assay

For metabolic labeling, 3 OD_{600} units of log phase strain DBY2063 or YJW150 were pelleted and resuspended in 100μl of SD containing 1 mM or 5 mM DTT. After 5 min, labeling was initiated with 150-350μCi ^{35}S-Met/Cys (Pro-Mix, Amersham). After 20-30 minutes, labeling was halted by resuspending cells in SD supplemented with 100 mM Cys, 100 mM Met, and 10 mM cycloheximide (1 mM DTT was included for folding assays conducted in the continuous presence of DTT). At the indicated chase times, an aliquot was removed and folding halted with ice cold chase solution (20 mM NaN_3, 40 mM NEM in PBS). Samples were lysed, immunoprecipitated and analyzed by SDS-PAGE as described (Simons et al., 1995). The ox p1CPY sample was obtained from the H393 strain as described (Simons et al., 1995), and red p1CPY was generated by addition of DTT to ox p1CPY.

β-lactamase folding

YJW171 and YJW172 were generated by transformation of YJW150 and DBY2063, respectively, with a *Kpn-bla* integrating plasmid (pKTH4544; Simonen et al., 1994) linearized by NcoI. β-lactamase activity was measured as follows: cultures were grown to log phase in YPD at 25°C and treated with 0 mM, 1 mM, or 5 mM DTT as indicated. After 20 min, cells were pelleted and resuspended in YPD for the 0 mM and 5 mM pulse treatments or YPD plus 1 mM DTT for the continuous DTT treatment. Kpn-bla expression was then induced by growth at 37°C for 90 minutes. β-lactamase activity in the medium was determined using amoxicillin and cephaloridine (Sigma) as substrates as described previously (Farmer et al., 1994).

Invertase folding and secretion assay

For assaying the kinetics of secretion, a *sec18; ero1* double mutant strain (YJW170) was created by crossing H393 with YJW150. External invertase activity was measured from whole cell suspensions, while internal activity was determined from lysed spheroplasts as described previously (Jämsä et al., 1994). One unit of activity was defined as 1 μmol of glucose released per min at 37° C.

Acknowledgments

Table 1. Yeast Strains

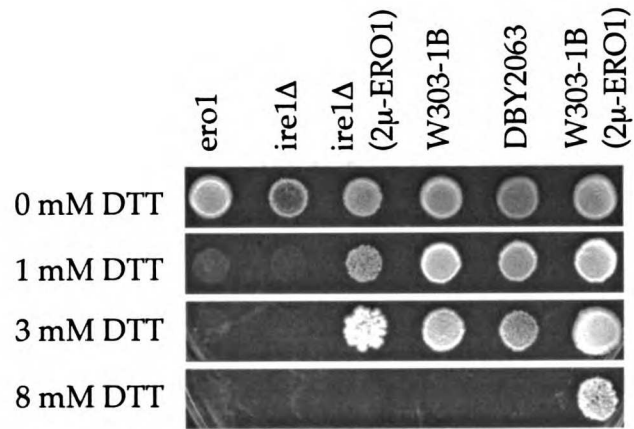| Strain	Genotype	Source/Reference
W303-1A	*leu2-3, -112; his3-11, -15; trp1-1; ura3-1; ade2-1; can1-100*; MATa	Cox et al., 1993
W303-1B	same as W303-1A, except MATα	Cox et al., 1993
JC103	Same as W303-1A, except *leu2-3, -112::LEU'UPRE-lacZ; his3-11, -15::HIS'UPRE-lacZ*	Cox et al., 1993
JC104	Same as JC103, except MATα	Cox et al., 1993
CS165 (ire1Δ)	Same as JC103, except *ire1::URA'*	Cox et al., 1993
DBY2063	*ura3-52; leu2-3, -112; GAL'*; MATa	Hardwick and Murray, 1995
DBY4033 (YJW029)	*ero1-2; his4-619;* MATα	Moir et al., 1982
EYO403	*pho84::LEU2; leu2-3, -112; his3-11, -15::PHO5pr'HIS3+; trp1-1; ura3-1; ade2-1; can1-100;* MATa	E. K. O'Shea
H393	*sec18-1; trp1-289; ura3-52::URA'Kpn-bla; leu2-3, -112; his-;* MATα	Simonen et al., 1994
YJW150	*ero1-2; ura3-52; leu2-3, -112;* MATa	This study
YJW155	Same as W303-1B, except *ura3::URA'UPRE-GFP'*	This study
YJW156	Same as YJW155, except *his3-11, -15::HIS'UPRE-lacZ*	This study
YJW169	Diploid product of W303-1A x W303-1B, except *ero1::TRP'/ERO1*	This study
YJW170	*leu2-3, -112; his3-11, -15; trp1-1; ura3-1; ero1-2; sec18-1;* MATa	This study
YJW171	Same as YJW150, except *ura3-52::URA'Kpn-bla*	This study
YJW172	Same as DBY2063, except *ura3-52::URA'Kpn-bla*	This study
YJW173	Same as YJW150, except *ura3::URA'UPRE-GFP'*	This study

Figure 1. DTT Sensitivity is Strongly Dependent on the Level of Functional Ero1p Protein

(A) Various yeast strains are shown growing on SD plates supplemented with the indicated DTT concentrations. W303-1B and DBY2063 are parental to the CS165 (ire1Δ) and YJW150 (ero1) strains, respectively. Strains carrying a high copy plasmid expressing *ERO1* are indicated (2μ-ERO1).
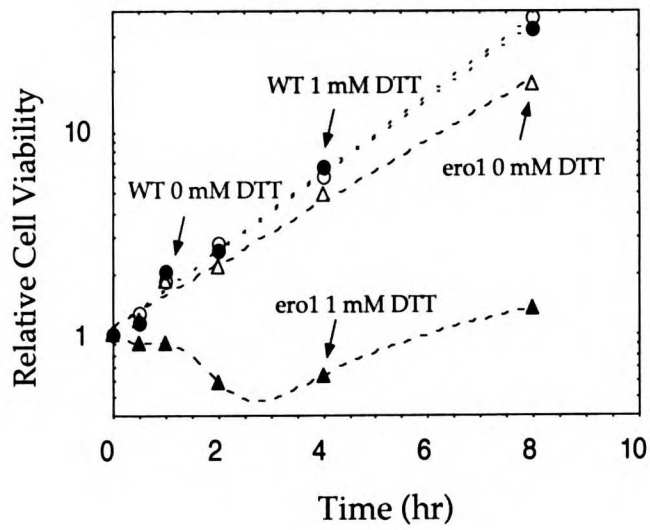
(B) Early log phase cultures of YJW150 (*ero1*, triangles) and parental DBY2063 (WT, circles) strains were transferred to YPD containing 0 mM (open symbols) or 1 mM (closed symbols) DTT. At the indicated times, the number of viable cells was determined by colony formation on YPD plates. Shown is the number of viable cells relative to the zero timepoint. The modest growth of the *ero1* 1 mM DTT culture at later times is likely the result of air oxidation of DTT and perhaps induction of the UPR.

A

	ero1	ire1Δ	ire1Δ (2μ-ERO1)	W303-1B	DBY2063	W303-1B (2μ-ERO1)
0 mM DTT						
1 mM DTT						
3 mM DTT						
8 mM DTT						

B

Relative Cell Viability vs Time (hr)

WT 1 mM DTT

WT 0 mM DTT

ero1 0 mM DTT

ero1 1 mM DTT

Figure 2. Induction of the UPR is Greatly Exaggerated in *ero1* Cells

(A) YJW150 (ero1) and parental DBY2063 (WT) strains, as well as two partially characterized DTT-sensitive mutant strains (dud2 and dud8), were transformed with a plasmid (pJC005) containing a β-galactosidase reporter driven by a UPRE and grown in the presence of DTT for 4 hr. The level of β-galactosidase activity is shown as a function of DTT concentration.

(B) The YJW173 (ero1) and YJW156 (WT) strains contain a GFP reporter driven by 4 repeats of the UPRE integrated into the genomes of YJW150 and W303-1B, respectively. Early log phase cultures of these strains were grown in the presence of 0 mM or 0.25 mM DTT, as indicated, for 2 hr. A plot of cell number versus GFP intensity derived by FACS analysis is shown. The molecular basis for the splitting of the ero1 histogram is unknown.

A

UPRE — lacZ

B

4X UPRE — GFP

0 mM DTT

0.25 mM DTT
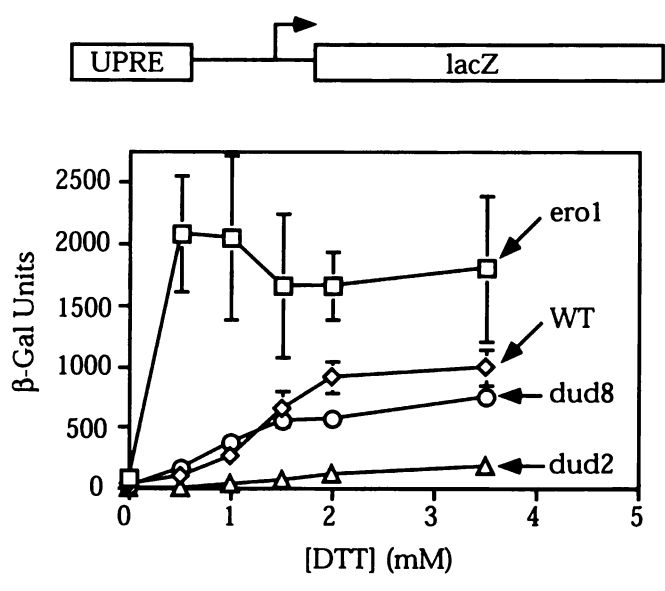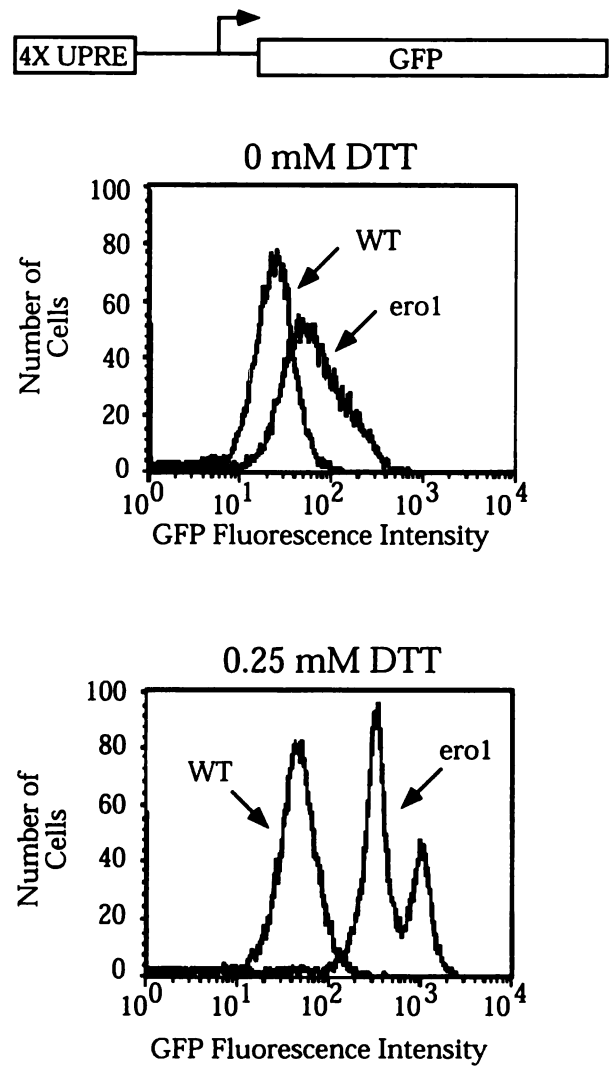
Figure 3. Amino Acid Sequence Comparison of Ero1p Homologs

Amino acid identities and similarities are indicated by dark gray and light gray boxes, respectively. Sequences were aligned using the ClustalW algorithm.

(A) Comparison among full length *S. cerevisiae* and trypanosome (*T. brucei*) proteins as well as human and mouse sequences compiled from EST fragments. The conserved histidine altered in *ero1-2* is indicated (*).

(B) Comparison among the TALK-Box domains from seven organisms. In addition to the sequences in (A), fragments from *S. pombe*, *C. elegans*, and *Arabidopsis* (*A. thaliana*) are presented. The conserved cysteines are indicated (*).

A

S. cerevisiae 1 MRLRTAIATLC----LTAFTSATSNNSYIATDQTQNAFNDTHFCKVDR-NDHVSP 50
trypanosoma 1 MLKMRLLIVVPVLLGLVWQILLRAELDGVSFFGMYISANNSGAGSYVRTKKGNALKEG 58
mouse 1 GDGPPGAC----SLDSWASCGCCAWATGGRRRIQR-TACFCQVS--GYLDDC 45
human 1 0

S. cerevisiae 51 SCNVTFNELNAINENIRDDLSALLKSDFFKYFRLDLYKQCSFWDANDGL----CLNRA 104
trypanosoma 59 FCSLTMDEVSQNTEGITGLLNNITSHPYFRYFKVNLDRECRYWVAEASCT---CDSNG 113
mouse 46 TCDVETIDK-FNNYRLFPRLQKLLESVYFRYYKVNLKRPCPFWNDINQCGRRDCAVKP 102
human 1 MLKPSDR-GNNYRLFPRLQKLLESDYFRYYKVNLKRPCPFWNDISQCGRRDCAVKP 55

S. cerevisiae 105 CSVDVVEDWDTLPEYWQPEILGSFNNDTMKEADDSDDECKFLDQLCQTSKKPVDIEDT 162
trypanosoma 114 CQICTCDDSGIPETLKYPYDMSDVSAVERRTAPDKHAAKGFEDEIKPID--P-D-- 164
mouse 103 CHSDEVPDGIKSASYKYSEEAN-RIEECEQAERLGAVDESLSEETQKAVLQWTKHDDS 159
human 56 CQSDEVPDGIKSASYKYSEEANNLIEECEQAERLGAVDESLSEETQKAVLQWTKHDDS 113

S. cerevisiae 163 IN-YCDVNDFNGKNAVLIDLTANPERFTGYGGKQAGQIWSTIYQDNCFT----- 210
trypanosoma 165 -----RDAT----YVDLLQNPEANTGYSGPKAARVWQAVYDNCNIDGLPS----- 205
mouse 160 SDSFCEIDDIQSPDAEYVDLLLNPERYTGYGKPQTIQRPLR 217
human 114 SDNFCEADDIQSPEAEYVDLLLNPERYTGYKGPDAWKIWNVIYEENCFKPQTIKRPLN 171

S. cerevisiae 211 -----IGETGESLAKDAFVR-LVSGFHASIGTHLSKEYLNTKITGKWEP 252
trypanosoma 206 -----NDTAGVENREKALLRQLLSGLHTSITMHVAAFFYNDTKGDSPL 248
mouse 218 ---SGRGKSKENTFYNWLEGLCVEKRAFYR-LISGLHASINVHLSARYLLQDTWLEKK 271
human 172 PLASGQGTSEENTFYSWLEGLCVEKRAFYR-LISGLHASINVHLSARYLLQETWVRKR 228

S. cerevisiae 253 ----NLDLFMARI----GNFPDRVTN-----MYPNYAVVAKALWKIQPYLP---- 290
trypanosoma 249 RSLGVLNNPNISFYPN--CGMFRRIVKNDEFIRNLFVVYQFVLRAVAKTKRAFLANSS 304
mouse 272 WG-HNVTEFQQRFDGILTEGEGPRRLRN-----LYFLYLIELRALSKVLPFFERPDF 322
human 229 NGGHNITEFQQRFDGILTEGEGPRRFKD-----LYFPLLNR---------- 264

S. cerevisiae 291 ----EFSFCDLVNKEIKNKMDNVISQLDT--KIFNEDLVFAND--LSLTLKDEFRSR 339
trypanosoma 305 LYNSGFNGAATDGDVRLYSNIGELFSSKLFRVATFDEQKFFESP-GAHLLVRQMKRV 360
mouse 323 QLFTGNKVQDAENKALLEILHEIKSFP----LHFDENSFFAGDKNEAHKLKEDFRLH 376
human 265 --NKIQDEENKMLLEILHEIKSFP----LHFDENSFFAGDKKEAHKLKEDFRLH 313

S. cerevisiae 340 FKNVTKIMDCVQCDRCRLWGKIQTTGYATATALKILFEINDADEFTKQHIVGKLTKYELI 397
trypanosoma 361 VHNVTTLMDCVTCEKCRAWGKLETAALATALKIVFGS- 397
mouse 377 FRNISRIMDCVGCFKCRLWGKLQTQGLGTALKILFS 412
human 314 FRNISRIMDCVGCFKCRLWGKLQTQGLGTALKILFSE 350

S. cerevisiae 398 ALLQTFGRLSESIESVNMFEKMYGKRLNGSENRLSSFFQNNFFNILKKAGKSIRYTIE 455
trypanosoma 398 AENVVELNRGE---- 408
mouse 413 412
human 351 KLIANMPSGPSY---- 363

S. cerevisiae 456 NINSTKEGKKKTNNSQSHVFDDLKMPKAEIVPRPSNGTVNKWKKAWNTEVNNVLEAFR 513
trypanosoma 409 R--VALIN 416
mouse 413 412
human 364 EFHLTRQEIVS------LFNAZG 380

S. cerevisiae 514 FIYRSYLDLPRNIWELSLMKVYKFWNKFIGVADYVSEETREPISYKLDIQ 563
trypanosoma 417 RQLAISVKNVR----------SLAAVCEKFNYTAMS 442
mouse 413 412
human 381 RIWKNFYKCER----------IRKLQELVTEYSLKKTS 408

B

Trypanosoma VHNVTTLMDCVTCEKCRAWGKLETAALATALKIVF
S. cerevisiae FKNVTKIMDCVQCDRCRLWGKIQTTGYATATALKILF
S. pombe FRDISRIMDCVGCDRCRLWGKVQITGYGTALKLLL
Mouse FRNISRIMDCVGCFKCRLWGKLQTQGLGTALKILF
Human FRNISRIMDCVGCFKCRLWGKLQTQGLGTALKILF
Arabidopsis FRNISAIMDCVGCEKCRLWGKLQILGLGTALZILF
C. elegans FVNISRIMDCVECDKCRLWGKVQTHGMGTALKILF

Figure 4. Ero1p is an ER-resident Glycoprotein that is Induced by the UPR

(A) Extracts were prepared from a parental strain (DBY2063) carrying a low copy plasmid encoding the HA-tagged *ERO1* gene (pMP008). Where indicated, the cells were induced for the UPR by DTT treatment prior to extract preparation. The samples were then subjected to endoglycosidase H (endo H) treatment, where indicated, and analyzed by SDS-PAGE and western blot analysis, probing with an α-HA antibody.

(B) Cells in (A) were analyzed by double immunofluorescence using antibodies to HA and the ER-resident protein BiP. From left to right are shown fluorescence images corresponding to BiP (green), Ero1p-HA$_3$ (red), or an overlay of the two.

(C) RNA samples were prepared from the JC103 strain (WT) and an isogenic UPR defective strain (ire1Δ) that, where indicated, had been induced for the UPR by DTT treatment. The samples were subjected to northern blot analysis using *ERO1* and *ACT1* probes. The results from the *ERO1* probe are shown and the intensity of the *ERO1* band, normalized relative to that of *ACT1*, is indicated below.

A

EndoH — —   — +
DTT — +   + +

← Ero1p-(HA)₃ →

B

BiP   Ero1p-(HA)₃   OVERLAY

C

WT   ire1Δ

DTT   −   +   −   +

ERO1 —

Normalized
Intensity   1   8.7   1.6   1.3

71
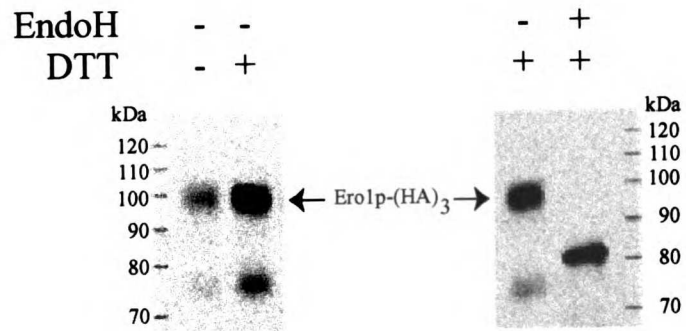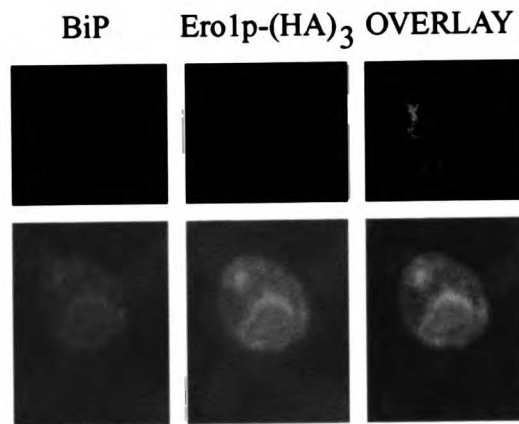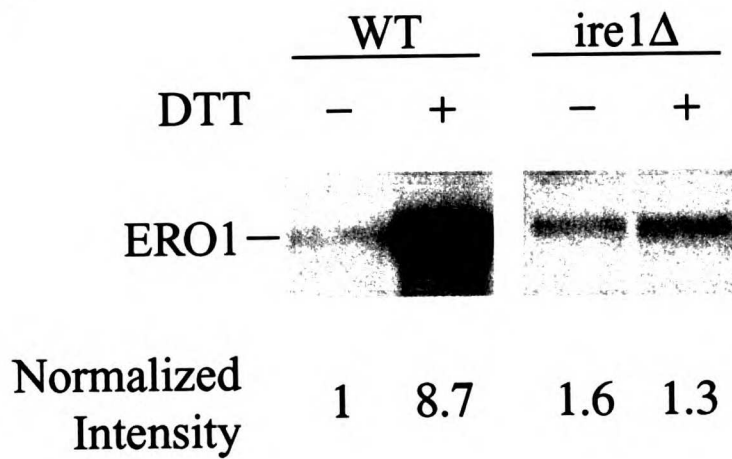
Figure 5. Defective Folding of Disulfide-Containing Proteins in an *ero1* Strain

The effects of *ero1* on the folding of CPY are analyzed in **A-D**. The parental DBY2063 (WT) and YJW150 (ero1) strains were ^{35}S radio-labeled for 20 min in the presence of either 5 mM DTT **(A, B)** or 1 mM DTT **(C, D)**. Labeling was stopped and folding allowed to proceed for a defined period of time either in the absence of DTT **(A, B)** or the continued presence of 1 mM DTT **(C, D)**. At the indicated times, CPY folding was analyzed by immunoprecipitation and SDS-PAGE under reducing **(A, C)** or nonreducing **(B, D)** conditions. The large fraction of mCPY in the 0 min timepoint of the WT sample in (C) results from folding of CPY during the 20 min labeling. The samples designated ox p1CPY and red p1CPY are the native and reduced ER forms of CPY, respectively. The positions of the ER (p1CPY), Golgi (p2CPY), and mature vacuolar (mCPY) forms are indicated.

(E) Parental YJW172 (WT) and YJW171 (ero1) strains, which each contain an integrated *Kpn-bla* reporter, were grown to early log phase. Cultures were treated with either 0 mM DTT, the continuous presence of 1 mM DTT, or a 5 mM DTT pulse as indicated, and Kpn-bla expression was induced. The total level of β-lactamase activity after 90 minutes of induction is shown relative to that seen in the 0 mM DTT WT sample.

A

WT   ero1

time (min)   0   15   30   60   0   7.5   15   22.5   30   60

p2CPY →
p1CPY →
mCPY →

B

WT   ero1   ox-   red-
                        p1CPY   p1CPY

time (min)   0   15   30   60   0   10   20   30

p1CPY →
mCPY →

C

WT   ero1

time (min)   0   10   20   30   0   10   20   30

p1CPY →
mCPY →

D

ero1   ox-   red-
                p1CPY   p1CPY

time (min)   0   10   20   30

red p1CPY →
ox p1CPY →

E

73
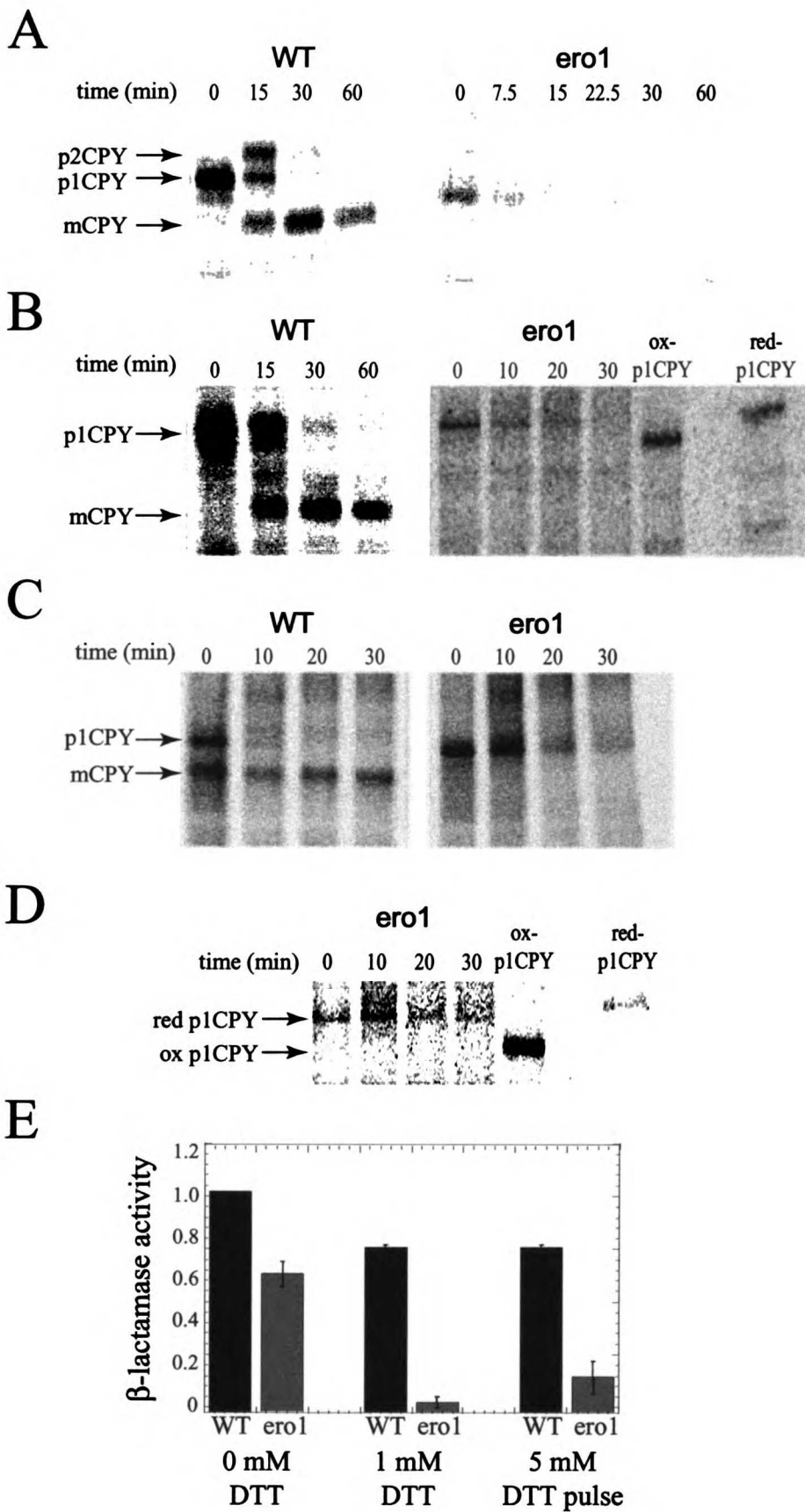
Figure 6. Invertase Folding and Secretion are not affected by the *ero1* Mutation

(A) Invertase was accumulated in the ER of the *sec18* (H393) and the *sec18*; *ero1* double mutant (YJW170) strains by incubation at 37°C in low glucose YPD. At 50 min, the samples were split into two portions either receiving (dashed lines) or not receiving (solid lines) 1 mM DTT and protein synthesis was inhibited with cycloheximide. At 60 min, secretion was initiated by shift to 25°C. Shown is the external (open symbols) and internal (filled symbols) invertase activity as a function of time. The ~4-fold greater total invertase activity in the *sec18* strain as compared to *sec18*; *ero1* is predominantly a consequence of the H393 strain background and not the *ero1* mutation (see B).

(B) The YJW150 (ero1) and parental DBY2063 (WT) strains were treated as indicated: 0 mM DTT, continuous 1 mM DTT during the entire time course, or 5 mM DTT for 20 min prior to induction of invertase. Shown is total invertase activity (external plus internal) as a function of time after initiating induction.
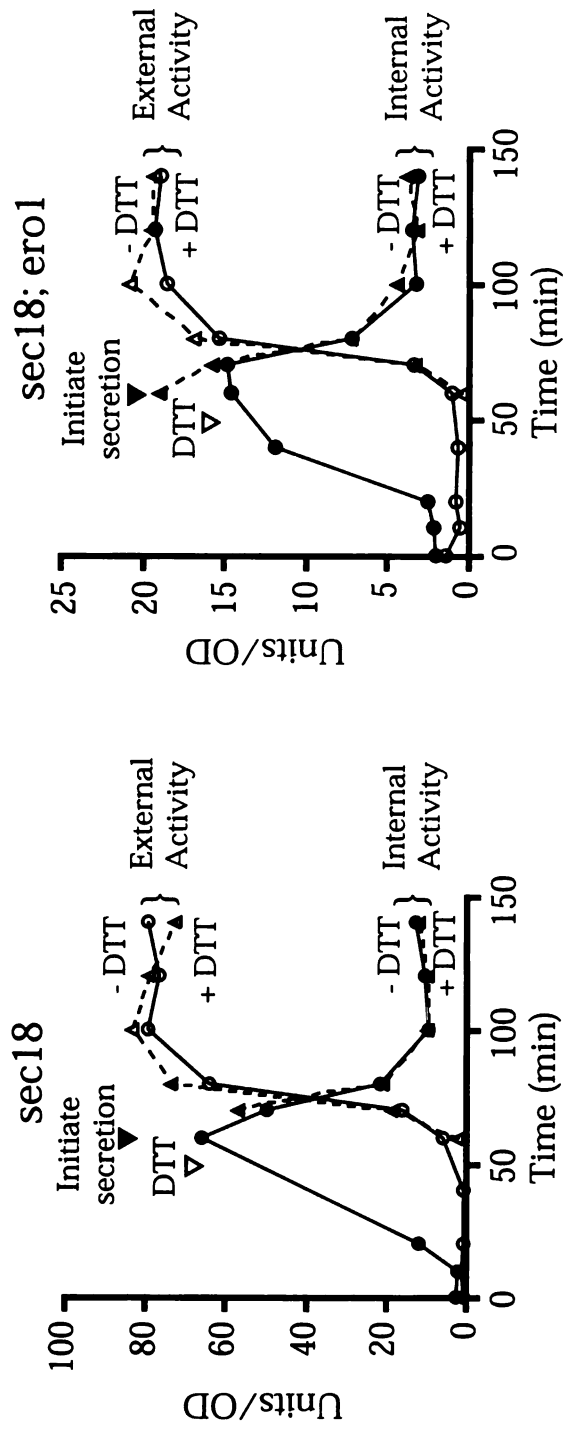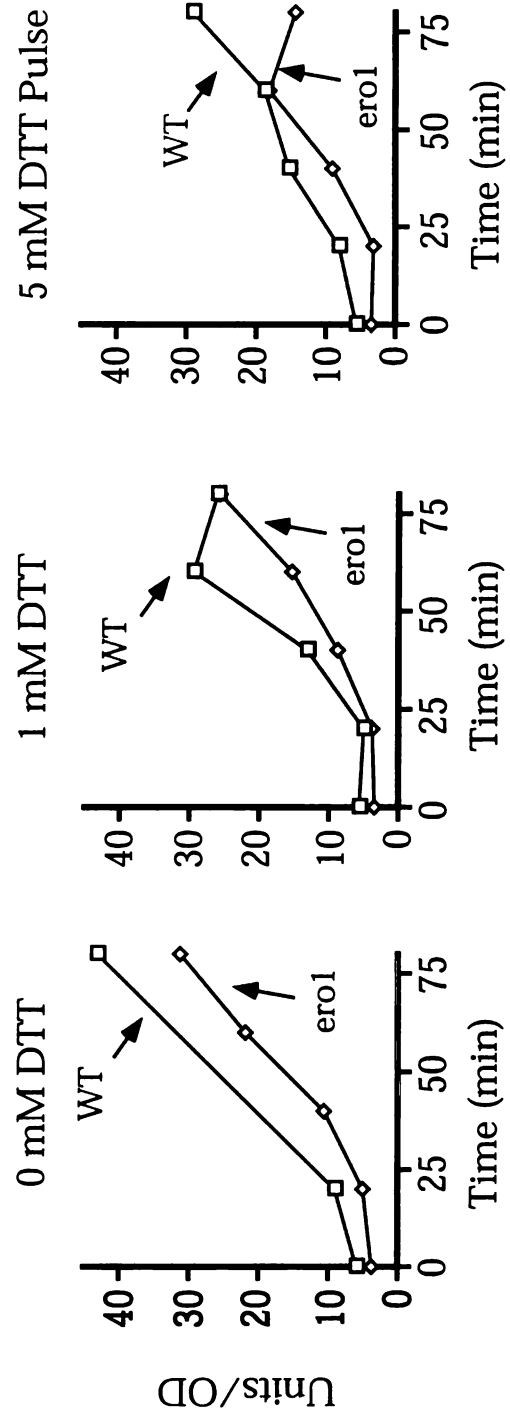
Figure 7. Schematic Model Comparing Bacterial and ER Protein-oxidation

Machinery

In the bacterial periplasm (for review see Missiakas and Raina, 1997) oxidized

DsbA acts directly to oxidize protein (P) disulfide bonds by a thiol-disulfide

exchange reaction, generating reduced DsbA. The transmembrane protein DsbB

is then thought to regenerate oxidized DsbA by a second thiol-disulfide exchange

step. In the eukaryotic ER, PDI and its homologs, which like DsbA have a

thioredoxin-like active site, are thought to act as the direct oxidant of folding

proteins. The phenotype of the *ero1* mutant most closely resembles that of the

dsbB mutants in bacteria (see text), although it is not known if Ero1p is acting

directly as an oxidant of reduced PDI.
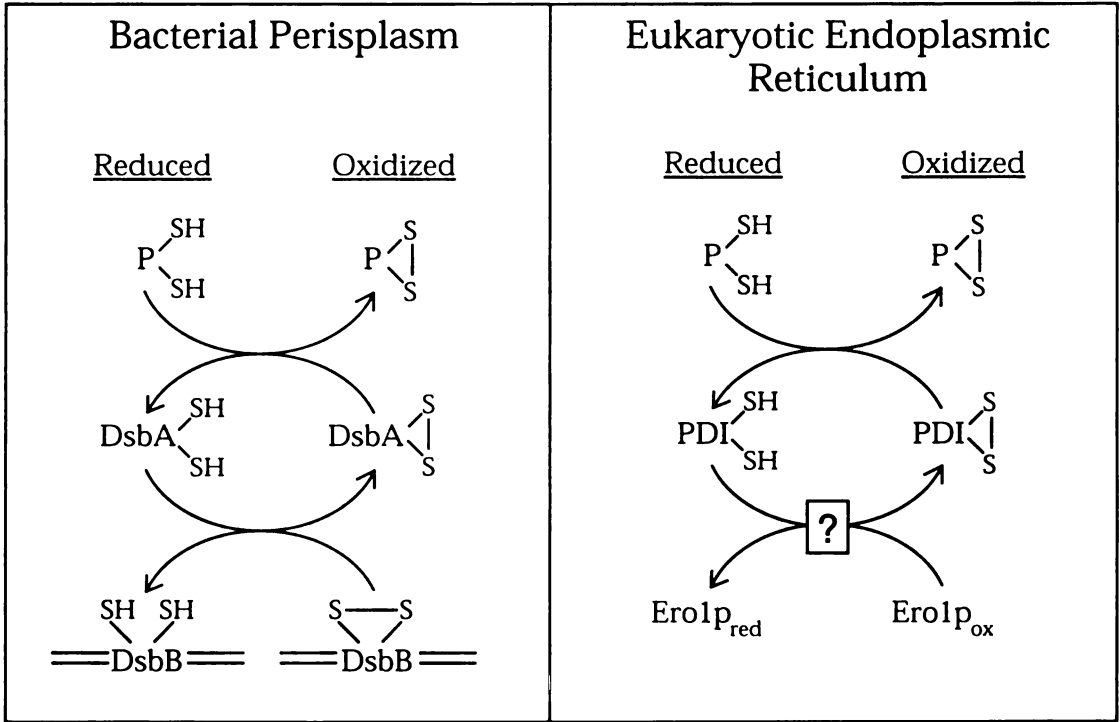
Chapter 3

Biochemical Basis of Oxidative Protein

Folding in the Endoplasmic Reticulum

Biochemical Basis of Oxidative Protein Folding in the Endoplasmic Reticulum

Benjamin P. Tu*, Siew C. Ho-Schleyer*, Kevin J. Travers, and

Jonathan S. Weissman[†]

Howard Hughes Medical Institute
Department of Cellular and Molecular Pharmacology
University of California-San Francisco
San Francisco, California 94143-0450
* These authors contributed equally to this work
[†] To whom correspondence should be addressed
E-mail: jsw1@itsa.ucsf.edu

Abstract

The endoplasmic reticulum (ER) supports disulfide bond formation by a poorly understood mechanism requiring protein disulfide isomerase (PDI) and Ero1p. In yeast, Ero1p-mediated oxidative folding was shown to depend on cellular flavin adenine dinucleotide (FAD) levels but not on ubiquinone or heme, and Ero1p was shown to be an FAD-binding protein. We reconstituted efficient oxidative folding *in vitro* using FAD, PDI and Ero1p. Disulfide formation proceeded by direct delivery of oxidizing equivalents from Ero1p to folding substrates via PDI. This kinetic shuttling of oxidizing equivalents could allow the ER to support rapid disulfide formation while maintaining the ability to reduce and rearrange incorrect disulfide bonds.

Introduction

Proteins that traverse the secretory pathway are typically stabilized by one or more disulfide bonds. To support efficient disulfide formation, cells actively promote oxidation in the two compartments where disulfide-linked folding commonly occurs: the eukaryotic ER (Frand et al., 2000) and the bacterial periplasm (Rietsch and Beckwith, 1998). In bacteria, an electron transport pathway links disulfide bond formation to the respiratory chain (Bader et al., 1999; Kobayashi et al., 1997). The integral membrane protein DsbB oxidizes the CxxC active site of the PDI homolog DsbA, which then catalyzes disulfide formation in folding proteins. DsbB is reoxidized by ubiquinone produced during respiration.

Over the past few decades, a number of factors have been suggested to contribute to disulfide formation in the ER, including secretion of reduced thiols, uptake of oxidized thiols, and a variety of redox enzymes and small molecule oxidants (Frand et al., 2000; Hwang et al., 1992; Ziegler and Poulsen, 1977). The physiological importance of any of these to disulfide formation has not been established. Genetic studies in *Saccharomyces cerevisiae* have identified an essential and conserved ER-resident protein, Ero1p (Frand and Kaiser, 1998; Pollard et al., 1998), loss of which results in the accumulation of reduced PDI and the cessation of disulfide bond formation, a phenotype resembling that of loss of DsbB in bacteria (Bardwell et al., 1993). Ero1p, however, has no apparent homology to DsbB or any other redox enzymes. Thus whether oxidative folding

occurs by a similar biochemical mechanism in eukaryotes and bacteria, or even if Ero1p can catalyze redox reactions, is not known.

To define the requirements for oxidative folding in the ER, we used reverse genetics in *S. cerevisiae* to eliminate components of the cellular redox machinery and examined the effects on disulfide-linked folding. We monitored disulfide formation by pulsing cells with the reductant dithiothreitol (DTT) and following the rate and efficiency of folding of newly synthesized carboxypeptidase Y (CPY), which contains five disulfide bonds required for folding and ER export (Stevens et al., 1982). Deletion of *COQ5* or *HEM1*, which blocks biosynthesis of ubiquinone (Barkovich et al., 1997; Poon et al., 1997) or heme (Astin and Haslam, 1977), respectively, inhibited respiration and ER-associated cytochromes, but did not alter the kinetics of CPY folding (Figure 1A). Depletion of Nfs1p, an essential protein required for iron-sulfur (Fe-S) cluster assembly (Kispal et al., 1999), also had little effect on CPY folding (Figure 1A). Moreover, under depletion conditions where the activities of known Fe-S cluster proteins are abolished (Kispal et al., 1999), the kinetics of Ero1p reoxidation were comparable to those of a wildtype strain (Figure 1B).

Finally, several lines of evidence indicate that the oxidation activity of Ero1p is not dependent on molecular oxygen. First, PDI, whose oxidation *in vivo* is dependent on Ero1p function, persisted in a predominantly oxidized state even when yeast were grown in anaerobic conditions (Figure 5). Second, in both the

presence (Pollard et al., 1998) and absence of oxygen, *ero1-2* mutant yeast were highly sensitive to DTT (Figure 6), and the *ero1-1* strain remained temperature-sensitive (B. P. Tu, S. C. Ho-Schleyer, K. J. Travers, J. S. Weissman, unpublished data). This suggested that Ero1p function was required for viability even in the absence of oxygen. Finally, preliminary experiments *in vitro* indicated that purified Ero1p could catalyze the oxidation of RNase A in an FAD-dependent reaction in the absence of oxygen (B. P. Tu, S. C. Ho-Schleyer, K. J. Travers, J. S. Weissman, unpublished data). In summary, Fe-S clusters, molecular oxygen, ubiquinone, and hemes are not required for Ero1p-mediated oxidative folding.

We then investigated the role of riboflavin and its metabolic derivatives (flavin mononucleotide [FMN] and FAD) in oxidative folding using a strain lacking the *RIB5* gene, which is required for riboflavin biosynthesis. Depletion of riboflavin from the growth media inhibited CPY folding in a Δ*rib5* strain (Figure 1A) and caused PDI (B. P. Tu, S. C. Ho-Schleyer, K. J. Travers, and J. S. Weissman, unpublished data) and Ero1p to accumulate in a reduced form even in the absence of DTT (Figure 1B). Depletion of riboflavin also results in loss of FMN and FAD, which are derived from the sequential activities of Fmn1p and Fad1p, respectively (Wu et al., 1995). To determine whether these components are important for Ero1p-mediated folding, we examined the effect of overexpression of *FMN1* or *FAD1* on a strain containing a temperature-sensitive allele of *ERO1* (*ero1-1*; Frand and Kaiser, 1998). Overexpression of *FMN1* led to

a modest enhancement of *ero1-1* viability, whereas overexpression of *FAD1* strongly suppressed the *ero1-1* temperature-sensitive phenotype (Figure 1C).

In principle, the sensitivity of oxidative folding to cellular FAD levels could result from an indirect effect, such as altering the cytosolic redox potential, rather than a specific requirement for FAD in the ER. We addressed this possibility by examining the effect of FAD on the *in vitro* reoxidation of endogenous PDI in microsomes produced from either wildtype or *ero1-1* strains (Figure 1D). The addition of FAD to wildtype microsomes greatly accelerated both the rate and yield of PDI reoxidation following DTT treatment, strongly arguing for a direct role of FAD in disulfide bond formation. Importantly, PDI oxidation depended on Ero1p function, as microsomes isolated from an *ero1-1* strain showed markedly slower PDI reoxidation in the presence of FAD.

Addition of GSSG to mammalian microsomes has previously been reported to re-oxidize substrates contained within the microsomes (Marquardt et al., 1993). Similarly, GSSG added to microsomes isolated from yeast supports reoxidation of PDI (Figure 7). However, performing a similar experiment in microsomes deficient in functional Ero1p reveals that the observed PDI reoxidation is independent of Ero1p activity. *In vivo*, reoxidation of PDI and folding proteins is both Ero1p-dependent and glutathione-independent (Cuozzo and Kaiser, 1999), making the physiological significance of oxidation by GSSG unclear. Taken together, our results indicated that Ero1p-mediated oxidative

folding is exquisitely sensitive to cellular FAD levels, and not other small molecules.

To directly assess the biochemical mechanism of oxidative folding, we developed an affinity-based purification which yielded highly purified polyoma epitope-tagged Ero1p (Ero1p-Py$_2$) from yeast microsomes (Figure 2A). Further purification of Ero1p-Py$_2$ using α-polyoma resin did not alter its activities in subsequent analyses, arguing that our Ero1p preparations contained no functional contaminants (B. P. Tu, S. C. Ho-Schleyer, K. J. Travers, and J. S. Weissman, unpublished data). Purified Ero1p displayed a distinct absorbance peak at 450 nm (B. P. Tu, S. C. Ho-Schleyer, K. J. Travers, and J. S. Weissman, unpublished data). Reverse-phase HPLC analysis of denatured Ero1p revealed a single fluorescence peak that co-eluted with an FAD standard (Figure 2B). Thus Ero1p itself is a flavoprotein that contains non-covalently bound FAD. Furthermore, Ero1p purified from yeast microsomes that were treated with Proteinase K in the absence of detergent remained active and still retained bound FAD, suggesting the existence of a mechanism for transporting FAD into the ER lumen (also see Figure 1D).

We next asked whether Ero1p could act as an oxidase *in vitro* by monitoring its activity on a well-characterized folding substrate, ribonuclease A (RNase A), which contains four disulfides necessary for its folding and activity (Lyles and Gilbert, 1991). In the presence of supplemental FAD and PDI,

catalytic amounts of Ero1p rapidly promoted reactivation of reduced RNase A (Figure 3A). SDS-PAGE analysis directly demonstrated that the reactivation of RNase A resulted from Ero1p-mediated reoxidation of its four disulfide bonds (Figure 3B). The observed refolding of RNase A was completely dependent on Ero1p, PDI, and supplemental FAD, but did not require reduced (GSH) or oxidized (GSSG) glutathione, and was not affected by pyridine nucleotide cofactors (e.g., NAD+, NADPH) (Figure 8). There was also a strong preference for FAD over FMN (Figure 9), in agreement with *in vivo* observations (Figure 1C). Increasing concentrations of Ero1p enhanced the rate of RNase A oxidative refolding (Figure 3A). Even at a stoichiometry of one Ero1p molecule per 340 RNase A disulfide bonds, refolding proceeded at a rate that was significantly faster than the refolding of RNase A in the presence of PDI and an optimal glutathione redox buffer (Figure 3A). Furthermore, an Ero1p mutant that is non-functional *in vivo* (B. P. Tu, S. C. Ho-Schleyer, K. J. Travers, and J. S. Weissman, unpublished data; Cabibbo et al., 2000) could not catalyze reoxidation of RNase A (Figure 3A, 3B). Thus Ero1p is an efficient oxidase that catalyzes *de novo* disulfide bond formation via an FAD-dependent mechanism.

In the absence of PDI, folding substrates remained reduced *in vitro* (Figure 3A, 3B) and *in vivo* (Frand and Kaiser, 1999) even with Ero1p present, suggesting that PDI acts as an intermediary in the disulfide formation process by transferring oxidizing equivalents derived from Ero1p to folding substrates. We examined whether a mutant PDI in which the second cysteine of both active sites

is changed to alanine [PDI (CxxA)$_2$] could support Ero1p-mediated oxidative refolding of RNase A. This mutant PDI retains disulfide isomerase activity but cannot function as an oxidase (Laboissiere et al., 1995). Consistent with PDI acting as an oxidant, PDI (CxxA)$_2$ did not support RNase A refolding (Figure 4A). Surprisingly, PDI (CxxA)$_2$ was a dominant inhibitor of Ero1p-dependent oxidative folding, as inclusion of equimolar amounts of PDI (CxxA)$_2$ with wildtype PDI resulted in a severe reduction of RNase A reactivation (Figure 4A). SDS-PAGE analysis revealed a disulfide crosslink between PDI (CxxA)$_2$ and Ero1p (Figure 4B), suggesting that inhibition of refolding by PDI (CxxA)$_2$ resulted from sequestration of Ero1p via a disulfide crosslink between the two proteins. A similar crosslink is observed *in vivo* when both Ero1p and a mutant PDI are overexpressed, albeit at much lower efficiency (Frand and Kaiser, 1999). Thus, a disulfide crosslink between PDI and Ero1p is likely to be an obligatory intermediate during the oxidation of the PDI active sites by Ero1p.

What is the role of glutathione in oxidative protein folding in the ER? Oxidized glutathione, produced as a consequence of Ero1p activity (Cuozzo and Kaiser, 1999), could contribute to protein oxidation. However, we found that Ero1p had no detectable activity as a direct oxidase of GSH to GSSG (B. P. Tu, S. C. Ho-Schleyer, K. J. Travers, and J. S. Weissman, unpublished data). Also, Ero1p-dependent folding of RNase A did not require glutathione. Furthermore, PDI, one of the most abundant proteins in the ER, is present at concentrations comparable to that of GSSG (Gilbert, 1990), and is a far better oxidant of

proteins than is GSSG (see, for example, Weissman and Kim, 1993). We have also demonstrated that oxidized PDI, at a 50-fold lower concentration than GSSG, oxidized RNase A at least 8-fold faster than GSSG (Figure 10). Given these considerations and that Ero1p-catalyzed oxidation *in vivo* (Cuozzo and Kaiser, 1999) and *in vitro* can occur independent of glutathione (Figure 3), the predominant pathway for flow of oxidizing equivalents in the ER is likely to be a protein-based relay from Ero1p to PDI and then directly to substrate proteins.

Consistent with this idea, Ero1p could efficiently drive oxidation of RNase A in the presence of a large excess of reducing agent (1 or 2 mM GSH, Figure 4C). During refolding, we then observed a gradual production of GSSG, suggesting that glutathione is not oxidized directly by Ero1p, but rather by reduction of Ero1p-derived disulfide bonds in PDI and/or substrates. Nonetheless, the glutathione buffer remained strongly reducing (e.g., at 20 min, GSH:GSSG ≈ 40:1) throughout the course of RNase A oxidation. These conditions were comparable to the reducing environment of the cytosol (Hwang et al., 1992), where PDI at equilibrium should be largely reduced (Lundström and Holmgren, 1993). Despite this, Ero1p- and PDI-driven oxidation of RNase A proceeded rapidly (within roughly a factor of two of the rate of oxidation without GSH) and PDI remained oxidized (B. P. Tu, S. C. Ho-Schleyer, K. J. Travers, and J. S. Weissman, unpublished data).

In summary, Ero1p is an FAD-dependent oxidase of PDI responsible for sustaining disulfide-linked protein folding in the ER. The FAD dependence of Ero1p is unexpected as Ero1p contains no known flavin-binding motifs, and DsbB, which plays an analogous role to Ero1p in the bacterial periplasm, uses ubiquinone as the proximal oxidant in a flavin-independent reaction (Bader et al., 1999). Furthermore, unlike many microsome-associated flavoproteins, which face the cytosol, protease-protection by microsomal membranes suggest that Ero1p is localized within the ER lumen (Figure 11). Given the sensitivity of Ero1p-mediated oxidation to FAD levels, regulation of the amount of FAD available to Ero1p could play an important role in modulating oxidative folding in the ER.

While previous studies of disulfide bond formation in the ER often focused on the bulk redox potential of the organelle, we demonstrated that oxidizing equivalents are delivered directly from Ero1p to folding substrates via PDI, thereby allowing disulfide formation to occur rapidly even in a reducing environment. Accordingly, *in vivo* PDI is found predominantly in the oxidized form (Frand and Kaiser, 1999), contrary to predictions that the reduced form should be significantly populated if it were in equilibrium with the bulk ER redox buffer (Frand et al., 2000; Lundström and Holmgren, 1993). In order to support efficient disulfide-linked folding, the ER must simultaneously be able to rapidly add disulfide bonds to unfolded proteins and remove them from misfolded proteins. The shuttling of disulfide bonds through a protein relay, by largely

insulating the Ero1p-driven oxidase machinery from other redox systems, could help prevent Ero1p from interfering with the reduction or rearrangement of incorrect disulfides.

Experimental Procedures

Yeast strains and manipulations

All deletion strains were generated by replacing the entire open reading frame with the indicated auxotrophic marker using the Pringle method (Longtine et al., 1998). The *Gal-NFS1* strain was kindly provided by Dr. Roland Lill (Kispal et al., 1999). Unless otherwise indicated, all strains were grown in synthetic defined media (SD) which lacks ubiquinone, heme and their immediate precursors (Guthrie and Fink, 1991). The Δ*hem1* strain was grown in the presence of 1% (v/v) Tween-80 and 20 mg/L ergosterol (Gollub et al., 1977). The growth medium for the Δ*rib5* strain contained 20 mg/L riboflavin (Santos et al., 1995).

Because *NFS1* is essential, we used a strain in which *NFS1* was controlled by a repressible promoter and assayed CPY folding after 24 hours of growth under repressing conditions. Although no Nfs1p could be detected at this time point, the kinetics of CPY folding and export from the ER were only modestly decreased compared to a wildtype strain (Figure 1A). It is possible that this folding activity was due to residual Fe-S clusters. We could not examine CPY folding at later time points due to the lack of *de novo* protein synthesis. Instead, we followed the kinetics of reoxidation of the pre-existing pool of Ero1p following DTT treatment.

91

For the CPY assays shown in Figure 1A, the *Gal-NFS1* strain was grown under repressing conditions (2% glucose) for 24 hours and the Δ*rib5* strain was grown in the absence of riboflavin for 17 hours prior to labeling.

In Figure 1B, the *Gal-NFS1* strain was grown under repressing conditions for 40 hours and the Δ*rib5* strain was grown in the absence of riboflavin for 17 hours prior to analysis of the Ero1p oxidation state.

Strain and Plasmid Construction

To recover the *ero1-2* allele, plasmid pKT001 was gapped with BglII and then transformed into strain YJW150 (Pollard et al., 1998). The *HIS3* gene from pRS313 was then inserted 326 bp downstream of the *ERO1* stop codon in this gap-repaired plasmid using the Seamless Cloning kit (Stratagene), producing plasmid pKT017. The *ero1-1* allele was recovered by performing inverse PCR on pKT017 using oligonucleotides that excluded exactly the coding sequence of *ERO1*, and transforming the PCR product into strain CKY559 (Frand and Kaiser, 1998). The resulting gap-repaired plasmid (pKT029) then consisted of a pRS316 backbone containing *ero1-1* with *HIS3* 326 bp past the stop codon. pKT029 was then cut with BamHI and the resulting fragment transformed into W303-1B, replacing the wildtype *ERO1* locus with a cassette consisting of *ero1-1* and *HIS3*.

Plasmid pKT014, encoding an HA epitope-tagged Ero1p, was constructed by subcloning a ClaI fragment from pMP003 which contains the *ERO1* promoter

and the majority of the *ERO1* coding sequence, into the ClaI sites of pMP008 (Pollard et al., 1998).

Plasmid pKT026, which contains *ERO1* tagged at its 3' end with sequences encoding a double polyoma epitope (MEYMPMEMEYMPME) (Schneider et al., 1994), a TEV protease cleavage site (ENLYFQG), and two immunoglobulin G (IgG)-binding "z" domains derived from protein A (ERO1-Py$_2$-zz), all under the control of the native *ERO1* promoter, was generated as follows. Complementary oligonucleotides encoding the polyoma epitope flanked by an XbaI and a NotI restriction site were annealed and ligated at the XbaI and NotI sites of plasmid pKT014, resulting in the intermediate plasmid pKT025. The TEV protease site and zz-domain were generated by PCR amplification of the zz domain from plasmid pKSZZ (Kaffman et al., 1998) with a 5' oligonucleotide encoding the TEV protease cleavage sequence. This PCR product was ligated at the NotI and SacI sites of plasmid pKT025. This plasmid pKT026 could fully complement a Δ*ero1* strain.

Plasmid pBT005, which contains ERO1-Py$_2$-zz under the control of the inducible yeast *GAL1* promoter, was constructed as follows. ERO1-Py$_2$-zz was generated by PCR amplication from pKT026 and then subcloned into the BamHI and SacI sites of a pRS315-based backbone containing ~500 bp of upstream promoter sequence of the *GAL1* gene.

Plasmid pBT006 was constructed by subcloning the GAL1 promoter-ERO1-Py$_2$-zz fragment from pBT005 into the XhoI and SacI sites of pRS425.

Plasmid pBT008, containing the *ERO1* gene in which cysteine 352 is changed to alanine, but otherwise identical to pBT006, was constructed using Quikchange site-directed mutagenesis (Stratagene).

Plasmid pBT101, containing a His$_6$-tagged derivative of yeast *PDI1* under control of the T7 promoter, was constructed as follows. *PDI1* (residues 28-522) was PCR amplified from yeast genomic DNA and subcloned into the XmaI and XhoI sites of pBH4, a pET-19b-derived vector designed for overxpression of His$_6$-tagged proteins in *E. coli* (Hillier et al., 1999).

Plasmid pBT104, expressing PDI (CxxA)$_2$ where cysteine residues 64 and 409 are changed to alanine, but otherwise identical to pBT101, was constructed using site-directed mutagenesis (Stratagene).

The pGal-*FMN1* and pGal-*FAD1* plasmids were constructed by subcloning the PCR fragments corresponding to the coding region of *FMN1* or *FAD1* into the *Sal1-Not1* restriction sites of the pBT005 plasmid.

Microsome reoxidation

Microsomes were prepared as described (Brodsky et al., 1993) and resuspended in Buffer 88 containing 20 mM DTT for one hour, washed with Buffer 88 to remove DTT and resuspended in Buffer 88 in the presence or absence of 200 µM FAD. At the indicated times, aliquots were quenched with TCA to 10% (w/v). TCA precipitates were resuspended in 1% SDS, 50 mM Tris•Cl pH 7.5, 1 mM PMSF, containing 20 mM AMS, incubated at room temperature for 15 min, 37°C for 10 min, and boiled for 2 min prior to Endo H treatment and SDS-PAGE analysis.

Ero1p purification

Plasmid pBT006 or pBT008 was transformed into YJW169 for overexpression of Ero1p in yeast. This strain was grown and induced as described previously (Worland and Wang, 1989). Microsomes were then prepared from the harvested cell pellets as described (Brodsky et al., 1993). All steps hereafter were performed at 4°C unless otherwise noted. Microsomes were solubilized in 50 mM HEPES pH 7.5, 400 mM KOAc, 8 mM $Mg(OAc)_2$, 1 mM $CaCl_2$, 10% glycerol, 1 mM β-mercaptoethanol, 2% digitonin, 1 mM PMSF, 20 µM leupeptin for 1 h and then spun at 35,000 g for 12 min. The supernatant was collected and the pellet resolubilized and respun once again. The solubilized extract was then allowed to bind IgG sepharose (Pharmacia) for 1-2 h. The resin was then washed twice with 50 mM HEPES pH 7.5, 150 mM NaCl, 10% glycerol, 0.1% digitonin, 1 mM PMSF, 20 µM leupeptin, followed by a wash

with the same buffer but with 300 mM NaCl. The resin was then resuspended in 50 mM HEPES pH 7.5, 100 mM NaCl, and 0.1% digitonin. TEV protease (Gibco) was then added (~0.5 U/μg Ero1p) and allowed to cleave Ero1p-Py$_2$ from the resin at room temperature for 1-2 h. TEV protease (which is His$_6$-tagged) was then depleted by incubating in the presence of Ni-NTA agarose (Qiagen) at 4°C for 30 min.

Purification of Ero1p over α-polyoma resin

Ero1p-Py$_2$ from the IgG sepharose purification step was allowed to bind α-polyoma protein G sepharose in a buffer containing 50 mM HEPES pH 7.5, 100 mM NaCl, 10% glycerol, 0.1% digitonin, 1 mM PMSF for 2 h at 4°C. The α-polyoma resin was washed twice with the same buffer, followed by a wash with the same buffer but with 300 mM NaCl. Ero1p-Py$_2$ was eluted off the resin by incubation in 50 mM HEPES pH 7.5, 100 mM NaCl, 0.1% digitonin, 0.002% n-octyl-β-glucoside, and 100 μg/mL polyoma peptide (EYMPME) for 10 min at room temperature.

HPLC analysis of Ero1p-bound FAD

Approximately 2-3 μg of Ero1p was denatured in 6 M guanidinium hydrochloride, 20 mM Tris•Cl pH 7.8, and analyzed using reverse-phase HPLC. Samples were run through a μRPC ST 4.6/100 C2/C18 column (Pharmacia) using a methanol/acetic acid/t-butylammonium phosphate solvent system (Fahey

and Newton, 1987). Flavins were identified using a scanning fluorescence detector (ex. 450 nm, em. 520 nm, Waters model 474).

PDI purification from *E. coli*

Plasmid pBT101 or pBT104 was transformed into *E. coli* BL-21 for overexpression. Cells were induced with 0.4 mM IPTG at OD ≈ 0.3 for 2 h at 37°C, harvested, and resuspended in 50 mM Tris•Cl pH 7.9, 50 mM NaCl, 10% sucrose. All steps hereafter were performed at 4°C. Lysozyme (100 µg/mL) was added and the suspension incubated for 30 min on ice. DNase I (2 U) and MgCl$_2$ (5 mM) were then added. Cells were sonicated and then spun at 15,000 rpm for 20 min at 4°C. The supernatant was filtered through a 0.45 µ filter and then mixed with pre-equilibrated Ni-NTA agarose (Qiagen) for 1-2 h. The resin was washed with 10 column volumes of 50 mM Tris•Cl pH 7.9, 50 mM NaCl, 10% sucrose, 1 mM β-mercaptoethanol, 1 mM PMSF, 20 µM leupeptin, followed by 5 column volumes of 50 mM Tris•Cl pH 7.9, 300 mM NaCl, 10% glycerol, 20 mM imidazole, 1 mM β-mercaptoethanol, 1 mM PMSF, 20 µM leupeptin. The protein was eluted with the same buffer but with 100 mM imidazole. Imidazole was removed using a PD-10 gel filtration column (Pharmacia).

Ero1p refolding reactions

Oxidative refolding was initiated by addition of reduced RNase A (Lyles and Gilbert, 1991) to the indicated concentration of purified Ero1p, bacterially expressed PDI, and/or FAD (100 µM) in a buffer containing 18 mM cCMP, 0.1 M

Tris•OAc pH 8.0, 65 mM NaCl, 2 mM EDTA, and 0.005% digitonin. RNase A

activity (hydrolysis of cCMP) was followed by the rate of change of absorbance at

296 nm at 25°C (Lyles and Gilbert, 1991). The disulfide content of RNase A was

monitored in a similar buffer, but without cCMP. Samples were analyzed at the

indicated times by the addition of SDS-PAGE buffer and 10 mM AMS, incubation

for 30 min at room temperature, followed by non-reducing SDS-PAGE.

Formation of Ero1p-PDI complexes

Reduced PDI (WT) or PDI (CxxA)$_2$ (1.7 µM) was added to Ero1p (1.3 µM)

in a buffer containing 50 mM HEPES pH 7.5, 100 mM NaCl, 2 mM EDTA, and

0.05% digitonin. After 10 min at room temperature, free sulfhydryls were

quenched by addition of SDS-PAGE buffer and 10 mM N-ethylmaleimide for 1 h.

The sample was then divided into two and subjected to SDS-PAGE under

reducing or non-reducing conditions.

Acknowledgments

Table 1. Yeast Strains

Strain	Genotype	Source/Reference
W303-1A	*leu2-3, -112; his3-11, -15; trp1-1; ura3-1; ade2-1; can1-100*; MATa	(Cox et al., 1993)
W303-1B (WT)	same as W303-1A, except MATα	(Cox et al., 1993)
Gal-NFS1	same as W303-1B, except Δ*nfs1::LEU2/Gal-NFS1*	(Kispal et al., 1999)
YJW169	same as W303-1A, except Δ*ero1::TRP1* [pKT026]	This study
YJW193	same as W303-1A, except Δ*ero1::TRP1* [pKT014]	This study
YJW208	same as W303-1A, except Δ*ero1::HIS3/ero1-2*	This study
YJW594 (*ero1-1*)	same as W303-1B, except Δ*ero1::HIS3/ero1-1*	This study
YJW598 (Δ*coq5*)	same as W303-1B, except Δ*coq5::URA3, trp1-1::TRP1 UPRE-lacZ*	This study
YJW604 (Δ*hem1*)	same as W303-1B, except Δ*hem1::LEU2, trp1-1::TRP1 UPRE-lacZ*	This study
YJW696 (Δ*rib5*)	same as W303-1B, except Δ*rib5::TRP1*	This study

Figure 1. Oxidative protein folding is highly sensitive to cellular FAD levels

(A) Contribution of various cellular redox cofactors to oxidative folding of CPY. The indicated yeast strains were ^{35}S-methionine labeled for 7 minutes in the presence of 5 mM DTT, and then chased in the absence of DTT for the indicated times. CPY was immunoprecipitated from cell lysates and analyzed by SDS-PAGE and autoradiography (Horazdovsky and Emr, 1993). The ER form (p1) was chased to the Golgi (p2) and vacuolar mature (m) forms after DTT removal except in the $\Delta rib5$ strain. The $\Delta coq5\Delta hem1$ double mutant also did not show a defect in CPY maturation (B. P. Tu, S. C. Ho-Schleyer, K. J. Travers, and J. S. Weissman, unpublished data). For a complete description of yeast strains and plasmids in this study, see Table 1.

(B) Contribution of various cellular redox cofactors to Ero1p reoxidation. The indicated yeast strains expressing an HA epitope-tagged version of Ero1p (Pollard et al., 1998) were treated with 5 mM DTT for 30 minutes. After the indicated chase times in the absence of DTT, cells were lysed in the presence of 20 mM AMS (Frand and Kaiser, 1999) and subjected to non-reducing SDS-PAGE and western blot analysis using an α-HA antibody. The positions of oxidized and reduced Ero1p are indicated.

(C) Overexpression of *FAD1* suppresses the temperature-sensitivity of *ero1-1*. An *ero1-1* strain carrying a vector with no insert, or an insert encoding *FMN1* or

FAD1 regulated by the *GAL1* promoter (pGal-*FMN1* or pGal-*FAD1,* respectively), or an isogenic *ERO1* (WT) strain carrying an empty vector were spotted on media containing glucose at 25°C, glucose at 37°C, or galactose at 37°C.

(D) FAD induces reoxidation of PDI in microsomes. Microsomes from wildtype (WT) and *ero1-1* yeast were treated with DTT, and incubated in buffer lacking DTT with or without 200 μM FAD for the indicated times. Samples were then subjected to AMS modification, SDS-PAGE, and western blot analysis using an α-PDI antibody. Addition of GSSG also induced reoxidation of PDI but in an Ero1p-independent manner (see Figure 7).

A

	WT	*Gal-NFS1* (+Glu.)	Δ*coq5*	Δ*hem1*	Δ*rib5*
Chase (min)	0 10 30 60	0 10 30 60	0 10 30 60	0 10 30 60	0 10 30 60

p2 →
p1 →
m →

CPY

B

	WT	*Gal-NFS1* (+Glu.)	Δ*rib5*	Δ*rib5* + RIB
DTT	- +	- +	- +	- +
Chase (min)	0 2 5 15 30	0 2 5 15 30	0 2 5 15 30	0 30

red →
ox →

Ero1p

C

	WT	ero1-1	ero1-1[pGal-FAD1]	ero1-1[pGal-FMN1]
25° Glu				
37° Glu				
37° Gal				

D

WT

PDI_red →
PDI_ox →

Chase (min)	0 2 10 30	0 2 10 30
	Buffer	Buffer + FAD

ero1-1

PDI_red →
PDI_ox →

Chase (min)	0 2 10 30	0 2 10 30
	Buffer	Buffer + FAD

103

Figure 2. Ero1p is a flavoprotein

(A) SDS-PAGE analysis of purified Ero1p-Py$_2$ either before or after further purification on an α-polyoma column, with or without Endoglycosidase H treatment, as indicated. No significant differences in oxidase activity or flavin binding properties between the α-polyoma and non-α-polyoma purified protein were observed (B. P. Tu, S. C. Ho-Schleyer, K. J. Travers, and J. S. Weissman, unpublished data).

(B) Purified Ero1p contains non-covalently bound FAD. Purified Ero1p from (A) was denatured and analyzed by reverse-phase HPLC coupled to a scanning fluorescence detector. The stoichiometry of bound oxidized FAD to Ero1p varied between 1:4 and 1:2. A fraction of Ero1p may have been misfolded or incapable of binding FAD. For comparison, a chromatogram of standards containing riboflavin, FMN, and FAD is shown (bottom trace).

A

Endo H   -   -   +

90 —

60 —

Ero1p

←Endo H

α–Py purified

B

Fluorescence

Ero1p

RIB   FMN

FAD

Standards

Retention time
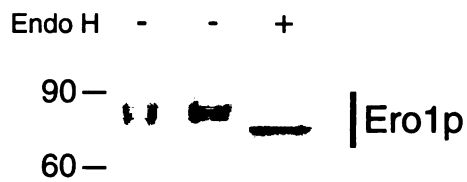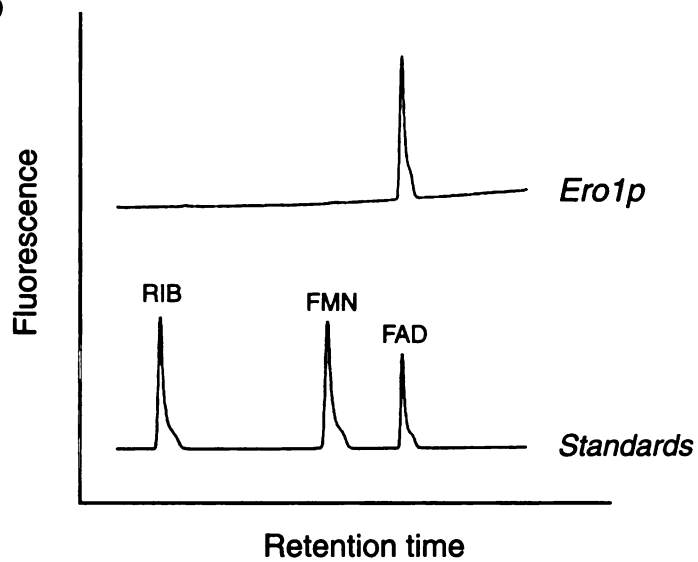
Figure 3. Ero1p is an FAD-dependent oxidase

(A) Reconstitution of oxidative protein folding *in vitro*. The conversion of reduced RNase A (15 µM) to its oxidized, active form in the presence or absence of the indicated concentrations of Ero1p, PDI (0.9 µM), and/or FAD (100 µM) was assayed by following hydrolysis of cCMP at 296 nm (Lyles and Gilbert, 1991). For comparison, the half-time of RNase A refolding in the presence of PDI and an optimal glutathione redox buffer (1 mM GSH, 0.2 mM GSSG) under the same conditions is ≈ 14 min. Ero1p (C352A) refers to a mutant Ero1p where Cys352 is changed to Ala.

(B) Direct observation of Ero1p-mediated catalysis of disulfide formation in RNase A. Refolding of reduced RNase A (15 µM) was followed in the absence or presence of Ero1p (0.36 µM), PDI (0.9 µM), and/or FAD (100 µM) as indicated, quenched at the indicated times with AMS, and analyzed by non-reducing SDS-PAGE.

A
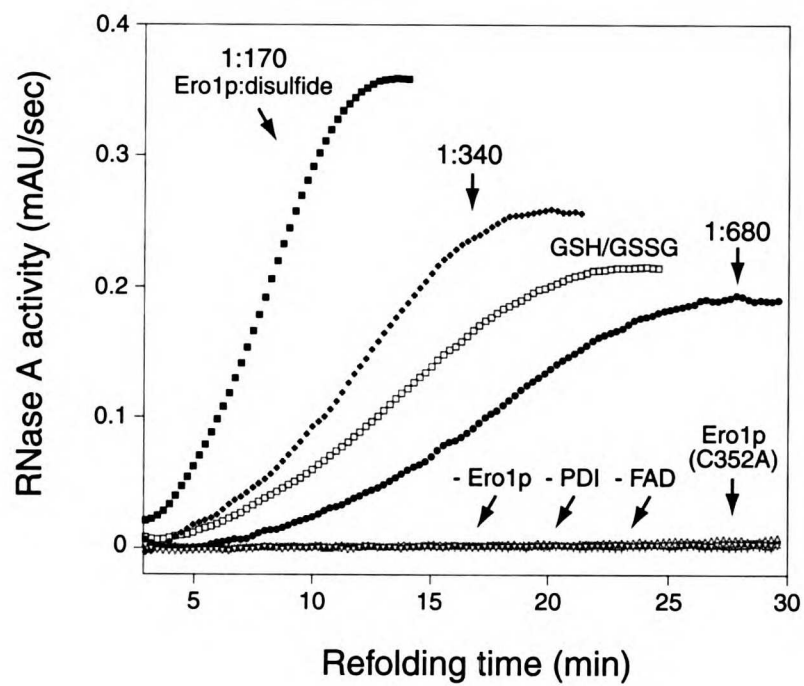
B
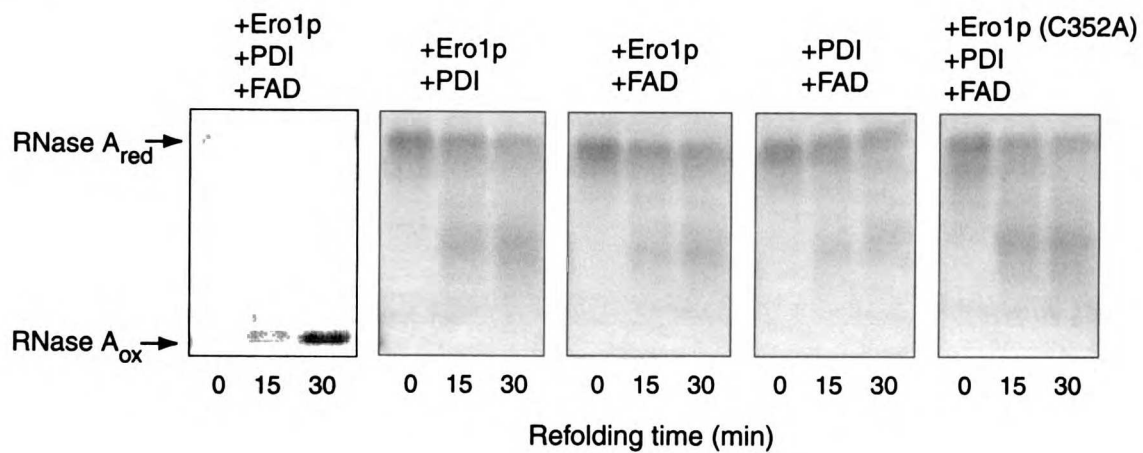
Figure 4. A protein cascade drives disulfide bond formation in the ER

(A) PDI (CxxA)$_2$ is a dominant inhibitor of Ero1p-dependent oxidative folding *in vitro*. Kinetics of oxidative refolding of RNase A (15 μM) in the presence of Ero1p (0.18 μM), FAD (100 μM), and WT PDI (0.9 μM), PDI (CxxA)$_2$ (0.9 μM) , or both.

(B) PDI (CxxA)$_2$ forms a disulfide crosslink with Ero1p. Following a brief incubation of Ero1p (1.3 μM) with either PDI (CxxA)$_2$ (1.7 μM) or WT PDI (1.7 μM), free cysteines were blocked and potential disulfides trapped with the addition of N-ethylmaleimide. Note the PDI-Ero1p disulfide crosslink (~200 kDa) in the sample containing Ero1p and PDI (CxxA)$_2$. Western blot analysis confirmed the presence of both PDI and Ero1p in this band (B. P. Tu, S. C. Ho-Schleyer, K. J. Travers, and J. S. Weissman, unpublished data). Below, schematic model of Ero1p-catalyzed oxidation of PDI. PDI first forms a mixed disulfide with Ero1p, which is resolved by nucleophilic attack of the second cysteine in the PDI active site, yielding oxidized PDI. When the second cysteine is not present, the PDI-Ero1p crosslinked species cannot be readily resolved.

(C) Ero1p can drive oxidative folding under reducing conditions. RNase A (15 μM) refolding was initiated in the presence of Ero1p (0.36 μM), PDI (0.9 μM), FAD (100 μM) and the indicated concentrations of reduced glutathione (GSH). At the specified times, disulfide content was monitored as described. The

observed GSH:GSSG ratio (Anderson, 1985) in the 2 mM GSH reactions at 10,

20, and 30 min was $\approx$ 120:1, 40:1 and 17:1, respectively.

A

B

PDI$_{SH}^{SH}$ + Ero1p$_{ox}$ → PDI$_{SH}^{S}$—Ero1p → PDI$_{S}^{S}$) + Ero1p$_{red}$

PDI$_{A}^{SH}$ + Ero1p$_{ox}$ → PDI$_{A}^{S}$—Ero1p ✗
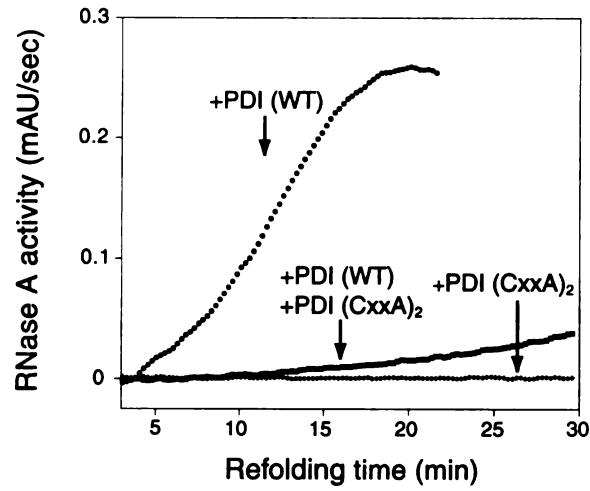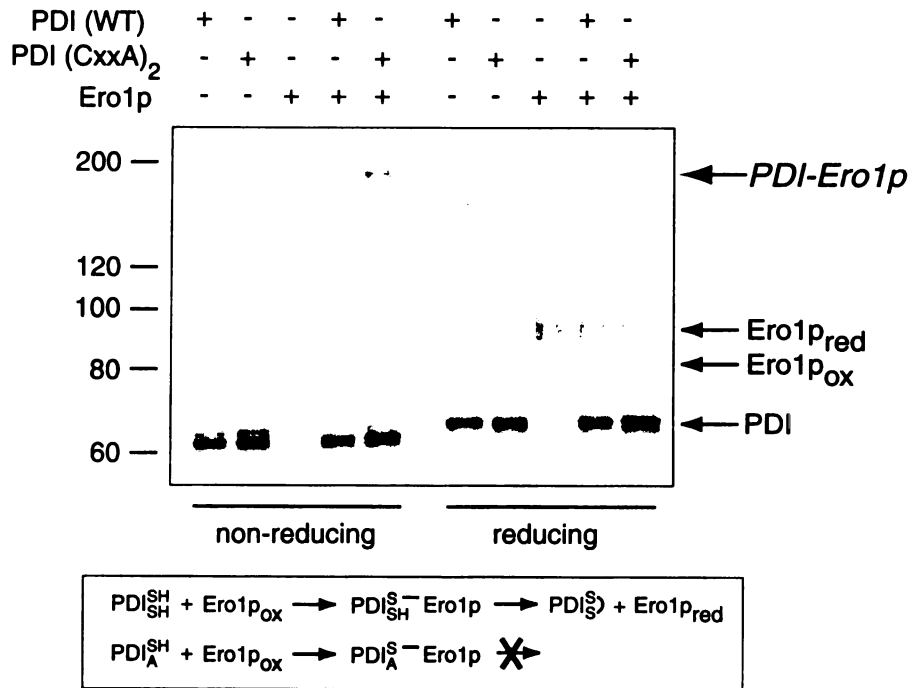
C
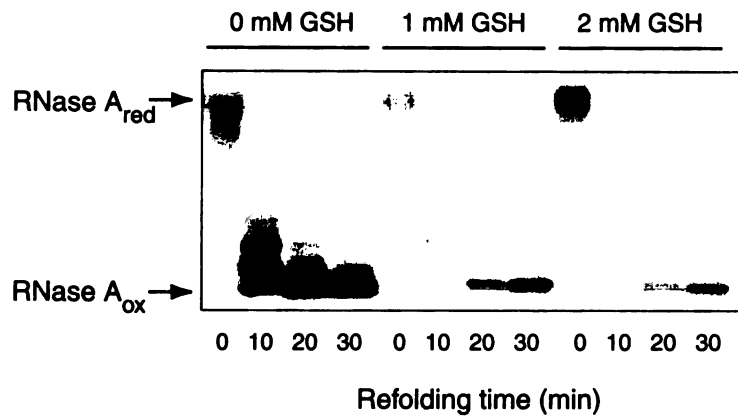
Figure 5. PDI is oxidized in yeast cells grown anaerobically

Synthetic complete media supplemented with 20 mg/L ergosterol and 1% (v/v) Tween-80 (Andreasen and Stier, 1953; Andreasen and Stier, 1954) was stirred overnight in a controlled atmosphere chamber (Plas Labs) filled with an anaerobic gas mixture (85% N_2, 5% CO_2, 10% H_2). The media was determined to be oxygen-free by measurement with a dissolved oxygen sensor (Corning). YJW193 was inoculated into the media and grown anaerobically to $OD_{600} \approx 1$. Cells were treated with TCA to a final concentration of 10% (w/v) and incubated on ice for 20 min in the controlled atmosphere chamber. The samples were then removed from the chamber, spun at 14,000 rpm and washed twice with acetone. Pellets were lysed in the presence of SDS and AMS as previously described (Frand and Kaiser, 1999). As a control, YJW193 grown aerobically was treated in a similar fashion, except an aliquot of cells was exposed to 10 mM DTT for 30 min prior to exposure to TCA. The AMS-treated lysates were subjected to SDS-PAGE and western blot analysis using an α-PDI antibody. The reduced (red) and oxidized (ox) forms of PDI are indicated with arrowheads.
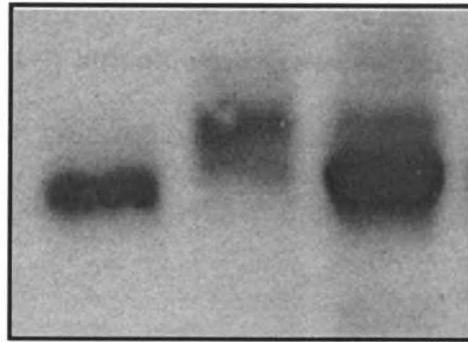
Figure 6. DTT resistance is dependent on functional Ero1p under anaerobic growth conditions

Wildtype and YJW208 (*ero1-2*) strains were grown on synthetic complete plates with or without DTT under anaerobic conditions at 30°C. Each successive column represents a tenfold dilution of cells from the previous column.

0 mM DTT   1 mM DTT

ero1-2

WT
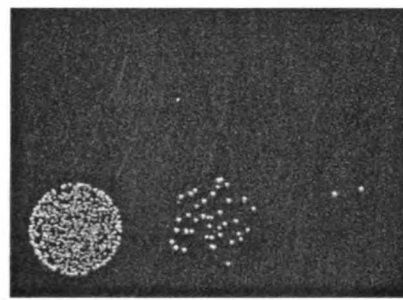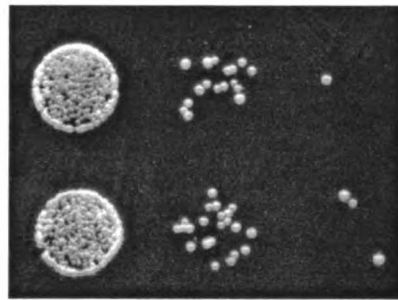
Figure 7. Addition of GSSG stimulates reoxidation of PDI independently of Ero1p activity

Microsomes were isolated from strains W303-1B and YJW594 (*ero1-1*) as described (Brodsky et al., 1993). Microsomes were treated with 20 mM DTT for 1 hour. Following removal of DTT, GSSG was added at a final concentration of 2 mM. At the indicated time points, aliquots were removed and quenched with 10% TCA. Pellets were resuspended in SDS buffer containing 20 mM AMS, treated with Endo H, and analyzed by SDS-PAGE. PDI was detected by western analysis using an α-PDI antibody.

WT   *ero1-1*

PDI$_{red}$ →

PDI$_{ox}$ →

0   2   10   30   0   2   10   30   Chase (min)

Buffer + GSSG   Buffer + GSSG

116
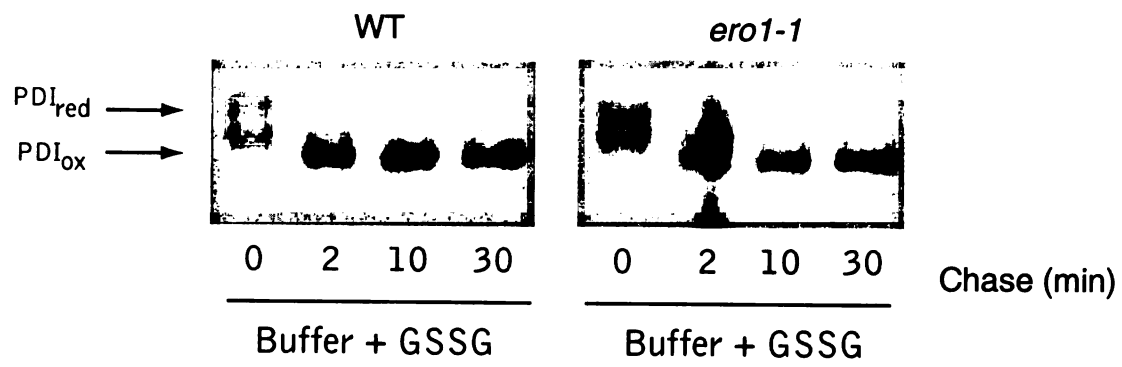
Figure 8. Ero1p specifically uses FAD as an oxidant

The oxidative refolding of reduced RNase A (12 μM) was assayed by following the hydrolysis of cCMP at 296 nm at 25°C (Lyles and Gilbert, 1991) in the presence of Ero1p (0.07 μM), PDI (0.9 μM), and either FAD (100 μM), NAD$^+$ (100 μM), NADP$^+$ (100 μM), or NADPH (100 μM) in a buffer containing 18 mM cCMP, 0.1 M Tris•OAc pH 8.0, 65 mM NaCl, 2 mM EDTA, and 0.005% digitonin. Note the specific requirement for FAD over these other cofactors during RNase A reoxidation catalyzed by Ero1p and PDI. These pyridine nucleotide cofactors also did not stimulate Ero1p activity in the presence of FAD (B. P. Tu, S. C. Ho-Schleyer, K. J. Travers, J. S. Weissman, unpublished data).
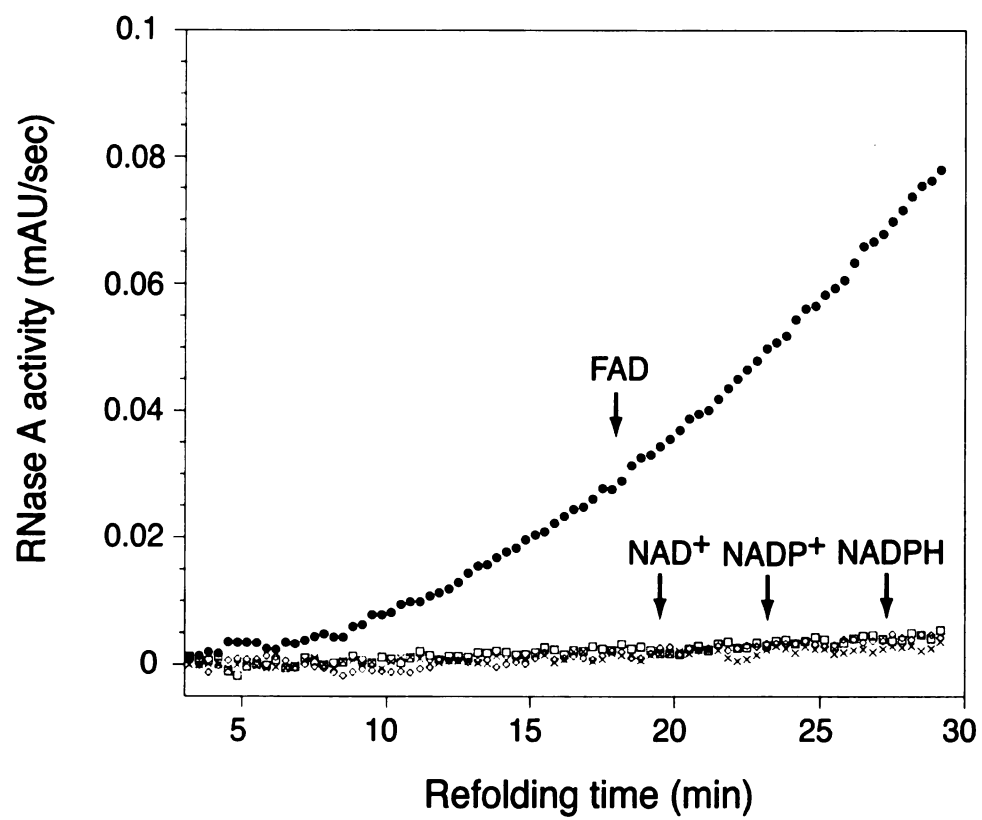
Figure 9. Ero1p shows a marked preference for FAD over FMN as an oxidant

RNase A refolding (11 μM) was assayed as in Figure 8 in the presence of Ero1p

(0.11 μM), PDI (0.9 μM), and either FAD (10 μM), FMN (10 μM), or no

supplemented flavins in a buffer containing 4.5 mM cCMP, 0.1 M Tris•OAc pH

8.0, 65 mM NaCl, 2 mM EDTA, and 0.005% digitonin. Note the preference for

FAD over FMN during RNase A reoxidation catalyzed by Ero1p and PDI.
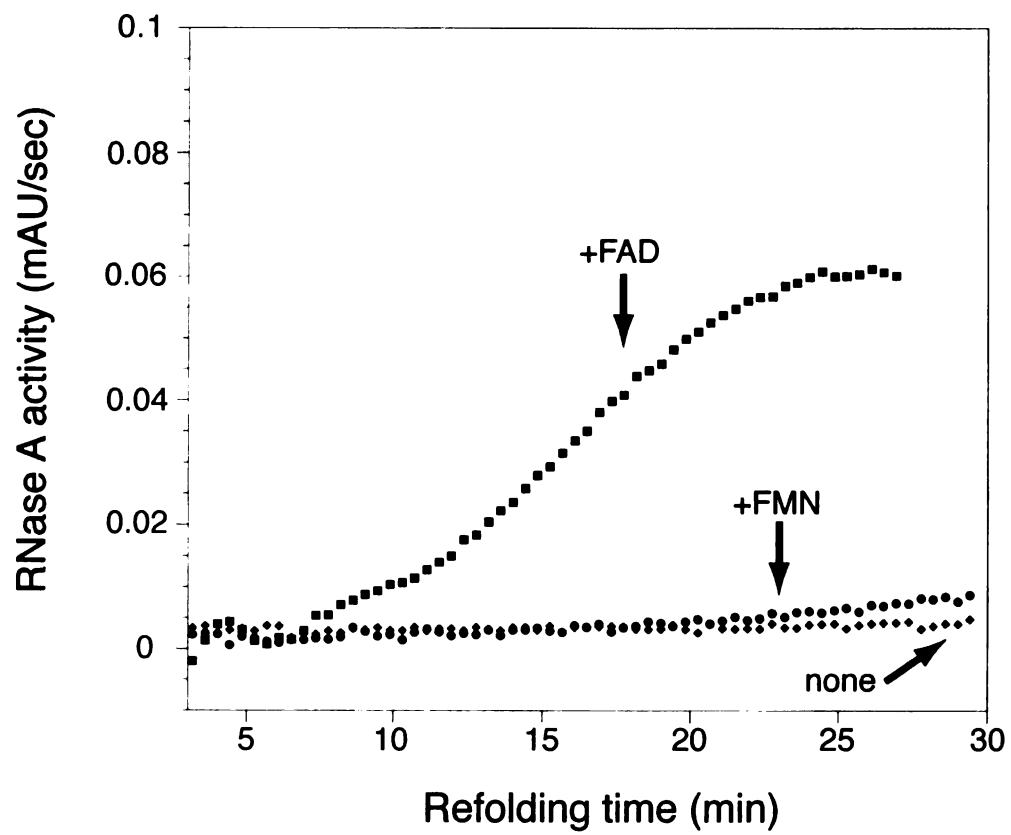
Figure 10. PDI is likely to be the predominant oxidant of proteins in the ER

Reduced RNase A (10 µM) was incubated with either GSSG (500 µM) or oxidized PDI (10 µM) in a buffer containing 50 mM Tris•Cl pH 7.3, 50 mM NaCl, 2 mM EDTA, quenched with 10 mM AMS in 1X SDS loading buffer at the indicated time points, and then analyzed using non-reducing SDS-PAGE. Oxidized PDI was prepared by incubation in the presence of 100 µM GSSG at 4°C for 30 min, followed by buffer exchange using a centrisep spin column (Princeton Separations). Note the rapid loss of the reduced form of RNase A within 15 seconds upon incubation with oxidized PDI. The PDI reaction stops short of complete RNase A oxidation because of depletion of oxidized PDI. A similar level of RNase A oxidation was achieved using a 50-fold higher concentration of GSSG as an oxidant, but after 120 seconds.

+GSSG   +PDI (ox.)

RNase A$_{red}$ →

0 15 45 120   0 15 45 120

oxidation time (s)
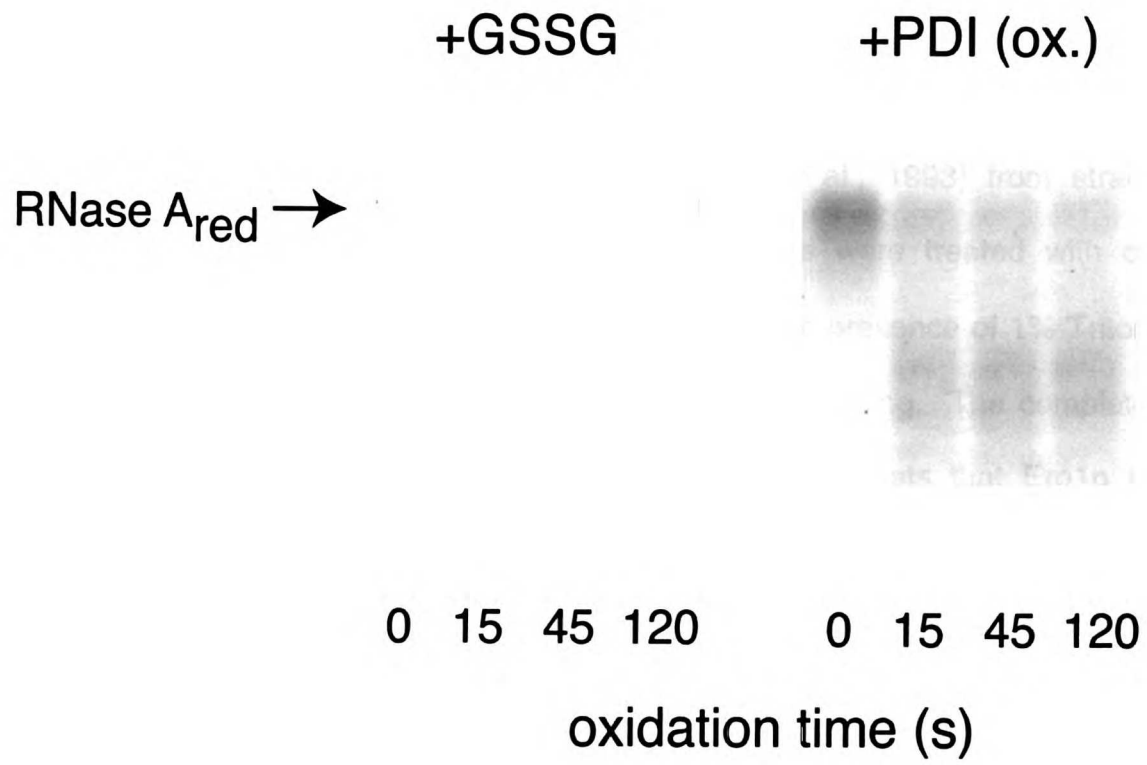
Figure 11. Ero1p is localized within the ER lumen

Microsomes were prepared as described (Brodsky et al., 1993) from strain W303-1B carrying plasmid pKT014. The microsomes were treated with or without Proteinase K at 10 μg/mL, and in the absence or presence of 1% Triton X-100, as indicated. Ero1p was visualized by western blotting. The complete protection against digestion provided by membranes suggests that Ero1p is entirely lumenal, with little or no protein extending beyond the membrane. This observation is consistent with the fact that Ero1p contains no apparent hydrophobic transmembrane domains.
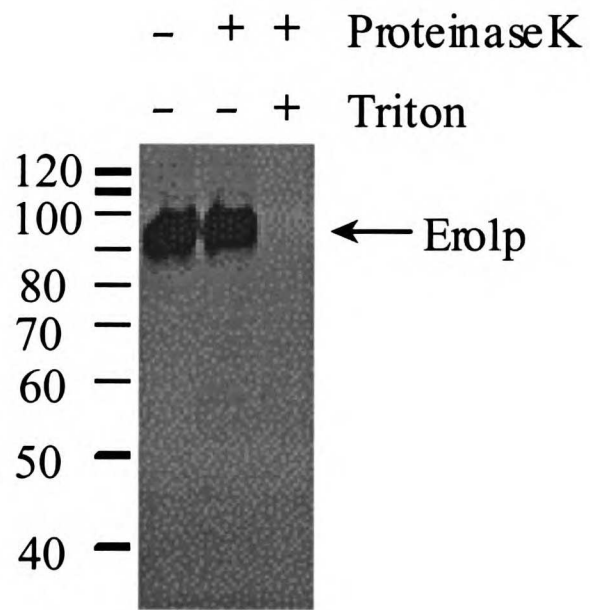
Chapter 4

Functional and Genomic Analyses Reveal Essential Coordination Between the Unfolded Protein Response and Endoplasmic Reticulum-associated Degradation

Functional and Genomic Analyses Reveal Essential Coordination Between the Unfolded Protein Response and Endoplasmic Reticulum-associated Degradation

Kevin J. Travers*[†], Christopher K. Patil*[‡], Lisa Wodicka[§], David J. Lockhart[§],
Jonathan S. Weissman[†#], and Peter Walter[‡#]

[‡]Howard Hughes Medical Institute
[†‡]Departments of Biochemistry and Biophysics, and [†]Cellular and Molecular
Pharmacology, University of California at San Francisco, San Francisco, CA
94143
[§]Affymetrix, Inc., 3380 Central Expressway, Santa Clara, CA 95051
[§]Present address: Genomics Institute of the Novartis Research Foundation
(GNF), 3115 Merryfield Row, San Diego, CA 92121

*These authors contributed equally to this work

#corresponding authors: jsw1@itsa.ucsf.edu, walter@cgl.ucsf.edu

Abstract

The unfolded protein response (UPR) regulates gene expression in response to stress in the endoplasmic reticulum (ER). We determined the transcriptional scope of the UPR using DNA microarrays. Rather than regulating only ER-resident chaperones and phospholipid biosynthesis, as anticipated from earlier work, the UPR affects multiple ER and secretory pathway functions. Studies of UPR targets engaged in ER-associated protein degradation (ERAD) reveal an intimate coordination between these responses: efficient ERAD requires an intact UPR, and UPR induction increases ERAD capacity. Conversely, loss of ERAD leads to constitutive UPR induction. Finally, simultaneous loss of ERAD and the UPR greatly decreases cell viability. Thus the UPR and ERAD are dynamic responses required for the coordinated disposal of misfolded proteins even in the absence of acute stress.

Introduction

Proteins entering the secretory pathway fold within the confines of the endoplasmic reticulum (ER). To support efficient folding, the ER maintains an environment enriched in chaperones, glycosylation enzymes, and oxidoreductases (for review, see Ellgaard et al., 1999). Despite this optimized environment, an inevitable consequence of the large flux of proteins through the ER is that the folding process occasionally fails, resulting in the production of irrevocably misfolded proteins. Two distinct processes have been described which help eukaryotic cells cope with this problem: ER-associated degradation (ERAD) and the unfolded protein response (UPR).

The ERAD system eliminates misfolded proteins via degradation in the cytosol (reviewed by Bonifacino and Weissman, 1998). Misfolded ER proteins are retrotranslocated across the ER membrane into the cytosol, where ubiquitin-conjugating enzymes target them for proteasomal degradation (Biederer et al., 1997; McCracken and Brodsky, 1996; Qu et al., 1996; Ward et al., 1995; Werner et al., 1996). ERAD requires a number of dedicated ER-resident factors, including the proteins Der1p, Der3p/Hrd1p, and Hrd3p (Bordallo et al., 1998; Hampton et al., 1996; Knop et al., 1996). ERAD substrates pass through the translocon as they exit the ER en route to the proteasome; hence, several components of the translocon and cytosolic degradation machinery are shared by ERAD and other cellular processes (Hiller et al., 1996; Pilon et al., 1997; Plemper et al., 1997; Wiertz et al., 1996b; Zhou and Schekman, 1999).

A second means of coping with unfolded ER proteins is the UPR (reviewed by Chapman et al., 1998). The accumulation of unfolded ER proteins activates the transmembrane kinase/nuclease Ire1p (Cox et al., 1993; Mori et al., 1993; Shamu and Walter, 1996), which initiates the nonconventional splicing of *HAC1* mRNA. This leads to production of Hac1p, a bZIP transcription factor (Cox and Walter, 1996; Mori et al., 1996; Sidrauski et al., 1996; Sidrauski and Walter, 1997), and ultimately transcriptional induction of UPR target genes. Regulation of gene expression by the UPR allows the cell to tolerate folding stress and presumably assists in correction of the insult that caused unfolded proteins to accumulate (Cox et al., 1993; Mori et al., 1993).

While the mechanism by which the UPR signal is transmitted from the ER to the nucleus is well characterized, it is less clear how this response corrects misfolding. Of the small number of UPR target genes identified thus far, most encode ER-resident chaperones, as might be expected for a response to the accumulation of unfolded proteins (Chapman et al., 1998). In addition, components of the phospholipid biosynthetic pathways are targets, suggesting a role for the UPR in maintenance and biogenesis of the ER membrane (Cox et al., 1997; Kagiwada et al., 1998). Identification of the complete set of UPR target genes thus promised to provide insight into the means by which the cell copes with folding stress and adjusts the capacity of protein folding in the ER according to need. Here, we have used genome-wide expression analysis in conjunction

with specific mutations to identify genes whose expression is specifically induced

by the UPR in the budding yeast *Saccharomyces cerevisiae*.

Results

Defining the targets of the UPR

We identified transcriptional targets of the UPR by monitoring mRNA levels using high-density oligonucleotide arrays (Wodicka et al., 1997). We induced the UPR by treating cells with two chemical agents that disrupt protein folding in the ER: the strong reducing agent dithiothreitol (DTT), which prevents disulfide bond formation, and the drug tunicamycin, which inhibits N-linked glycosylation. Neither of these agents is known to affect protein folding outside the secretory pathway. Furthermore, because these agents interfere with ER folding by different mechanisms, any gene regulation resulting from both treatments is likely to result from ER protein misfolding rather than nonspecific effects.

We prepared RNA samples for array hybridization from wildtype cells grown under five conditions: exposure to DTT for 15, 30, 60, or 120 minutes, or exposure to tunicamycin for 60 minutes. For each open reading frame (ORF), we determined the fold change in expression due to each drug treatment by comparing its expression level in the treated sample to its level in an untreated control. In order to eliminate from consideration ORFs with UPR-independent transcriptional changes, we also measured fold changes in strains bearing either a deletion of *IRE1* (Δ*ire1*) or *HAC1* (Δ*hac1*). These UPR-deficient strains are unable to transduce the UPR signal from the ER to the nucleus (Cox et al., 1993;

Cox and Walter, 1996; Mori et al., 1996; Mori et al., 1993). We treated both mutant strains with either DTT or tunicamycin for 60 minutes, and determined the fold change in expression by comparison to an untreated control. Thus, for each ORF, there are nine induction measurements: five from treatment of a wildtype strain, and four from treatment of UPR-deficient strains.

We then defined a canonical response profile for a UPR target gene by combining the array expression data for seven previously reported UPR targets: *KAR2*, *EUG1*, *PDI1*, *LHS1*, *FKB2*, *ERO1*, and *INO1* (Chapman et al., 1998). For each of the nine treatment conditions, we defined the canonical response as the average of the fold changes in that condition for each of the known target genes. As anticipated, UPR targets showed strong induction in each of the wildtype conditions and little or no induction in the four UPR-deficient conditions (Figure 1A). The canonical profile shows that the UPR is rapid: induction of target genes was essentially complete after 15 minutes and was maintained over the time course of DTT treatment. Thus, the time course of DTT induction in effect provides four independent measurements of UPR activity under fully induced conditions. The magnitude of the response was comparable in DTT- and tunicamycin-treated cells.

We employed three criteria to identify novel targets of the UPR. First, we required targets of the UPR to exhibit expression patterns that matched those of known UPR targets. For each ORF, we calculated the correlation between the

expression pattern of that ORF and the canonical profile. We selected ORFs as candidate targets if this correlation was no worse than that of *KAR2*, the previously identified UPR target with the lowest correlation to the canonical profile (P = 0.81). This analysis is illustrated in Figure 1B, in which the expression patterns for three DnaJ homologs are displayed along with their correlations to the canonical profile. The gene encoding the ER-resident chaperone Jem1p shows high correlation (P = 0.98), suggesting that *JEM1* is a target of the UPR. In contrast, genes encoding DnaJ homologs localized to the mitochondria (*MDJ1*) or the cytosol (*YDJ1*) show little correlation (P = -0.70 and -0.56, respectively) and are therefore excluded from the target set.

Second, we required that candidate UPR targets exhibit inductions that differ between wildtype and UPR-deficient mutant samples at a level of significance (3.6 standard deviations) corresponding to a difference that would occur by chance less than one time in 6400, i.e., less than one gene in the *S. cerevisiae* genome. Finally, in order to eliminate ORFs that passed the criteria established above due solely to decreases in expression in the UPR-deficient mutants, we required that UPR targets show a mean change in the wildtype of greater than 1.5-fold. The set of genes satisfying these criteria defines the *HAC1*- and *IRE1*-dependent response to ER protein misfolding.

Two genes that are known targets of the UPR (*KAR2* and *INO1*) did not pass the strict statistical criterion (2.75 and 3.0 standard deviations, respectively)

due to significant residual upregulation in the mutant strains, as previously observed (Cox et al., 1993). Thus, the high stringency of the criteria employed results in an underestimation of the full scope of the UPR. Despite this stringent selection, we identified a large set comprised of 381 ORFs that are induced by both DTT and tunicamycin in an *IRE1*- and *HAC1*-dependent manner. A database containing the complete data set can be found at http://www.cell.com/cgi/content/full/101/3/249/DC1. We have also included transcriptional data from a strain deleted for *OPI1*, a negative regulator of inositol and membrane biosynthesis which is inhibited upon activation of *HAC1* (Cox et al., 1997). These data reveal that loss of *OPI1* leads to induction of only a small subset of UPR target genes. We conclude that the vast majority of UPR target genes defined here are not upregulated as a secondary consequence of membrane proliferation.

For every ORF, we then determined the UPR-dependent induction due to a particular unfolding treatment (DTT or tunicamycin) by dividing the average fold change resulting from that treatment in wildtype cells by the average fold change in the UPR-deficient mutants. A scatter plot of DTT induction versus the tunicamycin induction (Figure 1C) reveals that, as with known UPR targets, the newly identified targets of the UPR (red points) are induced to similar levels by DTT and tunicamycin. Because the two unfolding agents have similar effects on gene expression, we projected this scatter plot onto the diagonal (equal induction by DTT and tunicamycin) and took the distance along this line as a measure of

combined DTT and tunicamycin induction. This analysis provides a single metric of UPR-dependent induction by the two unfolding agents. A histogram of this metric for all ORFs (Figure 1D) displays a significant degree of asymmetry, with the newly identified UPR targets (red bars) corresponding to the excess ORFs on the right side of the distribution. The fact that there is not a corresponding set of ORFs on the left side of the histogram indicates that the UPR is largely an inductive transcriptional response, with little specific repression.

Many aspects of secretory function are regulated by the UPR

Our analysis reveals that the scope of the UPR is far broader than anticipated by the functions of previously reported target genes. The 381 ORFs which passed our criteria include 208 genes for which some functional information is available (named genes or their homologs) and 173 genes for which no information is presently available. Of the functionally characterized genes, 103 are known or predicted by sequence homology to play roles in secretion or the biogenesis of secretory organelles. As expected, we observe induction of ER-resident chaperones and genes involved in phospholipid metabolism. However, these represent only a fraction of this set of target genes, which also includes several categories of genes with functions throughout the secretory pathway (Figure 2). These functional categories (detailed in Table 1) include translocation, protein glycosylation, vesicular transport, cell wall biosynthesis, vacuolar protein targeting, and ER-associated degradation (ERAD).

The UPR controls the rate of ERAD

The induction of ERAD components was particularly intriguing, as it suggested coordination between the UPR and another pathway related to protein misfolding in the ER. We confirmed the genomic array measurements of ERAD gene expression levels by northern blot analysis and found that the results were in good agreement. *DER1* and *HRD3*, nonessential genes required for ERAD, are strongly induced upon tunicamycin treatment of wildtype cells but not Δ*ire1* mutant cells (Figure 3). *SEC61*, an essential component of the translocon also required for ERAD (Pilon et al., 1997; Plemper et al., 1997; Zhou and Schekman, 1999), is similarly induced in an *IRE1*-dependent manner. In contrast, transcription of *SRP54*, which is also important for protein translocation but not known to influence the rate of ERAD, is unresponsive to tunicamycin treatment.

Since several genes important for ERAD are induced by the UPR, we examined candidate genes to identify novel ERAD components. One of these candidates, *YOL031c*, was chosen on the basis of its homology to a *Yarrowia lipolytica* gene (*SLS1*) which encodes a nonessential ER-lumenal protein that is physically associated with the translocon (Boisramé et al., 1999). Hereafter, we refer to this gene as *PER100* (protein processing in the ER; Ng et al., 2000).

136

We measured ERAD rates using strains expressing CPY* (prc1-1), a constitutively misfolded soluble secretory protein and a well-characterized substrate for ERAD (Knop et al., 1996). To facilitate immunoprecipitation of CPY*, the prc1-1 gene, which was driven by its native (PRC1) promoter, was modified by addition of sequences encoding a C-terminal HA tag (Ng et al., 2000). In each of the experiments described below, we pulse-labeled cells with ^{35}S-methionine/cysteine, chased over a 45-min time course, immunoprecipitated with antibodies against the HA epitope, and subjected samples to SDS-PAGE and autoradiography. The rate of disappearance of CPY* represents the rate of ERAD.

We compared the rate of degradation of CPY* in a Δper100 mutant to the rate in wildtype cells and in the Δder1 mutant, in which ERAD is completely blocked (Knop et al., 1996). In wildtype cells, CPY* was degraded with a half-life of 15 ± 1 minutes (Figure 4A, squares), a value in agreement with published observations. As anticipated, a Δder1 mutant failed to measurably degrade CPY* over the time course (Figure 4A, diamonds). The Δper100 mutant displayed an intermediate phenotype, with a CPY* half-life of 24 ± 2 minutes (Figure 4A, triangles). This stabilization is roughly comparable to that reported for strains containing ERAD-deficient alleles of KAR2 (Plemper et al., 1997) and deletion of the PMR1 ion transporter, also required for wildtype levels of ERAD (Dürr et al., 1998). Thus, the PER100 gene product plays a role in maintaining efficient ERAD, perhaps through an activity at the translocon.

Because several UPR target genes are required for ERAD, we asked whether mutant strains unable to induce the UPR are also deficient in ERAD. Indeed, the $\Delta ire1$ mutant degraded CPY* at a reduced rate (half-life of 25 ± 1 min, as compared to 15 ± 1 min in wildtype cells; Figure 4B, circles). Given that an intact UPR is necessary for efficient ERAD, we asked whether activation of the UPR is sufficient to increase the rate of degradation. We constructed strains bearing a plasmid system in which the spliced form of the *HAC1* gene is driven by a glucocorticoid-responsive element (GRE)-containing promoter; the *GRE-HAC1* gene and the glucocorticoid receptor, a ligand-regulated transcriptional activator, are expressed *in trans* on separate high copy (2µ) plasmids. This system allowed us to induce the UPR by expressing Hac1p upon addition of the glucocorticoid receptor ligand deoxycorticosterone (DOC). After 90 minutes of exposure to DOC, steady state levels of Hac1p reached a plateau, resulting in significant induction of several UPR target genes tested by northern blot (data not shown). The rate of CPY* degradation was dramatically increased in cells bearing *GRE-HAC1* and treated with DOC (half-life of 6 ± 1 min; Figure 4C, diamonds) compared to DOC-treated cells bearing the GRE vector alone (half-life of 30 ± 2 min; Figure 4C, squares). Cells bearing the GRE vector alone degrade CPY* more slowly than do the wildtype cells used in Figures 4A and 4B; this difference may be explained by the diminished growth rate we observe for these strains, which bear multiple 2µ plasmids. In any event, degradation of

CPY* is accelerated in the DOC-induced samples expressing *HAC1* even when compared to the wildtype samples displayed in Figure 4A and 4B.

In the GRE-inducible system, *HAC1*-expressing cells induce UPR target genes in the absence of high levels of unfolded protein. We also measured ERAD after activating the UPR in wildtype cells with chemical agents that interfere with protein folding. In marked contrast to the above experiments, in cells treated with tunicamycin (Figure 4D, circles) or DTT (Figure 4D, diamonds) for one hour prior to pulse-labeling, ERAD was completely blocked. These treatments generate pathologically high levels of misfolded protein; the blockage of ERAD may therefore result from saturation of the capacity of the ERAD system despite activation of the UPR and transcriptional upregulation of several ERAD components under these conditions (see Discussion). Consistent with this, expression of high levels of a single misfolded protein results in slower ERAD: cells expressing CPY* from the strong promoter *TDH3* grow at a normal rate but degrade CPY* with significantly slower kinetics than when the protein is expressed under control of the native (*PRC1*) promoter (half-life of 30 ± 1 min; Figure 4D, triangles).

Mutations in ERAD components result in constitutive activation of the UPR

Previous work has indicated that mutations in genes required for ERAD do not cause a detectable growth phenotype under normal growth conditions (Knop

et al., 1996). While it is possible that this is the case because degradation of misfolded proteins is required for life only under conditions of extreme folding stress, an alternative explanation is that the UPR can compensate for a defect in ERAD, eliminating misfolded proteins by other means. In the latter case, a loss of ERAD function would result in an accumulation of unfolded proteins in the ER and chronic activation of the UPR.

We tested for constitutive activation of the UPR in cells lacking *DER1*, *HRD1*, *HRD3*, or the newly identified ERAD gene *PER100* using a sensitive reporter of UPR activation. The reporter construct consists of the gene encoding green fluorescent protein (GFP) driven by four repeats of the unfolded protein response element from the *KAR2* promoter (UPRE; Cox and Walter, 1996; Mori et al., 1996). Comparison of steady state levels of GFP fluorescence in Δ*der1*, Δ*hrd1*, Δ*hrd3*, and Δ*per100* strains to those of wildtype cells (Figure 5A, left panel) reveals a ~2-fold induction of the UPR under normal growth conditions in these mutants. Both wildtype and ERAD-deficient cells showed similar levels of maximal GFP expression under DTT treatment (Figure 5A, right panel), indicating that the observed induction of the UPR is not the result of a nonspecific increase in GFP levels in the mutant cells.

Mutations in the UPR and ERAD are synthetically lethal

We have thus far demonstrated that the rate of ERAD is modestly decreased in the absence of a functional UPR (Figure 4B). In addition, ERAD-deficient cells show a constitutive, partial activation of the UPR. Together, these data suggest that the UPR and ERAD cooperate to eliminate misfolded proteins under normal growth conditions, predicting that simultaneous loss of both pathways should be more detrimental to the cell than the loss of either one alone.

To test for such synthetic effects, we constructed diploid strains containing heterozygous deletions in *IRE1* as well as one of the previously identified genes required for ERAD (*DER1*, *HRD1*, or *HRD3*) or the newly identified ERAD gene *PER100*. Following meiosis, spores bearing both Δ*ire1* and Δ*der1* mutations germinated normally, but showed poor growth and viability at room temperature, and entirely failed to grow at 37°C (Figure 5B). By contrast, the single mutants showed no growth defect under either condition. Consistent with the fact that there is a broader spectrum of substrates that are dependent on Hrd1p and Hrd3p for their ERAD-mediated degradation (Hampton et al., 1996; Knop et al., 1996), spores bearing both Δ*ire1* and either Δ*hrd1* or Δ*hrd3* mutations displayed a stronger phenotype than the Δ*ire1* Δ*der1* spores. These strains showed poor viability following meiosis, grew slowly at room temperature, and entirely failed to grow at 37°C (Figure 5B). Similarly, strains containing deletions in both the *IRE1*

and *PER100* genes failed to grow beyond the few cell stage despite the fact that

loss of *PER100* alone caused little or no growth defect (data not shown).

Discussion

Using high density oligonucleotide arrays in conjunction with strains bearing specific defects in the UPR, we have defined the transcriptional scope of the UPR. Remarkably, the UPR affects virtually every stage of the secretory pathway. From entry into the ER (translocation), through processing (folding, covalent modification, and sorting), until exit from the pathway (arrival at a target organelle, secretion from the cell, or degradation), a secretory protein's progress is influenced by the transcriptional targets of the UPR. The breadth of this response suggests that genes involved in many secretory functions, including but not limited to ER-resident chaperones, are required for maintenance of the specialized protein folding environment.

The scope of the UPR is focused in large part on the secretory pathway, with approximately half of the 208 UPR target genes for which functional data is available playing roles in secretion. The 173 transcriptional targets of the UPR with no known function are therefore excellent candidates for genes with important secretory functions. Indeed, our expression data and functional studies allowed us to identify the previously uncharacterized *S. cerevisiae* homolog of the *Y. lipolytica* gene *SLS1*, referred to above as *PER100*, as a novel component required for efficient ERAD.

Despite its breadth, the UPR results in a specific remodeling of the secretory pathway rather than an indiscriminate upregulation of all ER or

secretory pathway components. For example, many components of the COP-II vesicle coat involved in ER-Golgi trafficking are targets, including two strongly induced homologs of *SEC24* which have been suggested to play a role in export of specific cargo proteins (Roberg et al., 1999). In contrast, components of the COP-I/"coatomer" involved in retrograde transport are less well-represented, and those that are regulated by the UPR typically show only modest induction. Similarly, of the ER-resident chaperones involved in folding or secretion of specific substrates (Ellgaard et al., 1999), only *CHS7*, required for maturation of chitin synthase III (Trilla et al., 1999), is upregulated. This specificity suggests that rather than merely increasing the capacity of the secretory pathway, the UPR results in selective induction of those activities that are essential under folding stress, e.g., in the cases mentioned above, enhanced anterograde transport of a particular subset of secretory proteins or folding of proteins involved in maintaining cell wall integrity. The set of UPR target genes may therefore specify those activities required to optimize protein folding in the ER.

How might the set of UPR target genes act in a concerted manner to promote efficient folding? An attractive hypothesis is that a critical function of the UPR is to reduce the lumenal concentration of misfolded protein, by either directly refolding proteins or removing them from the ER (Figure 6). In this model, abundant chaperones would bind to misfolded species, prevent aggregation, and promote folding. Similarly, glycosylation enzymes would assist in the folding of proteins which require carbohydrate modification to attain their

proper conformation. Consistent with this suggestion, we found in an independent study that mutations which compromise either addition of GPI anchors or protein glycosylation are lethal in the absence of UPR function (Ng et al., 2000). Moreover, UPR induction in mammalian cells was recently shown to accelerate synthesis of the dolichol-oligosaccharides employed in N-linked glycosylation (Doerrler and Lehrman, 1999). In the event that direct attempts to increase the efficiency of folding fail, induction of specific COP-II components might enable efficient packaging of cargo proteins (possibly including unfolded proteins) into anterograde vesicles, or simply increase the overall capacity of anterograde transport. Such an increase in secretory capacity might facilitate targeting of misfolded species to the vacuole for degradation (Hong et al., 1996), consistent with our observation that several genes involved in vacuolar targeting are also UPR targets. Similarly, induction of phospholipid biosynthetic enzymes would generate new membranes, thereby increasing the volume of the ER, simultaneously diluting unfolded proteins and preparing the compartment to receive an influx of newly synthesized folding factors. Finally, induction of ERAD components directly enhances the clearance of misfolded proteins from the ER to the cytosol.

Our functional studies demonstrate that the capacity of the ERAD system is readily saturated under conditions of ER stress and that the UPR plays a direct role in counteracting this saturation. We find that the UPR is necessary for efficient ERAD function, as UPR-deficient cells degrade CPY* at a reduced rate;

these results are in qualitative agreement with recent reports that both full-length CPY* (Ng et al., 2000) and a truncated allele of CPY* (Casagrande et al., 2000) are stabilized in the Δire1 mutant. This decrease in ERAD rate is likely to result from chronic misfolding in Δire1 strains rather than from direct loss of the ERAD machinery, as Δire1 cells do not show decreased basal transcription of ERAD genes (Figure 3). The notion that ERAD capacity can be readily saturated is further supported by the observation that treatment with DTT or tunicamycin, both of which generate high levels of unfolded ER proteins, dramatically decreases the rate of CPY* degradation. High levels of even a single misfolded protein can substantially decrease the rate of degradation: expression of CPY* from a strong promoter resulted in accumulation of the protein and a doubling of its half-life, consistent with the idea that ERAD capacity can be saturated by high concentrations of substrate. In striking contrast to the DTT and tunicamycin treatments, we find that when the UPR is induced by expression of Hac1p, which does not cause accumulation of unfolded proteins, the rate of ERAD is significantly increased, thus demonstrating that the UPR plays a direct role in enhancing ERAD. It has recently been postulated that the rate-limiting step in the degradation of a protein through ERAD is the conversion of N-linked oligosaccharide from the Man9 to the Man8 form (Jakob et al., 1998), a reaction catalyzed by the glycosylase Mns1p. We found that UPR activation results in the upregulation of MNS1, raising the intriguing possibility that the UPR accelerates ERAD in part via increased expression of an enzyme which catalyzes the rate-limiting step; in this scenario, during times of folding stress, activation of the UPR

would reduce the time available for a protein to fold before being targeted for degradation.

Although the UPR enhances ER degradation capacity under acute folding stress, the ERAD pathway also plays a critical and previously undescribed role in the disposal of misfolded proteins even under normal growth conditions. Loss of ERAD function in Δder1 and Δper100 strains leads to chronic accumulation of unfolded proteins in the ER, as evidenced by constitutive activation of the UPR. Recently, Zhou and Schekman reported that SEC61 alleles with specific defects in ERAD, as well as deletion of several other ERAD components, also cause constitutive UPR induction (1999). Thus, the chronic accumulation of misfolded proteins in the ER appears to be a general consequence of loss of ERAD. Earlier studies suggested that even if it were constitutively active, ERAD has little physiological importance in the absence of an acute stress, as loss of ERAD function does not lead to a detectable growth phenotype (Knop et al., 1996; Zhou and Schekman, 1999). Here we show that this lack of phenotype results from a compensatory effect of UPR induction: deletion of any of three well-characterized ER-resident ERAD components (DER1, HRD1, HRD3) or the newly identified ERAD component PER100 results in dramatic loss of viability in a Δire1 strain. In a parallel study, we found that deletion of either of two genes encoding cytosolic ERAD components, the membrane-bound ubiquitin-conjugating enzyme Ubc7p and the proteasome regulator Son1p/Rpn4p, also shows a synthetic lethal phenotype when combined with loss of IRE1 (Ng et al., 2000).

Hence, loss of ERAD function at any location (ER lumen, ER membrane, or proteasome) results in a requirement for UPR-mediated clearance of misfolded proteins.

Taken together, our observations argue that a fraction of the proteins passing through the ER will inevitably misfold, and that removal of these misfolded polypeptides is an essential process under all growth conditions. The chronic misfolding of proteins in the ER is likely to reflect the inherent difficulty of folding secretory and membrane proteins, which unlike cytosolic proteins often require covalent modifications, such as disulfide bonds and glycosylation, as well as the precise ordering of transmembrane domains across and within the lipid bilayer. In the absence of a functional UPR, the ERAD capacity is sufficient to dispose of this flux provided the cell does not face an unusual stress. Conversely, when the UPR is available in a cell with diminished ERAD capacity, misfolded proteins can still be handled by multiple mechanisms, including refolding by chaperones, clearance from the ER by anterograde vesicular transport, or an alternate means of degradation, e.g., in the vacuole or by the action of other UPR-induced ERAD genes. Thus, the UPR and ERAD represent partially overlapping or compensatory means to the same essential end: elimination of misfolded secretory proteins, which are inevitably generated during the course of normal growth.

Experimental Procedures

General procedures

Yeast manipulations were performed using standard methods (Sherman, 1991), except that the pH of YPD was lowered to that of synthetic defined media (pH = 5.4) to inhibit oxidation of DTT. All incubations were at 30°C, unless otherwise indicated.

Plasmid construction

Plasmid pRS425-GRE, which contains the glucocorticoid responsive element upstream of a multiple cloning site, was generated by subcloning the XhoI-SacI fragment of p2UG (Schena et al., 1991) into the corresponding sites of pRS425 (Sikorski and Hieter, 1991). Plasmid pCP274, which contains the spliced form of the *HAC1* gene downstream of the GRE promoter, was generated by cloning the DraI/SmaI fragment of pRC43 (Cox et al., 1997) into the SmaI cloning site of pRS425-GRE. Plasmid pKT058, which encodes a GFP reporter gene driven by four repeats of the *KAR2* UPRE, was generated by subcloning the UPRE- and GFP-containing ClaI-SacI fragment of pKT007 (Pollard et al., 1998) into pRS304 (Sikorski and Hieter, 1991). Plasmid pCP280, which contains the *prc1-1* gene encoding CPY* under control of the *TDH3* promoter, was constructed by ligating a blunted AccI fragment of pDN431 (Ng et al., 2000) into blunted, BamHI-linearized pG-1 (2μ TRP1; Schena et al., 1991).

Yeast strains

The wildtype strains W303-1B and JC103 (which was derived from W303-1B by integration of a β-gal UPR reporter into the *HIS3* and *LEU2* loci), the Δ*ire1* strain CS165, and the Δ*hac1* strain JC408 are as described (Cox et al., 1993; Cox and Walter, 1996). The *PER100*, *HRD1*, and *HRD3* deletion strains were derived from a W303-1B parent by replacing the entire open reading frames of the appropriate genes with an auxotrophic marker (*LEU2* for *PER100*, or *HIS3* for *HRD1* and *HRD3*) using the method of Pringle and coworkers (Longtine et al., 1998). Strains used in the experiments described in Figure 4D were W303-1B transformed with pT2.GN795 (Schena et al., 1991), which contains the glucocorticoid receptor under control of the GPD promoter and either pRS425-GRE ("GRE-vector") or pCP274 ("GRE-*HAC1*").

Genomic arrays:

Sample preparation and hybridization

Biotinylated cRNA samples were prepared and processed largely as described previously (Wodicka et al., 1997). Briefly, cultures of wildtype (JC103), CS165 or JC408 strains were grown to mid-log phase in rich medium, and treated with either 1 μg/ml tunicamycin (Tm) or 2 mM DTT. At the indicated times, cells were treated with 20 mM azide, recovered from 250 ml aliquots by centrifugation, and frozen in liquid nitrogen. Total RNAs were prepared by freeze/thaw/hot phenol extraction (Schmitt et al., 1990) and mRNA was purified using the PolyATtract system (Promega) according to manufacturer's

instructions. First strand cDNA synthesis was performed using AMV (Promega) according to manufacturer's instructions. Second-strand syntheses, cRNA amplifications, fragmentations, and hybridizations were conducted as described previously (Wodicka et al., 1997).

Data analysis and categorization

For each treatment condition, fold changes in mRNA levels relative to untreated cultures were determined using the GeneChip software package (Wodicka et al., 1997). For all subsequent analyses, the base 2 logarithm (log_2) of the fold changes were utilized. For each ORF, the expression pattern was represented by a nine component vector composed of the following elements: <WT.D.15, WT.D.30, WT.D.60, WT.D.120, WT.T.60, Δire1.D.60, Δire1.T.60, Δhac1.D.60, Δhac1.T.60>. The first segment of each element indicates the strain, the second the treatment condition (DTT [D] or Tm [T]), and the third the treatment time (i.e., Δire1.D.60 is the log_2 of the fold change in a Δire1 strain treated with DTT for 60 minutes compared to the untreated Δire1 strain). An expression vector representing the canonical response profile was generated by averaging the vectors from seven known UPR targets: *KAR2*, *EUG1*, *PDI1*, *LHS1*, *FKB2*, *ERO1*, and *INO1*. Pearson correlations between a given ORF's vector and the canonical profile were calculated (Eisen et al., 1998). ORFs with a Pearson correlation coefficient at least as great as that of *KAR2* (P = 0.81) were subjected to a Z test with a null hypothesis of no difference between the five treatments of the wildtype strain and four treatments for the UPR-deficient

strains. ORFs with a Z score of greater than 3.6, corresponding to a chance occurrence of approximately 1 in 6400, were called as UPR targets provided that the average induction of the wildtype strain was greater than 1.5. Assignment of known/named ORFs to functional categories followed curated data available online at SGD (http://genome-www.stanford.edu/Saccharomyces) and YPD@Proteome (http://www.proteome.com/databases/index.html).

The calculation of UPR-dependent DTT induction used in Figure 1C is:

$$\frac{1}{4}((WT.D.15)+(WT.D.30)+(WT.D.60)+(WT.D.120))-\frac{1}{2}((\Delta ire1.D.60)+(\Delta hac1.D.60))$$

The calculation of UPR-dependent tunicamycin induction used in Figure 1C is:

$$(WT.T.60)-\frac{1}{2}((\Delta ire1.T.60)+(\Delta hac1.T.60))$$

CPY* degradation assay

Strains bearing a low copy CPY*-HA expression plasmid (Ng et al., 2000) were grown to $OD_{600}=1.0$. Cell pellets were washed twice, resuspended at 3 OD/ml in medium lacking methionine, and incubated for one hour at 30°C with 1 µg/ml tunicamycin, 2 mM DTT, or 100 µM DOC as indicated. Newly synthesized polypeptides were pulse-labeled by addition of 20 µCi/OD ProMix (Amersham) for 20 minutes and chased by addition of 2 mM each cold methionine and cysteine. Time points were taken by transferring 1 ml aliquots into chilled tubes containing 100 µl 100% TCA and 3 µl 3M sodium azide, and freezing immediately in liquid nitrogen. Immunoprecipitations were performed by the

method of Gaynor et al. (1994) except that after pre-clearing, supernatants were incubated for 4 hours at 4°C with 7 µl of 16B11 anti-HA antibody (BAbCo), and immunoprecipitated by addition of 1 µl rabbit anti-mouse antibody (Jackson) and 25 µl protein A-Sepharose slurry and incubation for 30 minutes.

FACS analysis

Strains containing an integrated UPRE-GFP reporter were constructed by transforming W303-1B (wildtype), Δder1, Δhrd1, and Δhrd3 with EcoRV-linearized pKT007 or by transforming Δper100 with EcoRV-linearized pKT058. Integrations were confirmed by genomic PCR analysis. All strains were grown to mid-log phase (OD_{600} = 0.5), and then cultures were grown in the presence or absence of 2 mM DTT for 1.5 hours to induce the UPR. GFP fluorescence was measured by FACS analysis on a FACScan instrument (Becton-Dickinson).

Acknowledgments

Table 1. Secretory pathway genes upregulated by the UPR

TRANSLOCATION

Translocon	*SEC61, SBH1, SLS1*
Post-translational translocation	*SEC62, SEC71, SEC72*
Signal peptidase	*SPC2*

GLYCOSYLATION/MODIFICATION

Core oligosaccharide synthesis	*DPM1, PMI40, RHK1, SEC59*
Oligosaccharyltransferase	*OST2, OST3, SWP1, WBP1*
Glycoprotein processing	*ALG6, ALG7, MNS1, RAM2, STE24*
GPI anchoring	*GAA1, GPI12, LAS21, MCD4*
Golgi/O-linked glycosylation	*KTR1, MNN11, PMT1, PMT2, PMT3, PMT5*

PROTEIN FOLDING

Chaperones	*FKB2, JEM1, LHS1, SCJ1, YFR041C*[a]
Disulfide bond formation	*ERO1, EUG1, MPD1, MPD2, PDI1*

PROTEIN DEGRADATION

ER-associated degradation (ERAD)	*DER1, HRD1/DER3, HRD3, UBC7*
Ubiquitin/proteasome	*DOA4, PEX4*

VESICLE TRAFFICKING/TRANSPORT

Budding (ER-Golgi)	*ERV25, SEC12, SEC13, SEC16, SEC24, SED4, SFB2, SFB3, YMR040W*[b]
Fusion (ER-Golgi)	*BOS1, TRS120*
Retrieval (Golgi-ER)	*ERD2, RER2, RET2, SEC26, SEC27*
Distal secretion	*APL3, ARL3, BFR1, MYO5, SEC6, TUS1, YPT10*

LIPID/INOSITOL METABOLISM

Fatty acid metabolism	*ACB1, HAP1, MGA2, YJR107W*[c]
Heme biosynthesis	*DFR1, HEM12, HEM13, HEM15, RIB1*
Phospholipid biosynthesis	*EPT1, INP51, LPP1, OP13, SCS3, SLC1*
Sphingolipid biosynthesis	*LCB1*
Sterol metabolism	*ARE1, HMG2, YHR073W*[d]

VACUOLAR PROTEIN SORTING   *LUV1, STP22, VPS17, VPS35*

CELL WALL BIOGENESIS   *CHS7, CSR1, ECM3, ECM8, ECM31, EXG2, GAS5, PKC1, SPF1, YKR027W*[e]*, YOR239W*[f]

Bold headings correspond to functional categories illustrated in Figure 2. Genes are assigned to subcategories according to summaries of published data listed in the Saccharomyces Genome Database (SGD) and Yeast Protein Database (YPD). [1]DnaJ homolog with predicted signal sequence. [b]Homolog of BAP-29 and BAP-31, sorting proteins that control anterograde transport of certain membrane proteins from the ER to the Golgi complex (Ng et al., 1997). [c]Homolog of acylglycerol lipase. [d]Homolog of human oxysterol-binding protein (OSBP). [e]Homolog of Chs6p, involved in localization of Chs3p. [f]Homolog of Chs5p, required for protease activation of Chs3p.

Figure 1. Identification of the transcriptional targets of the UPR

(A) Determination of the canonical UPR. For each of the indicated nine conditions (wildtype cells treated with DTT for 15, 30, 60, or 120 minutes; wildtype cells treated with tunicamycin (Tm) for 60 minutes; Δ*ire1* cells treated with DTT or Tm for 60 minutes; or Δ*hac1* cells treated with DTT or Tm for 60 minutes), the average of the $\log_2$ of fold induction for seven known UPR targets (*KAR2*, *LHS1*, *ERO1*, *PDI1*, *EUG1*, *FKB2*, and *INO1*) was calculated.

(B) Graphical representation of the expression pattern for three DnaJ homologs. Correlation coefficients (P) were calculated for each gene in the yeast genome, comparing its expression pattern in the nine conditions to that of the canonical profile. Represented here are three DnaJ homologs, with their respective correlation values. *JEM1* encodes an ER-resident protein, while *MDJ1* and *YDJ1* encode mitochondrial and cytosolic proteins, respectively.

(C) Comparison of UPR-dependent induction by DTT and tunicamycin. UPR-dependent induction was calculated by dividing the average of fold changes in wildtype cells by the average of fold changes in two UPR-deficient strains (see Experimental Procedures). Points representing ORFs that satisfy the criteria for being targets of the UPR (i.e., P value > 0.81, Z-test > 3.6, and average induction in wildtype cells > 1.5) are red, while points representing all other genes are green. For illustration, positions of three previously known targets of the UPR

(*ERO1*, *PDI1*, and *LHS1*) are indicated, as well as two targets identified in this work (*DER1* and *HRD3*).

(D)   Distribution of UPR induction.   Shown is a histogram of the number of ORFs at a given distance along the diagonal of the scatter plot in Panel C, which we take as a combined measure of DTT and tunicamycin UPR-dependent induction.   Green bars represent data from genes called as non-targets of the UPR, while red bars represent the contribution from the set of target genes. Shown with a dotted line is the Gaussian fit to the distribution of non-targets, which highlights the asymmetry of induction.
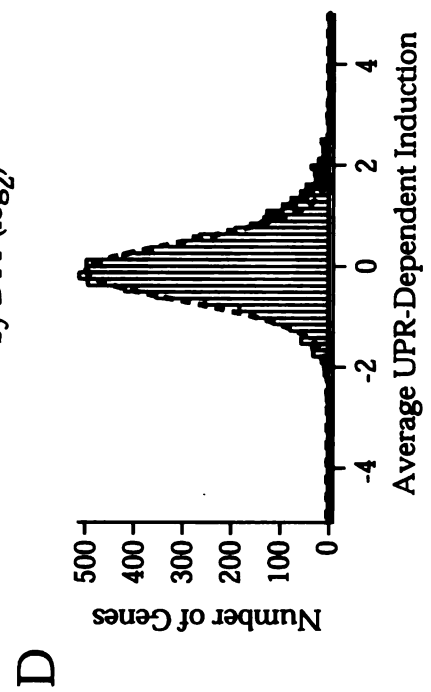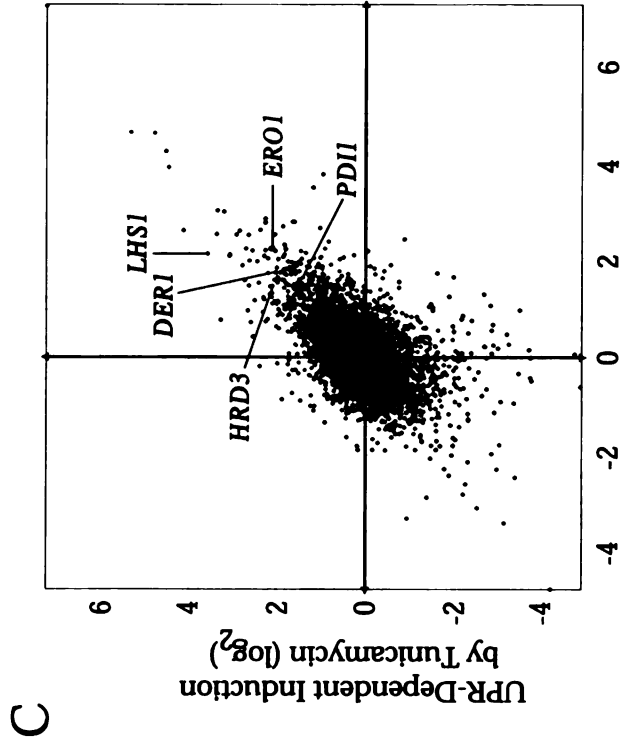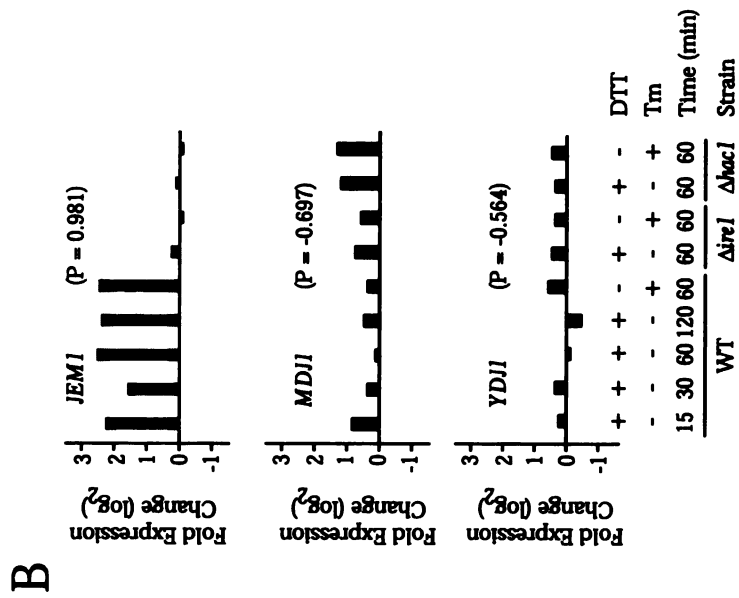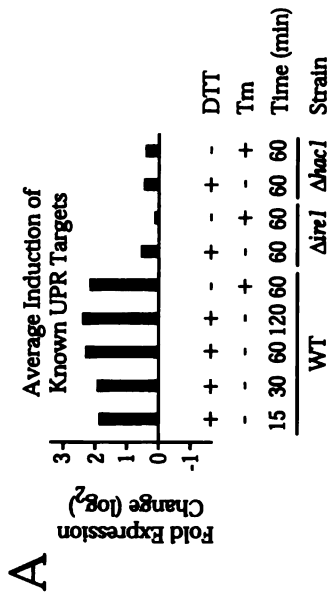
Figure 2. Many aspects of secretory pathway function are regulated by the UPR

A schematic diagram of the secretory pathway, with a classification of the genes identified as targets of the UPR. See Table 1 for details.

TRANSLOCATION
7 genes

LIPID/INOSITOL METABOLISM
19 genes

PROTEIN FOLDING
10 genes

GLYCOSYLATION (ER)
17 genes

PROTEIN DEGRADATION
6 genes

ER-GOLGI
TRANSPORT
11 genes

GOLGI-ER RETRIEVAL
5 genes

GLYCOSYLATION (GOLGI)
6 genes

VACUOLAR TARGETING
4 genes

DISTAL SECRETION
7 genes

CELL WALL BIOGENESIS
11 genes
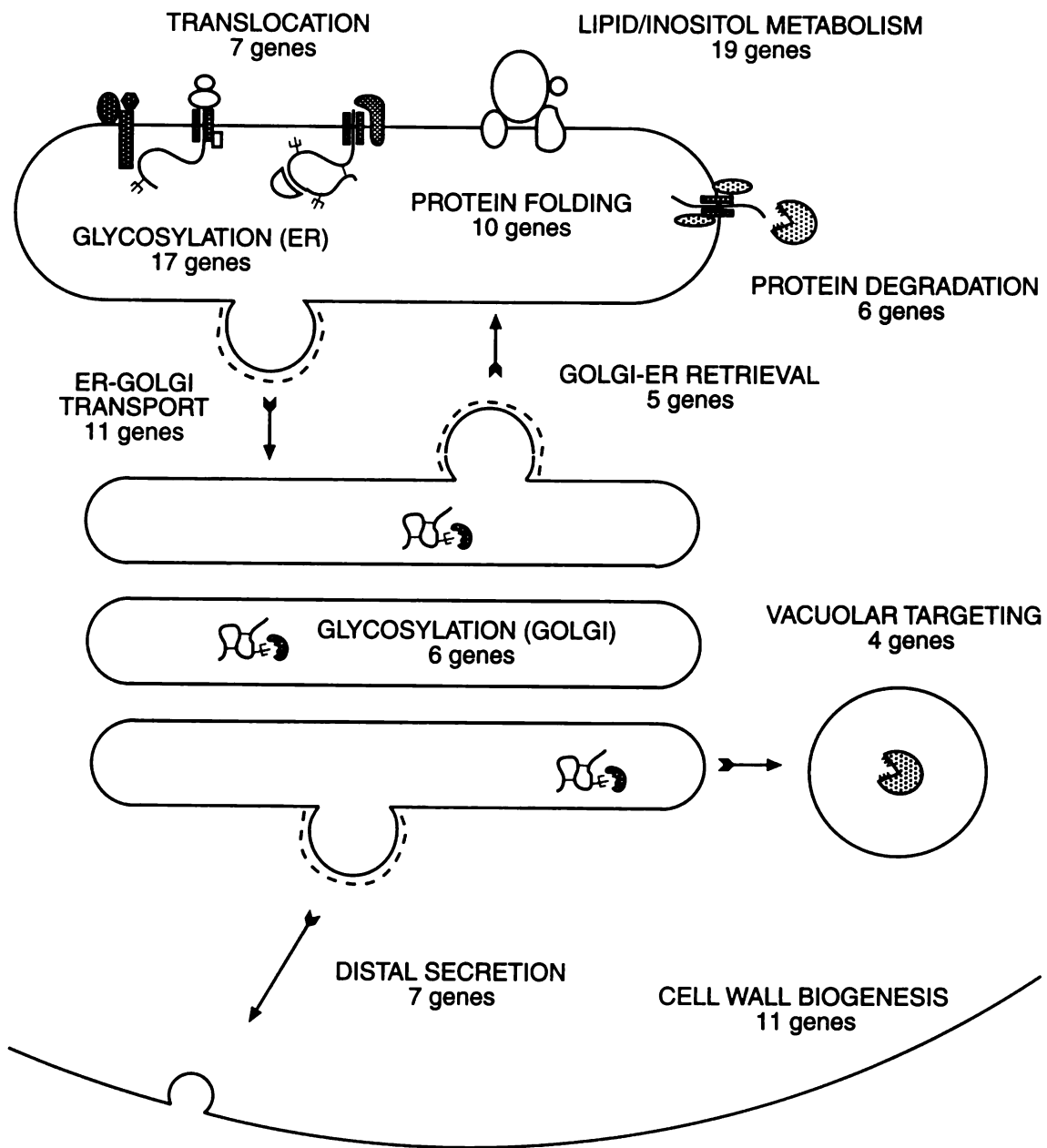
Figure 3. Northern blot analysis confirms UPR-dependent induction of genes involved in ERAD

Northern blot analysis was performed on the same RNA samples that were used to collect the microarray data for cells treated with tunicamycin (Tm) for 60 minutes. Shown are data for *DER1* and *HRD3*, encoding dedicated ERAD components; *SEC61*, encoding a protein shared with the general translocation machinery; and *SRP54*, which is involved in translocation but not ERAD. All expression levels were normalized against the *ACT1* message levels, and then against the expression level for the untreated wildtype sample. For comparison, the microarray data for wildtype cells treated with tunicamycin (Tm) found 3.9-fold, 3.4-fold, 2-fold, and 0.66-fold changes compared to untreated cells for *DER1*, *HRD3*, *SEC61*, and *SRP54*, respectively.
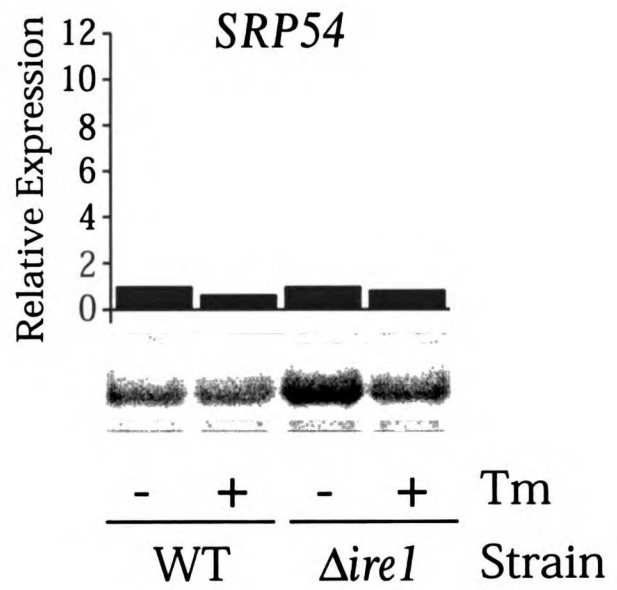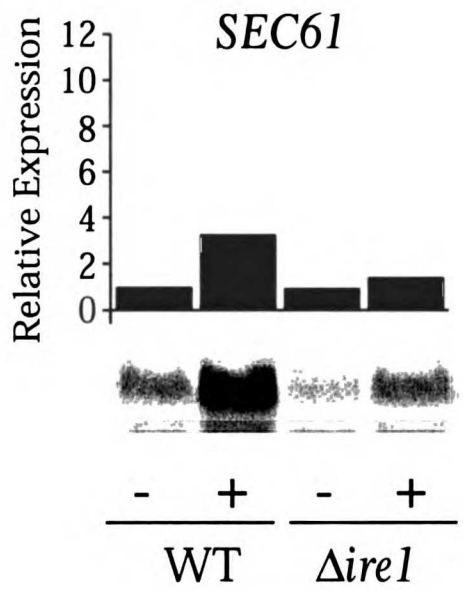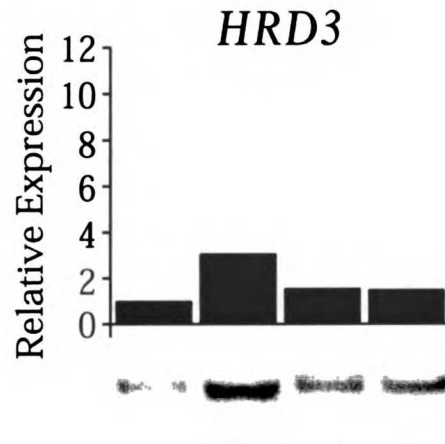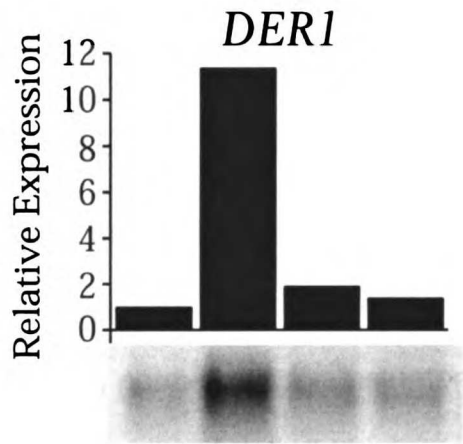
Figure 4. The rate of degradation of CPY* is controlled by the UPR

Cells expressing an HA-tagged copy of CPY* were ^{35}S-radiolabeled and then chased for the indicated time. The rate of degradation of CPY* was analyzed by immunoprecipitation followed by SDS-PAGE and autoradiography. Quantitation of CPY*, normalized against intensity in the time=0 sample, was plotted against chase time, and a half-life (see text) computed by fitting a single exponential curve to each graph. Error bars indicate standard deviation from the average of four (A, B, D) or three (C) independent experiments. Comparison of the rate of CPY* degradation in:

(A) cells deleted for the known ERAD component *DER1* (*Δder1*) or *PER100* (*Δper100*) versus wildtype cells (WT).

(B) cells deleted for *IRE1* (*Δire1*) versus wildtype cells (WT).

(C) cells expressing Hac1p under control of the glucocorticoid-responsive promoter (*GRE-HAC1*) versus cells not expressing Hac1p (GRE-vector). Both samples were treated with DOC for 90 minutes prior to pulse labeling.

(D) cells treated with DTT or tunicamycin (Tm) or expressing CPY* under control of the strong promoter *TDH3* (high CPY*) versus a control (untreated).
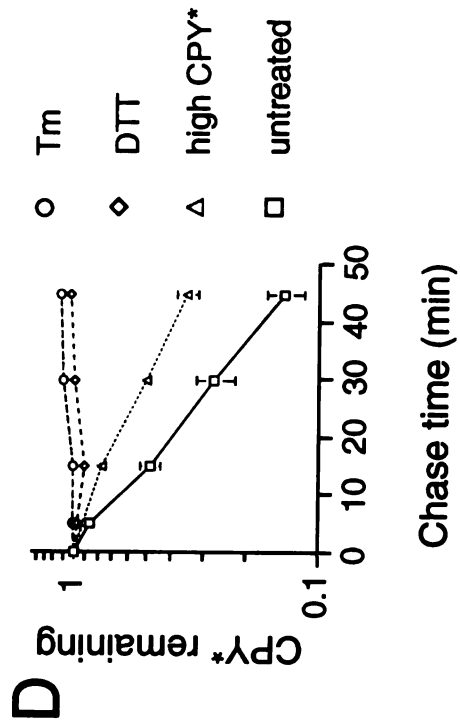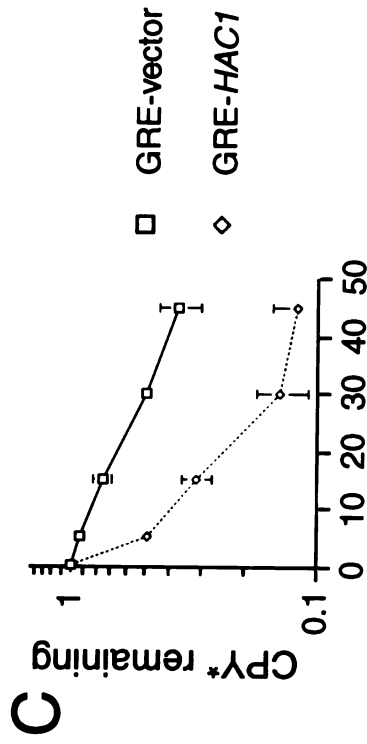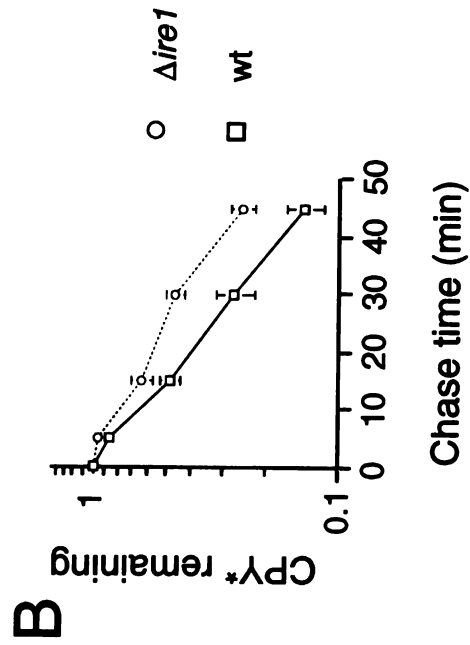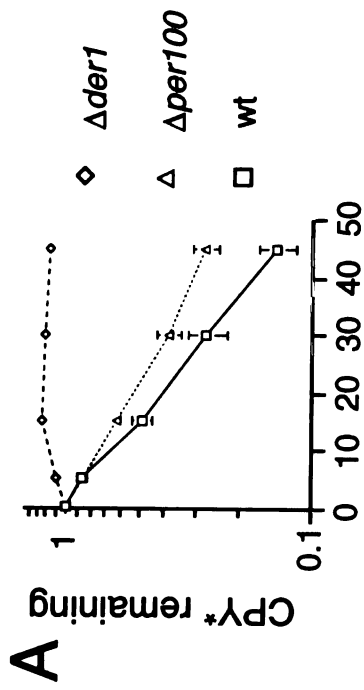
Figure 5. Genetic interaction between mutations in UPR and ERAD genes

(A) Deletion of genes involved in ERAD potentiates the UPR.

Cells contained an integrated reporter gene in which GFP was driven by four copies of the unfolded protein response element (UPRE). Wildtype cells (WT), cells deleted for one of the known ERAD components *DER1* (Δ*der1*), *HRD1*, (Δ*hrd1*), or *HRD3* (Δ*hrd3*) as well as cells deleted for *PER100* (Δ*per100*) were grown to mid-log phase, and analyzed for GFP expression by FACS. Shown on the left is the mean GFP fluorescence for each strain. Strains were analyzed for constitutive expression of GFP ("0 mM DTT") or UPR-induced expression after exposure to 2 mM DTT for 90 minutes ("2 mM DTT").

(B) Deletion of genes involved in ERAD is synthetically lethal with absence of the UPR.

The indicated yeast strains bearing either a single deletion in one of three well-characterized ERAD genes (*DER1*, *HRD1*, or *HRD3*) or this deletion combined with a deletion of *IRE1* were plated at 25°C and 37°C. For comparison, a strain bearing a deletion of *IRE1* and an isogenic parent (WT) are shown. In all cases, roughly equal numbers of cells were spotted.

A
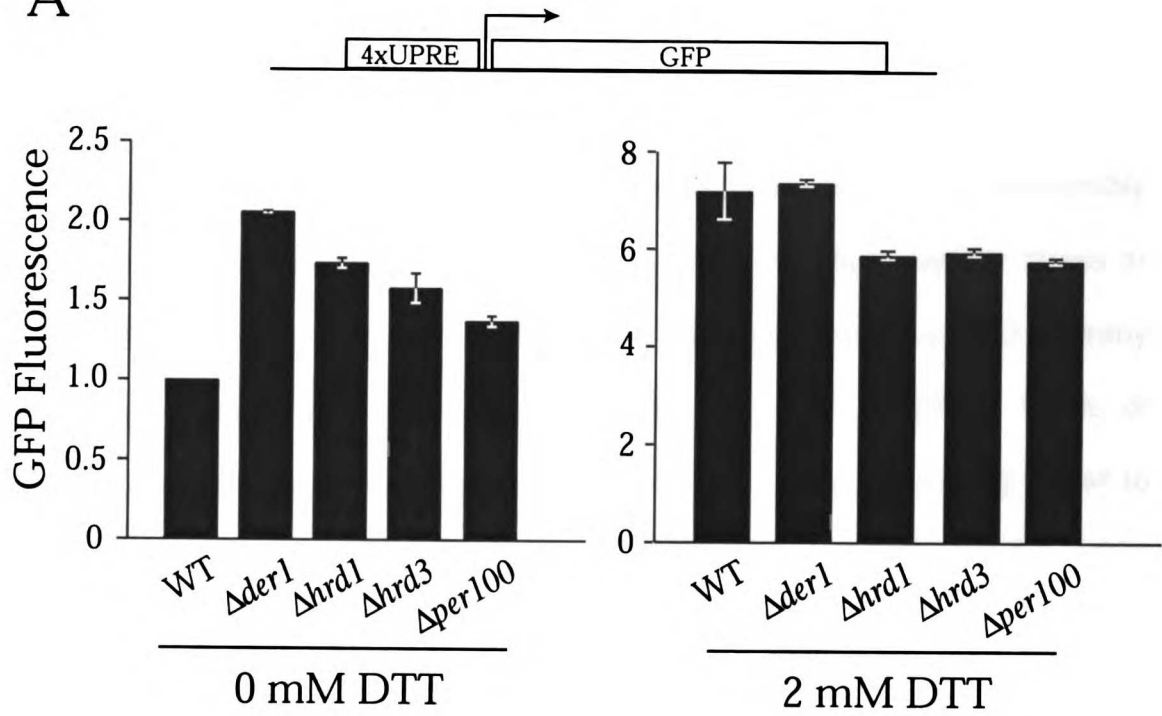
B
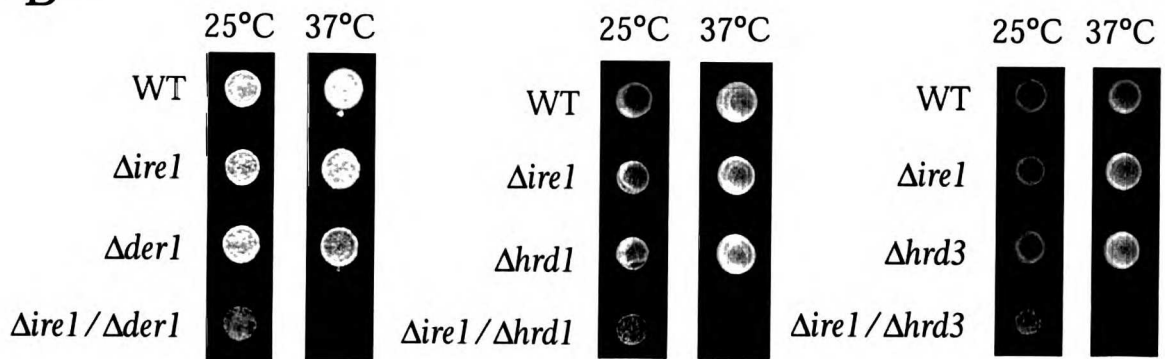
Figure 6. Schematic model illustrating the coordinated action of the UPR and ERAD

Proteins enter the ER in an unfolded form, whereupon they either fold, oligomerize, and pass on to the later secretory pathway, or become irreversibly misfolded and are eliminated by the ERAD machinery. Either cellular stress or loss of ERAD results in accumulation of misfolded proteins and thereby activation of the UPR (filled-in arrow). The UPR acts to reduce levels of misfolded proteins by enhancing folding to the native state, promoting transit to the distal secretory pathway, and enhancing the rate of ERAD, while simultaneously reducing the formation of misfolded species.

unfolded *native*

SECRETION

misfolded UPR

ERAD
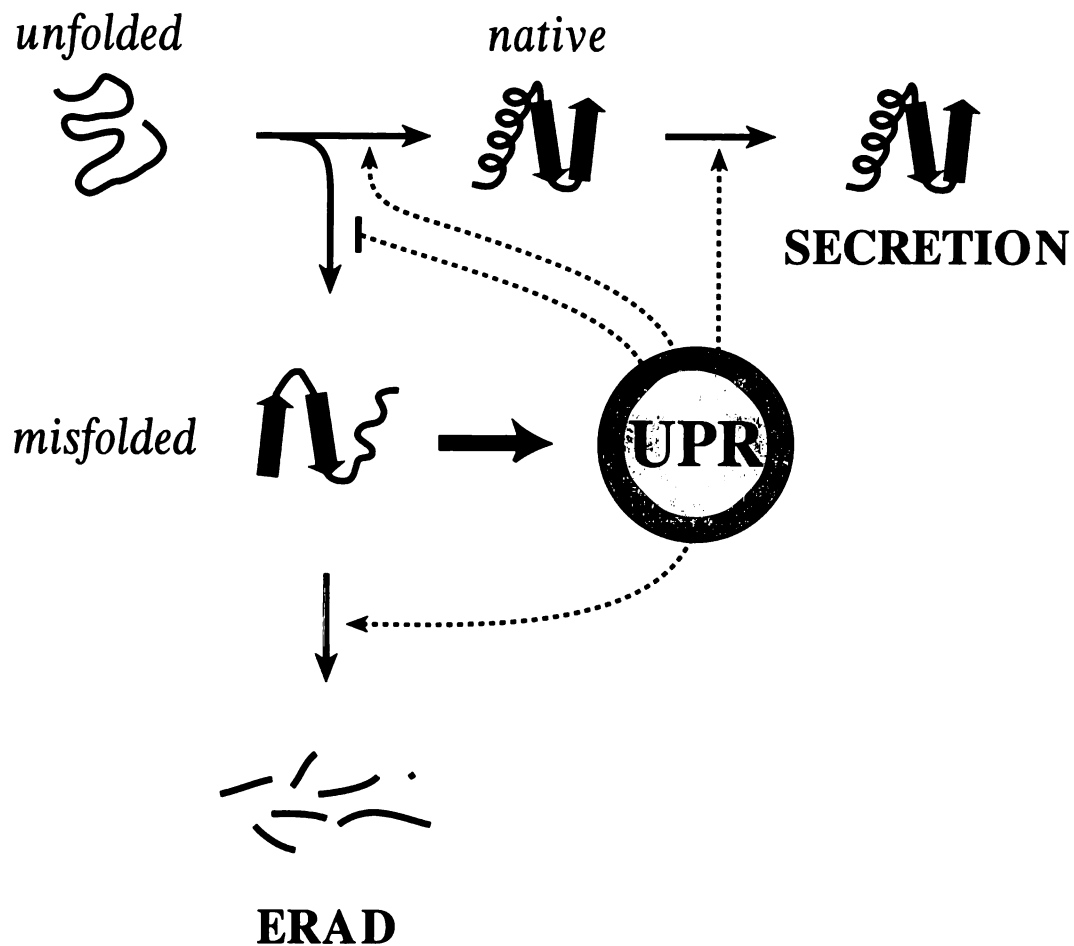
Chapter 5

Summary

The work described in this thesis takes two very different approaches to understanding the requirements for protein folding in the secretory pathway. The first approach, described in Chapters 2 and 3 of this thesis, was to look at a specific event that occurs during the process of protein folding, that of disulfide bond formation, and to try to determine how it is that cells are able to assist this process. The second approach, described in Chapter 4 of this thesis, was to take a more general look at protein folding, using a cellular response, the unfolded protein response (UPR), to have the yeast tell us what it does to create a more efficient protein folding environment.

At the time this work was begun, relatively little was known about the molecular mechanism that catalyzes the formation of disulfide bonds. The rate at which disulfides were observed to form *in vivo* relative to their rates *in vitro* suggested that their formation was likely to be catalyzed within cells (Gilbert, 1990). Protein disulfide isomerase had been identified as a biochemical fraction that accelerated the formation of native structure of disulfide-containing proteins (Goldberger et al., 1963). Furthermore, it was observed that the oxidized form of glutathione was present at significantly higher levels within the secretory pathway than in the cytosol (Hwang et al., 1992). This difference was presumed to be responsible for the relatively greater stability of disulfide bonds within the secretory pathway than in the cytosol. However, it was not clear what maintained the glutathione buffer in a relatively more oxidizing state in the ER than elsewhere in the cell.

Using approaches that had already been successfully applied to understanding oxidative protein folding in the bacterial periplasm, we were able to identify a novel factor that plays a critical role in the formation of disulfide bonds in the ER of eukaryotic cells, *ERO1*. In many respects, this protein is analogous to the DsbB protein which is responsible for introducing oxidizing equivalents into the bacterial periplasm: both are membrane proteins; they share a number of phenotypes, including resistance to reducing agent upon over-expression of the wild-type proteins and sensitivity when mutated; and mutation in either results in the accumulation of reduced protein. Despite these parallels, however, they share no sequence similarity. This is perhaps not surprising, as the proteins reside in quite different physical environments and would therefore be expected to utilize very different mechanisms to affect their respective oxidation reactions.

The subsequent demonstration of a biochemical activity for the Ero1p protein has further distinguished the mechanisms used in the bacterial periplasm and the eukaryotic ER to oxidize substrate proteins. Whereas DsbB is coupled through ubiquinone to the electron transport pathway used in respiration, Ero1p is coupled to FAD metabolism. At this point, it is unclear how the electrons that are passed to FAD are disposed of, but it seems unlikely that the respiratory chain plays a role, as the depletion of heme or iron-sulfur clusters, which are key components of respiratory chain function, has no effect on the ability of yeast

171

cells to undergo oxidative protein folding. A number of important questions remain then concerning the mechanism of oxidation of Ero1p. Does the $FADH_2$ that results from oxidation of Ero1p react directly with oxygen, or is $FADH_2$ recycled enzymatically? How does Ero1p gain access to FAD in the first place?

In any event, the finding that glutathione is not required for oxidation *in vivo* (Cuozzo and Kaiser, 1999) or *in vitro* has dramatically altered our view of the requirements for oxidation of the ER. Rather than participating directly in oxidation, it now appears that oxidized glutathione is merely a by-product of the direct oxidation of proteins by an Ero1p-PDI system. In fact, the finding that deletion of glutathione from yeast allows an oxidation-defective strain to grow (Cuozzo and Kaiser, 1999) strongly supports the notion that protein oxidation is hampered by the presence of glutathione. Although this idea has yet to be tested directly, it now seems more likely that the relevant form of glutathione may be its reduced species, which can interact with a misfolded protein, reduce an incorrect disulfide, and, in the process, form oxidized glutathione.

Glutathione is now hypothesized to be responsible for preventing the ER from becoming overly-oxidizing, a condition in which disulfide bonds may become so favorable that the ER is unable to either maintain a protein in the reduced form necessary to re-arrange disulfide bonds or to directly reduce the incorrect bond. It is also possible that eukaryotes have a system analogous to

the bacterial DsbC/DsbD system for rearranging disulfide bonds, in which case further genetic screens should identify these putative factors.

The more general project actually grew out of the interest in disulfide bond formation. We made what seemed at the time to be a simple assumption: that the vast majority of the targets of the UPR would be factors involved in protein folding and that if we had a list of all UPR targets, we would have a thorough candidate list for identifying new factors that might be involved in oxidative folding. This seemed to be a reasonable assumption, as only seven genes had previously been shown to be targets of the UPR, and of those, six (*KAR2*, *EUG1*, *PDI1*, *LHS1*, *FKB2*, and *ERO1*) encoded members of recognized molecular chaperone families or other folding factors (Chapman et al., 1998).

The surprise of this work came when we realized that the transcriptional output of the UPR is quite prodigious. First, rather than being limited to ER factors, we found that genes encoding proteins with activities throughout the entire secretory pathway were activated, from the ER all the way out to the plasma membrane. Second, the UPR was not limited to just folding activities, although we did find that a large number of genes encoding chaperones and other folding factors were induced. Rather, a wide range of biochemical activities appeared to be activated by the UPR, from translocation into the ER, to transport between the ER and Golgi, to maintenance of the plasma membrane.

We chose to focus on one activity in particular, that of ER-associated degradation (ERAD), because it suggested the existence of a regulatory link that had not been previously recognized, despite the intensive research into the process of ERAD. This work demonstrated that UPR activation does indeed lead to an increase in the rate of protein degradation, and that without the ability to remove misfolded proteins through the process of ERAD, misfolded proteins accumulate to a significant degree. Most importantly, we were able to demonstrate that the UPR and ERAD together provide an essential function for the cell: the removal of the misfolded proteins that inevitably arise during normal cellular growth.

The work carried out so far in analyzing the transcriptional output of the UPR has likely only scratched the surface. First, there are many unknown ORFs within the list of UPR targets. Given the central importance to secretory pathway function of many of the UPR targets that have already been characterized, it is likely that many of the uncharacterized ORFs represent significant candidates for further study.

Second, in a more general sense, we have only examined the significance of one of the regulatory relationships detected from the transcriptional analysis of the UPR, that between the process of ERAD and the UPR. In that case, further analysis demonstrated a need for mechanisms to clear misfolded proteins from the secretory pathway: without them, cells could not survive. Although it has not

yet been thoroughly tested, we would propose that similar relationships exist between the UPR and other aspects of secretory pathway function. It would be of clear interest to look for such regulatory relationships. Some hint that they exist has already come from experiments performed by Davis Ng and colleagues. In the process of identifying mutations in genes that result in synthetic lethality with an inability to induce the UPR, it was found that defects in glycosylation interact genetically with the UPR (Ng et al., 2000).

Appendix A

Invertase Secretion During

Activation of the

Unfolded Protein Response

Introduction

Examination of all transcriptional targets of the unfolded protein response (UPR) has revealed that genes involved in processes distributed throughout the secretory pathway are induced in response to the accumulation of misfolded proteins (Chapter 4; Travers et al., 2000). These processes include translocation; protein glycosylation; vesicular transport between the ER and Golgi in both the antero- and retrograde directions; cell wall biosynthesis and maintenance; vacuolar protein targeting; and protein degradation, with a particular focus on those factors that are involved in ER-associated degradation (ERAD).

Mechanistic studies from a number of labs have now established the physiological significance of the relationship between ERAD and the UPR. First, efficient ERAD requires an intact UPR. In particular, deletion of *IRE1* decreased the ERAD of CPY* (Chapter 4; Travers et al., 2000) and MHC class I heavy chain (H-2K^b) in yeast (Casagrande et al., 2000). Second, loss of ERAD function leads to chronic UPR induction. Mutants defective for CPY* degradation show a small but significant induction of the UPR (Friedlander et al., 2000; Knop et al., 1996; Chapter 4; Travers et al., 2000). Alleles of *SEC61* with specific defects in ERAD, as well as deletions of several other ERAD components, also caused constitutive UPR induction (Zhou and Schekman, 1999). Thus, the accumulation of misfolded proteins in the ER appears to be a general consequence of loss of ERAD. Third, simultaneous loss of ERAD and UPR function greatly decrease

cell viability (Friedlander et al., 2000; Ng et al., 2000; Chapter 4; Travers et al., 2000).

In addition, the importance of the UPR regulation of another class of genes, those involved in glycosylation, has recently been demonstrated. While screening for mutations that are synthetically lethal with the inability to induce the UPR, Ng et al. (2000) identified genes involved in the addition of GPI anchors to proteins as well as genes involved in N-linked glycosylation. This finding is consistent with the importance in the folding process generally given to the attachment of sugars to proteins in the secretory pathway (Helenius and Aebi, 2001).

The significance of the UPR regulation of the other classes of genes has not been determined, although we would suggest that they would show phenotypes similar to those found for genes involved in ERAD and glycosylation. In the experiments described in this Appendix, we began to look for possible alterations in secretion during UPR activation. As components involved in multiple aspects of vesicle transport are activated by the UPR, including both antero- and retrograde transport, it was not clear whether we should expect quality control, and therefore secretion, to increase or decrease.

We chose to follow the secretion of a mutant form of invertase known as s11-invertase (Bohni et al., 1987). This mutant contains an alanine to isoleucine

substitution at the amino acid immediately preceding the signal peptidase cleavage site, amino acid 19. This mutation at the cleavage site results in greatly reduced secretion kinetics, such that s11-invertase is secreted with a half-life approximately 200-fold longer than the wild-type protein (Bohni et al., 1987). The mechanism that leads to retention of s11-invertase is not clear.

s11-invertase serves as a useful measure of secretion in two respects. First, it is not itself induced by the UPR, which allows us to independently control both UPR induction and the expression of s11-invertase. Second, the s11 mutant shows detectable levels of secretion. This is important because we do not know if we should expect secretion to increase or decrease during UPR induction and want to be able to detect a change in either direction.

Results and Discussion

We first examined the effect of varying the level of s11-invertase expression on the secretion of the protein. To do this, we created a strain in which the wild-type *SUC2* gene was replaced with a copy carrying the s11 mutation. This strain was then transformed with an empty vector, a low-copy (CEN/ARS) vector carrying the s11 allele, or a high-copy (2μ) vector carrying the s11 allele. Each of these strains was then induced for invertase expression, and the levels of external and internal activity were examined as a function of time (Figure 1).

Whereas wild-type invertase is secreted very rapidly following transfer to low glucose conditions, with little or no accumulation of internal activity, the s11-invertase is almost entirely retained within the cell, as expected from previous results with this mutation (Bohni et al., 1987). As the number of copies of the s11 allele is increased by transforming the strain with a CEN/ARS plasmid carrying the s11 allele, the overall expression goes up approximately three-fold, with a small increase in the external activity, although most of the invertase remains internal. If the levels of s11-invertase are dramatically increased by transformation with a 2μ plasmid carrying the s11 allele, the total level of expression again increases as expected. In this case, there is a much greater increase in the amount of invertase secreted from the cell, as approximately 30% of the total activity is found extracellularly when s11-invertase is over-expressed in this manner. The change in the amount of secreted protein indicates that the

mechanism responsible for preventing the progression of s11-invertase through the secretory pathway is saturable.

We next wished to examine the effect of UPR activation on the secretion of s11-invertase. This was accomplished using the hormone-inducible $HAC1^i$ expression system developed in our analysis of the UPR (Chapter 4; Travers et al., 2000). With this system, the addition of deoxycorticosterone to yeast cells carrying the glucocorticoid receptor (GR) activates expression from a promoter containing the glucocorticoid-responsive element (GRE). To look for a potential effect of UPR activation on s11-invertase secretion, we began with a strain that showed a slightly elevated level of s11-invertase secretion, the strain carrying the s11 allele both chromosomally and on a CEN/ARS plasmid. This strain was transformed with the GR-expressing plasmid and either an empty vector or the vector carrying $HAC1^i$. For comparison, a wild-type strain was also transformed with the GR-expressing plasmid and either an empty vector or the vector carrying $HAC1^i$.

In comparing the rates of accumulation of external invertase activity, we found that UPR activation had no effect on the secretion of wild-type invertase (Figure 2A). Furthermore, the secretion of the s11-invertase is also not changed by activation of the UPR (Figure 2B).

A number of modifications to this experiment will be necessary before drawing any definitive conclusions about the role of UPR activation in the retention of misfolded proteins. First, we previously observed that the levels of Hac1^{i}p protein expression peaked at approximately ninety minutes (Chapter 4; unpublished observations), after which the Hac1^{i}p protein rapidly disappeared from cells. In the experiment described here, invertase expression did not begin until after the ninety minutes of hormone treatment. Perhaps to see an effect, we would need invertase expression to occur coincident with the peak of UPR activation.

Second, our examination of the external expression of invertase may not have enough resolution to observe the changes that are occurring. As speculated in Chapter 4, perhaps UPR activation results in an increase in trafficking between the ER and Golgi. Such changes could not be observed with a simple activity assay, but would instead be observed by following the change in glycosylation of s11-invertase. Invertase undergoes extensive modification of its glycosylation structure in the Golgi, resulting in a dramatic alteration of its size. A change of this type could be followed in a pulse-chase IP analysis.

Finally, it may be worthwhile to repeat these experiments using cells carrying a 2μ version of the s11 allele. It is possible that the levels of s11-invertase that are secreted by cells carrying the CEN/ARS plasmid are not high enough to detect an effect of UPR activation. In this case, the higher levels of

expression seen with the 2μ plasmid may sensitize the cells enough to allow us to detect an alteration in the kinetics of s11-invertase secretion.

One potential drawback to the use of s11-invertase is that it is not at all clear what mechanism is used to retain it within the ER, although it has been suggested that this protein is a substrate of the quality control machinery (Elrod-Erickson and Kaiser, 1996). If s11-invertase were retained by a component of the secretory pathway that is not a target of the UPR, we would not expect UPR activation to have any effect on the distribution of s11-invertase. In this sense, it may be better to find another secretory protein whose mechanism of retention is known.

Experimental Procedures

General procedures and reagents

All nucleic acid manipulations were performed according to standard laboratory protocols (Ausubel et al., 1995). Yeast transformations were carried out by an optimized lithium acetate procedure (Geitz and Schiestl, 1995). Other yeast manipulations were carried out using standard methods (Sherman, 1991). The following oligonucleotides were used in this study:

P1,   AGGTTGAATTCCAAATTACCAGTCGGTATGCTACG;

P2,   3' Yeast GenePairs primer for *SUC2* (Research Genetics);

P3,   CGCTAGTTTCGTTTGTCATTGATATCGATATTTTGGCTGCAAAACCAGCC;

P4,   ATTACGGCAGGAGGTTTCCC;

P5,   GAGTTGGCAGCTAAAACAGG.

s11-Invertase Construction

The *SUC2* gene was cloned from the wild-type yeast strain W303-1B using oligonucleotides P1 and P2. The resulting PCR product includes 600 bp of sequence upstream of the start codon of *SUC2* and ends at the stop codon of *SUC2*. This PCR product was cloned into the pCR-Blunt II-TOPO vector (Invitrogen), and then sub-cloned into pRS306 using EcoRI and XmaI sites introduced by the PCR reaction, generating plasmid pKT049. The s11 allele was created in pKT049 using site-directed mutagenesis and oligonucleotide P3, generating plasmid pKT051. In addition to the A19I mutation, this

oligonucleotide includes a silent mutation that introduces an EcoRV site into the *SUC2* gene.

Strain Construction

Plasmid pKT051 was linearized with MluI. The wild-type strain W303-1B was transformed with the linearized plasmid using a standard yeast transformation protocol. Correct integration was confirmed by PCR using primers P4 and P5. Strains containing the correct insert were grown on YEPD and then on 5-FOA. Loss of the wild-type copy of *SUC2* was confirmed by PCR amplification using primers P4 and P5, followed by restriction analysis of the PCR product with EcoRV.

Invertase Assay

Assays were performed on whole cells for external activity measurements or on lysed spheroplasts for internal measurements as previously described (Chapter 2), with the following modifications to fit a 96-well plate format. Following the addition of sucrose and incubation at 30°C, 24 μl of each sample was transferred to a well in a 96-well plate. Assay mix (88 μl; 10 Units/ml glucose oxidase, 2.5 μg/ml peroxidase, 150 μg/ml o-dianisidine, 20μM NEM, 0.1M KP$_i$, pH 7.0) was then added to each well. After 10 to 15 minutes, the reaction was quenched with 88 μl 6N HCl.

UPR Activation

Wild-type cells containing pRS316, pCP220 (Chapter 4), and either pRS425-GRE or pCP274 (Chapter 4) were grown to mid-log phase, and then treated with 100μM deoxycorticosterone (DOC) for ninety minutes to induce *HAC1ⁱ* expression. Cells were then resuspended in SD media containing 0.1% glucose and 100μM DOC. For the 0 minute time points, cells were collected prior to resuspension in low glucose media. At 15, 30, 60, and 120 minutes, cells were collected and treated with 10mM NaN$_3$, and assayed for invertase activity as described above.

Figure 1. Retention of s11-invertase is saturable

Wild-type cells (WT + Ø) or cells carrying a genomic copy of s11-invertase with no additional copies (s11 + Ø), two to three extra copies (s11 + CEN/ARS s11), or many extra copies (s11 + 2μ s11) were induced for invertase expression by transferring to low glucose media. At the indicated time points, aliquots of cells were assayed for external invertase activity. Increased expression of s11-invertase results in an increase in secretion of the protein, although its secretion does not reach the levels of the wild-type protein at even the highest levels of expression.

Secreted Invertase Activity

Legend:
- s11 + Ø
- WT + Ø
- s11 + CEN/ARS s11
- s11 + 2μ s11

Y-axis: Invertase Activity
X-axis: Time (min)
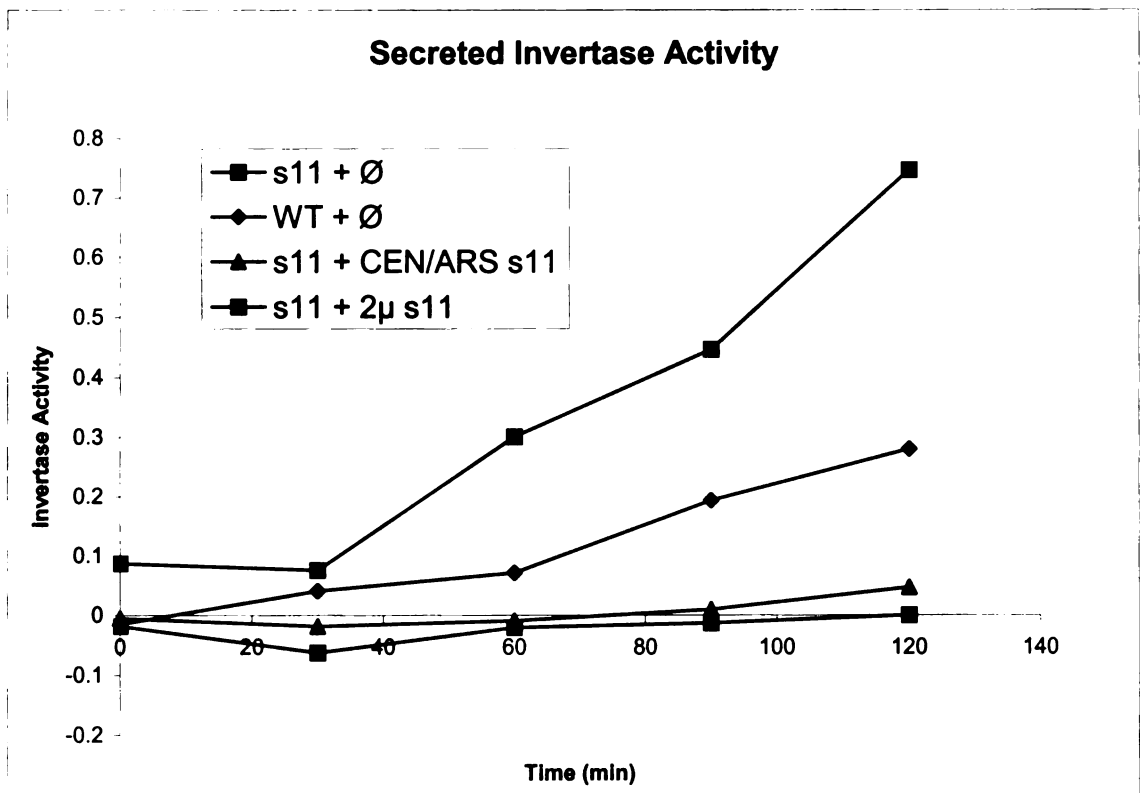
Figure 2. UPR induction does not alter the kinetics of secretion of wild-type or s11-invertase

(A) Cells carrying either an empty vector (WT + Ø) or a deoxycorticosterone (DOC)-inducible *HAC1^i* construct (WT + HAC1i) were treated with DOC for 90 minutes prior to transfer to low glucose media. At the indicated times, aliquots of cells were removed and assayed for invertase activity either on the cell surface (External) or within the cell (Internal). Quantitatively similar kinetics of invertase secretion are seen with and without UPR induction.

(B) Cells carrying a genomic copy of s11-invertase in addition to a CEN/ARS plasmid copy of s11-invertase were treated as in (A). As was seen with wild-type invertase, UPR activation does not alter the kinetics of secretion of s11-invertase.

A

Effect of UPR induction on invertase secretion

Legend:
- ◆ WT + Ø - External
- ▲ WT + HAC1i - External
- ■ WT + Ø - Internal
- ● WT + HAC1i - Internal

Y-axis: Invertase Activity (0 to 0.35)
X-axis: Time (min) (0 to 140)

B

Effect of UPR induction on s11-invertase secretion

Legend:
- ■ s11 + Ø - Internal
- ● s11 + HAC1i - Internal
- ▲ s11 + Ø - External
- ◆ s11 + HAC1i - External

Y-axis: Invertase Activity (0 to 0.4)
X-axis: Time (min) (0 to 140)
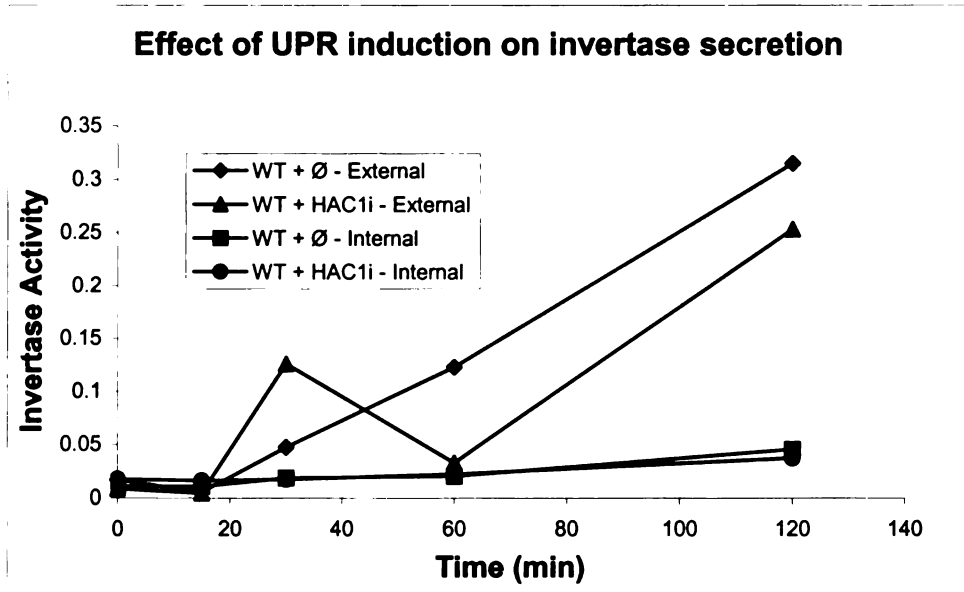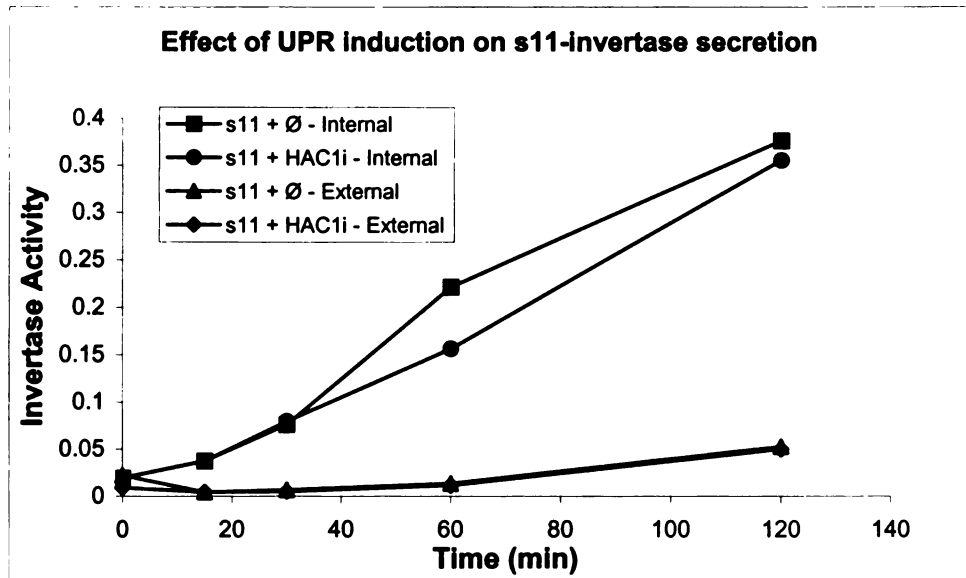
Appendix B

References

Anderson, M. E. (1985). Determination of glutathione and glutathione disulfide in biological samples, Meth. Enzymol. *113*, 548-55.

Andreasen, A. A., and Stier, T. J. B. (1953). J. Cell. Comp. Physiol. *41*, 23-6.

Andreasen, A. A., and Stier, T. J. B. (1954). J. Cell. Comp. Physiol. *43*, 271-81.

Anfinsen, C. B. (1973). Principles that govern the folding of protein chains, Science *181*, 223-30.

Astin, A. M., and Haslam, J. M. (1977). The manipulation of cellular cytochrome and lipid composition in a haem mutant of Saccharomyces cerevisiae, Biochem J *166*, 275-85.

Ausubel, F. M., Brent, R., Kingston, R. E., Moore, R. D., Seidman, J. G., Smith, J. A., and Struhl, K. (1995). Current Protocols in Molecular Biology (New York, John Wiley and Sons, Inc.).

Ayalon-Soffer, M., Shenkman, M., and Lederkremer, G. Z. (1999). Differential role of mannose and glucose trimming in the ER degradation of asialoglycoprotein receptor subunits, J. Cell Sci. *112*, 3309-18.

Bader, M., Muse, W., Ballou, D. P., Gassner, C., and Bardwell, J. C. (1999). Oxidative protein folding is driven by the electron transport system, Cell *98*, 217-27.

Baker, E. K., Colley, N. J., and Zuker, C. S. (1994). The cyclophilin homolog NinaA functions as a chaperone, forming a stable complex in vivo with its protein target rhodopsin, EMBO J. *13*, 4886-95.

Bardwell, J. C., Lee, J. O., Jander, G., Martin, N., Belin, D., and Beckwith, J. (1993). A pathway for disulfide bond formation in vivo, Proc. Natl. Acad. Sci. USA *90*, 1038-42.

Bardwell, J. C., McGovern, K., and Beckwith, J. (1991). Identification of a protein required for disulfide bond formation in vivo, Cell *67*, 581-9.

Barkovich, R. J., Shtanko, A., Shepherd, J. A., Lee, P. T., Myles, D. C., Tzagoloff, A., and Clarke, C. F. (1997). Characterization of the COQ5 gene from Saccharomyces cerevisiae. Evidence for a C-methyltransferase in ubiquinone biosynthesis, J. Biol. Chem. *272*, 9182-8.

Baumeister, W., Walz, J., Zühl, F., and Seemüller, E. (1998). The proteasome: paradigm of a self-compartmentalizing protease, Cell *92*, 367-80.

Bays, N. W., Gardner, R. G., Seelig, L. P., Joazeiro, C. A., and Hampton, R. Y. (2001). Hrd1p/Der3p is a membrane-anchored ubiquitin ligase required for ER-associated degradation, Nat. Cell Biol. *3*, 24-29.

Beinert, H., Holm, R. H., and Munck, E. (1997). Iron-sulfur clusters: nature's modular, multipurpose structures, Science *277*, 653-9.

Bertolotti, A., Zhang, Y., Hendershot, L. M., Harding, H. P., and Ron, D. (2000). Dynamic interaction of BiP and ER stress transducers in the unfolded-protein response, Nat. Cell Biol. *2*, 326-32.

Biederer, T., Volkwein, C., and Sommer, T. (1996). Degradation of subunits of the Sec61p complex, an integral component of the ER membrane, by the ubiquitin-proteasome pathway, EMBO J. *15*, 2069-76.

Biederer, T., Volkwein, C., and Sommer, T. (1997). Role of Cue1p in ubiquitination and degradation at the ER surface, Science *278*, 1806-9.

Bohni, P. C., Schauer, I., Tekamp-Olson, P., and Schekman, R. (1987). Signal peptide cleavage mutants of yeast invertase. In Proteases in biological control and biotechnology, D. Cunningham, and G. L. Long, eds. (New York, Liss), pp. 255-64.

Boisramé, A., Beckerich, J. M., and Gaillardin, C. (1999). A mutation in the secretion pathway of the yeast Yarrowia lipolytica that displays synthetic lethality in combination with a mutation affecting the signal recognition particle, Mol. Gen. Genet. *261*, 601-9.

Bonifacino, J. S., and Weissman, A. M. (1998). Ubiquitin and the control of protein fate in the secretory and endocytic pathways, Annu. Rev. Cell. Dev. Biol. *14*, 19-57.

Bordallo, J., Plemper, R. K., Finger, A., and Wolf, D. H. (1998). Der3p/Hrd1p is required for endoplasmic reticulum-associated degradation of misfolded lumenal and integral membrane proteins, Mol. Biol. Cell. *9*, 209-22.

Bose, S., Weikl, T., Bugl, H., and Buchner, J. (1996). Chaperone function of Hsp90- associated proteins, Science *274*, 1715-17.

Bowman, S., Churcher, C., Badcock, K., Brown, D., Chillingworth, T., Connor, R., Dedman, K., Devlin, K., Gentles, S., Hamlin, N., *et al.* (1997). The nucleotide sequence of Saccharomyces cerevisiae chromosome XIII, Nature *387*, 90-3.

Braakman, I., Helenius, J., and Helenius, A. (1992). Manipulating disulfide bond formation and protein folding in the endoplasmic reticulum, EMBO J. *11*, 1717-22.

Brodsky, J. L., Hamamoto, S., Feldheim, D., and Schekman, R. (1993).

Reconstitution of protein translocation from solubilized yeast membranes reveals

topologically distinct roles for BiP and cytosolic Hsc70, J. Cell Biol. *120*, 95-102.

Brodsky, J. L., and McCracken, A. A. (1999). ER protein quality control and

proteasome-mediated protein degradation, Sem. Cell Dev. Biol. *10*, 507-13.

Brodsky, J. L., Werner, E. D., Dubas, M. E., Goeckeler, J. L., Kruse, K. B., and

McCracken, A. A. (1999). The requirement for molecular chaperones during

endoplasmic reticulum-associated protein degradation demonstrates that protein

export and import are mechanistically distinct, J. Biol. Chem. *274*, 3453-60.

Brown, M. S., Ye, J., Rawson, R. B., and Goldstein, J. L. (2000). Regulated

intramembrane proteolysis: a control mechanism conserved from bacteria to

humans, Cell *100*, 391-8.

Buchner, J. (1999). Hsp90 & Co. - a holding for folding, Trends Biochem. Sci. *24*,

136-41.

Bukau, B., and Horwich, A. L. (1998). The Hsp70 and Hsp60 chaperone

machines, Cell *92*, 351-66.

Burns, N., Grimwade, B., Ross-Macdonald, P. B., Choi, E. Y., Finberg, K., Roeder, G. S., and Snyder, M. (1994). Large-scale analysis of gene expression, protein localization, and gene disruption in Saccharomyces cerevisiae, Genes Dev. *8*, 1087-105.

Cabibbo, A., Pagani, M., Fabbri, M., Rocchi, M., Farmery, M. R., Bulleid, N. J., and Sitia, R. (2000). ERO1-L, a human protein that favors disulfide bond formation in the endoplasmic reticulum, J. Biol. Chem. *275*, 4827-33.

Caplan, A. J. (1999). Hsp90's secrets unfold: new insights from structural and functional studies, Trends Cell Biol. *9*, 262-68.

Casagrande, R., Stern, P., Diehn, M., Shamu, C., Osario, M., Zuniga, M., Brown, P. O., and Ploegh, H. (2000). Degradation of proteins from the ER of S. cerevisiae requires an intact unfolded protein response pathway, Mol. Cell *5*, 729-35.

Chapman, R., Sidrauski, C., and Walter, P. (1998). Intracellular signaling from the endoplasmic reticulum to the nucleus, Annu. Rev. Cell. Dev. Biol. *14*, 459-85.

Cheng, M. Y., Hartl, F. U., Martin, J., Pollock, R. A., Kalousek, F., Neupert, W., Hallberg, E. M., Hallberg, R. L., and Horwich, A. L. (1989). Mitochondrial heat-

shock protein hsp60 is essential for assembly of proteins imported into yeast mitochondria, Nature *337*, 620-5.

Chillaron, J., Adan, C., and Haas, I. G. (2000). Mannosidase action, independen of glucose trimming, is essential for proteasome-mediated degradation of unassembled glycosylated Ig light chains, Biol. Chem. *381*, 1155-64.

Christianson, T. W., Sikorski, R. S., Dante, M., Shero, J. H., and Hieter, P. (1992). Multifunctional yeast high-copy-number shuttle vectors, Gene *110*, 119-22.

Chung, D. H., Ohashi, K., Watanabe, M., Miyasaka, N., and Hirosawa, S. (2000). Mannose trimming targets mutant alpha-2-plasmin inhibitor for degradation by the proteasome, J. Biol. Chem. *275*, 4981-87.

Colley, N. J., Baker, E. K., Stamnes, M. A., and Zuker, C. S. (1991). The cyclophilin homolog ninaA is required in the secretory pathway, Cell *67*, 255-63.

Cox, J. S., Chapman, R. E., and Walter, P. (1997). The unfolded protein response coordinates the production of endoplasmic reticulum protein and endoplasmic reticulum membrane, Mol. Biol. Cell. *8*, 1805-14.

Cox, J. S., Shamu, C. E., and Walter, P. (1993). Transcriptional induction of genes encoding endoplasmic reticulum resident proteins requires a transmembrane protein kinase, Cell *73*, 1197-206.

Cox, J. S., and Walter, P. (1996). A novel mechanism for regulating activity of a transcription factor that controls the unfolded protein response, Cell *87*, 391-404.

Creighton, T. E. (1977). Conformational restrictions on the pathway of folding and unfolding of the pancreatic trypsin inhibitor, J. Mol. Biol. *113*, 275-93.

Cuozzo, J. W., and Kaiser, C. A. (1999). Competition between glutathione and protein thiols for disulphide-bond formation, Nat. Cell Biol. *1*, 130-5.

Danese, P. N., and Silhavy, T. J. (1997). The sigma(E) and the Cpx signal transduction systems control the synthesis of periplasmic protein-folding enzymes in Escherichia coli, Genes Dev. *11*, 1183-93.

de Virgilio, M., Kitzmuller, C., Schwaiger, E., Klein, M., Kreibich, G., and Ivessa, N. E. (1999). Degradation of a short-lived glycoprotein from the lumen of the endoplasmic reticulum: the role of N-linked glycans and the unfolded protein response, Mol. Biol. Cell *10*, 4059-73.

de Virgilio, M., Weninger, H., and Ivessa, N. E. (1998). Ubiquitination is required for the retro-translocation of short-lived luminal endoplasmic reticulum glycoprotein to the cytosol for degradation by the proteasome, J. Biol. Chem. *273*, 9734-43.

Deak, P. M., and Wolf, D. H. (2001). Membrane topology and function of Der3/Hrd1p as an ubiquitin-ligase (E3) involved in endoplasmic reticulum degradation, J. Biol. Chem. *276*, 10663-69.

Doerrler, W. T., and Lehrman, M. A. (1999). Regulation of the dolichol pathway in human fibroblasts by the endoplasmic reticulum unfolded protein response, Proc. Natl. Acad. Sci. USA *96*, 13050-13055.

Dürr, G., Strayle, J., Plemper, R., Elbs, S., Klee, S. K., Catty, P., Wolf, D. H., and Rudolph, H. K. (1998). The medial-Golgi ion pump Pmr1 supplies the yeast secretory pathway with Ca2+ and Mn2+ required for glycosylation, sorting, and endoplasmic reticulum-associated protein degradation, Mol. Biol. Cell. *9*, 1149-62.

Edman, J. C., Ellis, L., Blacher, R. W., Roth, R. A., and Rutter, W. J. (1985). Sequence of protein disulphide isomerase and implications of its relationship to thioredoxin, Nature *317*, 267-70.

Eisen, M. B., Spellman, P. T., Brown, P. O., and Botstein, D. (1998). Cluster analysis and display of genome-wide expression patterns, Proc. Natl. Acad. Sci. USA *95*, 14863-8.

Ellgaard, L., Molinari, M., and Helenius, A. (1999). Setting the standards: Quality control in the secretory pathway, Science *286*, 1882-1888.

Elrod-Erickson, M. J., and Kaiser, C. A. (1996). Genes that control the fidelity of endoplasmic reticulum to Golgi transport identified as suppressors of vesicle budding mutations, Mol. Biol. Cell *7*, 1043-58.

Fahey, R. C., and Newton, G. L. (1987). Determination of low-molecular-weight thiols using monobromobimane fluorescent labeling and high-performance liquid chromatography, Meth. Enzymol. *143*, 85-96.

Farmer, T. H., Page, J. W., Payne, D. J., and Knowles, D. J. (1994). Kinetic and physical studies of beta-lactamase inhibition by a novel penem, BRL 42715, Biochem. J. *303*, 825-30.

Fenton, W. A., and Horwich, A. L. (1997). GroEL-mediated protein folding, Prot. Sci. *6*, 743-60.

Fernandez, F., D'Alessio, C., Fanchiotti, S., and Parodi, A. J. (1998). A misfolded protein conformation is not a sufficient condition for in vivo glucosylation by the UDP-Glc:glycoprotein glucosyltransferase, EMBO J. *17*, 5877-86.

Frand, A. R., Cuozzo, J. W., and Kaiser, C. A. (2000). Pathways for protein disulphide bond formation, Trends Cell Biol. *10*, 203-10.

Frand, A. R., and Kaiser, C. A. (1998). The ERO1 gene of yeast is required for oxidation of protein dithiols in the endoplasmic reticulum, Mol. Cell *1*, 161-70.

Frand, A. R., and Kaiser, C. A. (1999). Ero1p oxidizes protein disulfide isomerase in a pathway for disulfide bond formation in the endoplasmic reticulum, Mol. Cell *4*, 469-77.

Freedman, R. B., Hirst, T. R., and Tuite, M. F. (1994). Protein disulphide isomerase: building bridges in protein folding, Trends Biochem. Sci. *19*, 331-6.

Freeman, B. C., and Morimoto, R. I. (1996). The human cytosolic molecular chaperones hsp90, hsp70 (hsc70) and hdj-1 have distinct roles in recognition of a non-native protein and protein refolding, EMBO J. *5*, 2969-79.

Friedlander, R., Jarosch, E., Urban, J., Volkwein, C., and Sommer, T. (2000). A regulatory link between ER-associated protein degradation and the unfolded-protein response, Nat. Cell Biol. *2*, 379-84.

Gardner, R. G., Swarbrick, G. M., Bays, N. W., Cronin, S. R., Wilhovsky, S., Seelig, L., Kim, C., and Hampton, R. Y. (2000). Endoplasmic reticulum degradation requires lumen to cytosol signaling. Transmembrane control of Hrd1p by Hrd3p, J. Cell Biol. *151*, 69-82.

Gaynor, E. C., te Heesen, S., Graham, T. R., Aebi, M., and Emr, S. D. (1994). Signal-mediated retrieval of a membrane protein from the Golgi to the ER in yeast, J. Cell. Biol. *127*, 653-665.

Geitz, R. D., and Schiestl, R. H. (1995). Transformation of yeast with DNA, Meth. Mol. Cell. Biol. *5*, 255-269.

Gething, M. J., and Sambrook, J. (1992). Protein folding in the cell, Nature *355*, 33-45.

Gilbert, H. F. (1990). Molecular and cellular aspects of thiol-disulfide exchange, Adv. Enzymol. Relat. Areas Mol. Biol. *63*, 69-172.

Gillece, P., Luz, J. M., Lennarz, W. J., de La Cruz, F. J., and Römisch, K. (1999). Export of a cysteine-free misfolded secretory protein from the endoplasmic reticulum for degradation requires interaction with protein disulfide isomerase, J. Cell Biol. *147*, 1443- 56.

Goldberger, R. F., Epstein, C. J., and Anfinsen, C. B. (1963). Purification and properties of a microsomal enzyme system catalyzing the reactivation of reduced ribonuclease and lysozyme, J. Biol. Chem. *238*, 1406-1410.

Gollub, E. G., Liu, K. P., Dayan, J., Adlersberg, M., and Sprinson, D. B. (1977). Yeast mutants deficient in heme biosynthesis and a heme mutant additionally blocked in cyclization of 2,3-oxidosqualene, J. Biol. Chem. *252*, 2846-54.

Gonzalez, T. N., Sidrauski, C., Dörfler, S., and Walter, P. (1999). Mechanism of non-spliceosomal mRNA splicing in the unfolded protein response pathway, EMBO J. *18*, 3119-32.

Grenert, J. P., Johnson, B. D., and Toft, D. O. (1999). The importance of ATP binding and hydrolysis by hsp90 in formation and function of protein heterocomplexes, J. Biol. Chem. *274*, 17525-33.

Guilhot, C., Jander, G., Martin, N. L., and Beckwith, J. (1995). Evidence that the pathway of disulfide bond formation in Escherichia coli involves interactions

between the cysteines of DsbB and DsbA, Proc. Natl. Acad. Sci. USA *92*, 9895-9.

Guthrie, C., and Fink, G. (1991). Guide to Yeast Genetics and Molecular Biology, Meth. Enzymol. *194*, 933.

Hamman, B. D., Hendershot, L. M., and Johnson, A. E. (1998). BiP maintains the permeability barrier of the ER membrane by sealing the lumenal end of the translocation pore before and early in translocation, Cell *92*, 747-58.

Hammond, C., Braakman, I., and Helenius, A. (1994). Role of N-linked oligosaccharide recognition, glucose trimming, and calnexin in glycoprotein folding and quality control, Proc. Natl. Acad. Sci. USA *91*, 913-17.

Hammond, C., and Helenius, A. (1994). Quality control in the secretory pathway: retention of a misfolded viral membrane glycoprotein involves cycling between the ER, intermediate compartment, and Golgi apparatus, J. Cell Biol. *126*, 41-52.

Hammond, C., and Helenius, A. (1995). Quality control in the secretory pathway, Curr. Opin. Cell Biol. *7*, 523-9.

Hampton, R. Y., and Bhakta, H. (1997). Ubiquitin-mediated regulation of 3-hydroxy-3-methylglutaryl-CoA reductase, Proc. Natl. Acad. Sci. USA *94*, 12944-8.

Hampton, R. Y., Gardner, R. G., and Rine, J. (1996). Role of 26S proteasome and HRD genes in the degradation of 3-hydroxy-3-methylglutaryl-CoA reductase, an integral endoplasmic reticulum membrane protein, Mol. Biol. Cell *7*, 2029-44.

Harding, H. P., Zhang, Y., and Ron, D. (1999). Protein translation and folding are coupled by an endoplasmic-reticulum-resident kinase, Nature *397*, 271-4.

Hardwick, K. G., and Murray, A. W. (1995). Mad1p, a phosphoprotein component of the spindle assembly checkpoint in budding yeast, J. Cell Biol. *131*, 709-20.

Hartl, F. U. (1996). Molecular chaperones in cellular protein folding, Nature *381*, 571-9.

Hartwell, L. H. (1967). Macromolecule synthesis in temperature-sensitive mutants of yeast, J. Bacteriol. *93*, 1662-70.

Haze, K., Yoshida, H., Yanagi, H., Yura, T., and Mori, K. (1999). Mammalian transcription factor ATF6 is synthesized as a transmembrane protein and

activated by proteolysis in response to endoplasmic reticulum stress, Mol. Biol. Cell *10*, 3787-99.

Hebert, D. N., Foellmer, B., and Helenius, A. (1995). Glucose trimming and reglucosylation determine glycoprotein association with calnexin in the endoplasmic reticulum, Cell *81*, 425-33.

Helenius, A., and Aebi, M. (2001). Intracellular functions of N-linked glycans, Science *291*, 2364-9.

Helenius, A., Marquardt, T., and Braakman, I. (1992). The endoplasmic reticulum as a protein-folding compartment, Trends Cell Biol. *2*, 227-31.

Hemmingsen, S. M., Woolford, C., van der Vies, S. M., Tilly, K., Dennis, D. T., Georgopoulos, C. P., Hendrix, R. W., and Ellis, R. J. (1988). Homologous plant and bacterial proteins chaperone oligomeric protein assembly, Nature *333*, 330-4.

Hiller, M. M., Finger, A., Schweiger, M., and Wolf, D. H. (1996). ER degradation of a misfolded luminal protein by the cytosolic ubiquitin-proteasome pathway, Science *273*, 1725-8.

Hillier, B. J., Christopherson, K. S., Prehoda, K. E., Bredt, D. S., and Lim, W. A. (1999). Unexpected modes of PDZ domain scaffolding revealed by structure of nNOS-syntrophin complex, Science *284*, 812-5.

Holst, B., Tachibana, C., and Winther, J. R. (1997). Active site mutations in yeast protein disulfide isomerase cause dithiothreitol sensitivity and a reduced rate of protein folding in the endoplasmic reticulum, J. Cell Biol. *138*, 1229-38.

Hong, E., Davidson, A. R., and Kaiser, C. A. (1996). A pathway for targeting soluble misfolded proteins to the yeast vacuole, J. Cell. Biol. *135*, 623-33.

Horazdovsky, B. F., and Emr, S. D. (1993). The VPS16 gene product associates with a sedimentable protein complex and is essential for vacuolar protein sorting in yeast, J. Biol. Chem. *268*, 4953-62.

Hurtley, S. M., and Helenius, A. (1989). Protein oligomerization in the endoplasmic reticulum, Annu. Rev. Cell Biol. *5*, 277-307.

Hwang, C., Sinskey, A. J., and Lodish, H. F. (1992). Oxidized redox state of glutathione in the endoplasmic reticulum, Science *257*, 1496-502.

Jakob, C. A., Burda, P., Roth, J., and Aebi, M. (1998). Degradation of misfolded endoplasmic reticulum glycoproteins in Saccharomyces cerevisiae is determined by a specific oligosaccharide structure, J. Cell Biol. *142*, 1223-33.

Jämsä, E., Simonen, M., and Makarow, M. (1994). Selective retention of secretory proteins in the yeast endoplasmic reticulum by treatment of cells with a reducing agent, Yeast *10*, 355-70.

Jämsä, E., Vakula, N., Arffman, A., Kilpelainen, I., and Makarow, M. (1995). In vivo reactivation of heat-denatured protein in the endoplasmic reticulum of yeast, EMBO J. *14*, 6028-33.

Jensen, T. J., Loo, M. A., Pind, S., Williams, D. B., Goldberg, A. L., and Riordan, J. R. (1995). Multiple proteolytic systems, including the proteasome, contribute to CFTR processing, Cell *83*, 129-35.

Johnson, A. E., and van Waes, M. A. (1999). The translocon: a dynamic gateway at the ER membrane, Annu. Rev. Cell Dev. Biol. *15*, 799-842.

Johnson, B. D., Schumacher, R. J., Ross, E. D., and Toft, D. O. (1998). Hop modulates Hsp70/Hsp90 interactions in protein folding, J. Biol. Chem. *273*, 3679-86.

Kaderbhai, M. A., and Austen, B. M. (1985). Studies on the formation of intrachain disulphide bonds in newly biosynthesised bovine prolactin. Role of protein-disulphide isomerase, Eur. J. Biochem. *153*, 167-78.

Kaffman, A., Rank, N. M., and O'Shea, E. K. (1998). Phosphorylation regulates association of the transcription factor Pho4 with its import receptor Pse1/Kap121, Genes Dev. *12*, 2673-83.

Kagiwada, S., Hosaka, K., Murata, M., Nikawa, J., and Takatsuki, A. (1998). The Saccharomyces cerevisiae SCS2 gene product, a homolog of a synaptobrevin-associated protein, is an integral membrane protein of the endoplasmic reticulum and is required for inositol metabolism, J. Bacteriol. *180*, 1700-8.

Kaiser, C. A., and Schekman, R. (1990). Distinct sets of SEC genes govern transport vesicle formation and fusion early in the secretory pathway, Cell *61*, 723-33.

Katayama, T., Imaizumi, K., Sato, N., Miyoshi, K., Kudo, T., Hitomi, J., Morihara, T., Yoneda, T., Gomi, F., Mori, Y., *et al.* (1999). Presenilin-1 mutations downregulate the signalling pathway of the unfolded-protein response, Nat. Cell Biol. *1*, 479-85.

Kawahara, T., Yanagi, H., Yura, T., and Mori, K. (1997). Endoplasmic reticulum stress-induced mRNA splicing permits synthesis of transcription factor Hac1p/Ern4p that activates the unfolded protein response, Mol. Biol. Cell. *8*, 1845-62.

Kemmink, J., Darby, N. J., Dijkstra, K., Nilges, M., and Creighton, T. E. (1997). The folding catalyst protein disulfide isomerase is constructed of active and inactive thioredoxin modules, Curr. Biol. *7*, 239-45.

Kishigami, S., Akiyama, Y., and Ito, K. (1995a). Redox states of DsbA in the periplasm of Escherichia coli, FEBS Lett. *364*, 55-8.

Kishigami, S., Kanaya, E., Kikuchi, M., and Ito, K. (1995b). DsbA-DsbB interaction through their active site cysteines. Evidence from an odd cysteine mutant of DsbA, J. Biol. Chem. *270*, 17072-4.

Kispal, G., Csere, P., Prohl, C., and Lill, R. (1999). The mitochondrial proteins Atm1p and Nfs1p are essential for biogenesis of cytosolic Fe/S proteins, EMBO J. *18*, 3981-9.

Knittler, M., Dirks, R. S., and Haas, I. G. (1995). Molecular chaperones involved in protein degradation in the endoplasmic reticulum: quantitative interaction of the heat shock cognate protein BiP with partially folded immunoglobulin light

chains that are degraded in the endoplasmic reticulum, Proc. Natl. Acad. Sci. USA *92*, 764-68.

Knop, M., Finger, A., Braun, T., Hellmuth, K., and Wolf, D. H. (1996). Der1, a novel protein specifically required for endoplasmic reticulum degradation in yeast, EMBO J. *15*, 753-63.

Kobayashi, T., Kishigami, S., Sone, M., Inokuchi, H., Mogi, T., and Ito, K. (1997). Respiratory chain is required to maintain oxidized states of the DsbA-DsbB disulfide bond formation system in aerobically growing Escherichia coli cells, Proc. Natl. Acad. Sci. USA *94*, 11857-62.

Koivunen, P., Pirneskoski, A., Karvonen, P., Ljung, J., Helaakoski, T., Notbohm, H., and Kivirikko, K. I. (1999). The acidic C-terminal domain of protein disulfide isomerase is not critical for the enzyme subunit function or for the chaperone or disulfide isomerase activities of the polypeptide, EMBO J. *18*, 65-74.

Konishi, Y., Ooi, T., and Scheraga, H. A. (1982a). Regeneration of ribonuclease A from the reduced protein. Energetic analysis, Biochemistry *21*, 4741-8.

Konishi, Y., Ooi, T., and Scheraga, H. A. (1982b). Regeneration of ribonuclease A from the reduced protein. Rate-limiting steps, Biochemistry *21*, 4734-40.

Laboissiere, M. C., Sturley, S. L., and Raines, R. T. (1995). The essential function of protein-disulfide isomerase is to unscramble non-native disulfide bonds, J. Biol. Chem. *270*, 28006-9.

Lambert, N., and Freedman, R. B. (1985). The latency of rat liver microsomal protein disulphide-isomerase, Biochem. J. *228*, 635-45.

Lang, K., Schmid, F. X., and Fischer, G. (1987). Catalysis of protein folding by prolyl isomerase, Nature *329*, 268-70.

Leegwater, P. A., Strating, M., Murphy, N. B., Kooy, R. F., van der Vliet, P. C., and Overdulve, J. P. (1991). The Trypanosoma brucei DNA polymerase alpha core subunit gene is developmentally regulated and linked to a constitutively expressed open reading frame, Nuc. Acids Res. *19*, 6441-7.

Liberek, K., Marszalek, J., Ang, D., Georgopoulos, C., and Zylicz, M. (1991). Escherichia coli dnaJ and grpE heat shock proteins jointly stimulate ATPase activity of dnaK, Proc. Natl. Acad. Sci. USA *88*, 2874-2878.

Liu, Y., Choudhury, P., Cabral, C. M., and Sifers, R. N. (1999). Oligosaccharide modification in the early secretory pathway directs the selection of a misfolded glycoprotein for degradation by the proteasome, J. Biol. Chem. *274*, 5861-67.

Loayza, D., and Michaelis, S. (1998). Role for the ubiquitin-proteasome system in the vacuolar degradation of Ste6p, the a-factor transporter in Saccharomyces cerevisiae, Mol. Cell. Biol. *18*, 779-89.

Longtine, M. S., McKenzie, A., 3rd, Demarini, D. J., Shah, N. G., Wach, A., Brachat, A., Philippsen, P., and Pringle, J. R. (1998). Additional modules for versatile and economical PCR-based gene deletion and modification in Saccharomyces cerevisiae, Yeast *14*, 953-61.

Lu, Y., Turnbull, I. R., Bragin, A., Carveth, K., Verkman, A. S., and Skach, W. R. (2000). Reorientation of aquaporin-1 topology during maturation in the endoplasmic reticulum, Mol. Biol. Cell *11*, 2973-85.

Lundström, J., and Holmgren, A. (1993). Determination of the reduction-oxidation potential of the thioredoxin-like domains of protein disulfide-isomerase from the equilibrium with glutathione and thioredoxin, Biochemistry *32*, 6649-55.

Lyles, M. M., and Gilbert, H. F. (1991). Catalysis of the oxidative folding of ribonuclease A by protein disulfide isomerase: dependence of the rate on the composition of the redox buffer, Biochemistry *30*, 613-9.

Marquardt, T., Hebert, D. N., and Helenius, A. (1993). Post-translational folding of influenza hemagglutinin in isolated endoplasmic reticulum-derived microsomes, J. Biol. Chem. *268*, 19618-25.

Martin, J. L., Bardwell, J. C., and Kuriyan, J. (1993). Crystal structure of the DsbA protein required for disulphide bond formation in vivo, Nature *365*, 464-8.

Matsumura, M., Signor, G., and Matthews, B. W. (1989). Substantial increase of protein stability by multiple disulphide bonds, Nature *342*, 291-3.

Mayer, M. P., and Bukau, B. (1999). Molecular chaperones: the busy life of Hsp90, Curr. Biol. *9*, R322-5.

McCarty, J. S., Buchberger, A., Reinstein, J., and Bukau, B. (1995). The role of ATP in the functional cycle of the DnaK chaperone system, J. Mol. Biol. *249*, 126-37.

McCracken, A. A., and Brodsky, J. L. (1996). Assembly of ER-associated protein degradation in vitro: dependence on cytosol, calnexin, and ATP, J. Cell. Biol. *132*, 291-8.

McCracken, A. A., Karpichev, I. V., Ernaga, J. E., Werner, E. D., Dillin, A. G., and Courchesne, W. E. (1996). Yeast mutants deficient in ER-associated degradation of the Z variant of alpha-1-protease inhibitor, Genetics *144*, 1355-62.

McGee, T. P., Cheng, H. H., Kumagai, H., Omura, S., and Simoni, R. D. (1996). Degradation of 3-hydroxymethyl-3-glutaryl-CoA reductase in endoplasmic reticulum membranes is accelerated as a result of increased susceptibility to proteolysis, J. Biol. Chem. *271*, 25630-38.

Melnick, J., Dul, J. L., and Argon, Y. (1994). Sequential interaction of the chaperones BiP and GRP94 with immunoglobulin chains in the endoplasmic reticulum, Nature *370*, 373-75.

Missiakas, D., Georgopoulos, C., and Raina, S. (1993). Identification and characterization of the Escherichia coli gene dsbB, whose product is involved in the formation of disulfide bonds in vivo, Proc. Natl. Acad. Sci. USA *90*, 7084-8.

Missiakas, D., Georgopoulos, C., and Raina, S. (1994). The Escherichia coli dsbC (xprA) gene encodes a periplasmic protein involved in disulfide bond formation, EMBO J. *13*, 2013-20.

Missiakas, D., and Raina, S. (1997). Protein folding in the bacterial periplasm, J. Bacteriol. *179*, 2465-71.

Missiakas, D., Schwager, F., and Raina, S. (1995). Identification and characterization of a new disulfide isomerase-like protein (DsbD) in Escherichia coli, EMBO J. *14*, 3415-24.

Moir, D., Stewart, S. E., Osmond, B. C., and Botstein, D. (1982). Cold-sensitive cell-division-cycle mutants of yeast: isolation, properties, and pseudoreversion studies, Genetics *100*, 547-63.

Mori, K., Kawahara, T., Yoshida, H., Yanagi, H., and Yura, T. (1996). Signalling from endoplasmic reticulum to nucleus: transcription factor with a basic-leucine zipper motif is required for the unfolded protein-response pathway, Genes Cells *1*, 803-17.

Mori, K., Ma, W., Gething, M., and Sambrook, J. (1993). A transmembrane protein with a cdc2+/CDC28-related kinase activity is required for signaling from the ER to the nucleus, Cell *74*, 743-56.

Mori, K., Sant, A., Kohno, K., Normington, K., Gething, M. J., and Sambrook, J. F. (1992). A 22 bp cis-acting element is necessary and sufficient for the induction of the yeast KAR2 (BiP) gene by unfolded proteins, EMBO J. *11*, 2583-93.

Nakatsukasa, K., Nishikawa, S., Hosokawa, N., Nagata, K., and Endo, T. (2001). Mnl1p, an alpha-mannosidase-like protein in yeast Saccharomyces cerevisiae, is

required for ER associated degradation of glycoproteins, J. Biol. Chem. *276*, 8635-8638.

Nasmyth, K. A., and Reed, S. I. (1980). Isolation of genes by complementation in yeast: molecular cloning of a cell-cycle gene, Proc. Natl. Acad. Sci. USA *77*, 2119-23.

Nathan, D. F., Vos, M. H., and Lindquist, S. (1997). In vivo functions of the Saccharomyces cerevisiae Hsp90 chaperone, Proc. Natl. Acad. Sci. USA *94*, 12949-56.

Nehls, S., Snapp, E. L., Cole, N. B., Zaal, K. J., Kenworthy, A. K., Roberts, T. H., Ellenberg, J., Presley, J. F., Siggia, E., and Lippincott-Schwartz, J. (2000). Dynamics and retention of misfolded proteins in native ER membranes, Nat. Cell Biol. *2*, 288-95.

Ng, D. T., Spear, E. D., and Walter, P. (2000). The unfolded protein response regulates multiple aspects of secretory and membrane protein biogenesis and endoplasmic reticulum quality control, J. Cell Biol. *150*, 77-88.

Ng, F. W., Nguyen, M., Kwan, T., Branton, P. E., Nicholson, D. W., Cromlish, J. A., and Shore, G. C. (1997). p28 Bap31, a Bcl-2/Bcl-XL- and procaspase-8-associated protein in the endoplasmic reticulum, J. Cell. Biol. *139*, 327-38.

Nishikawa, S., and Endo, T. (1997). The yeast Jem1p is a DnaJ-like protein of the endoplasmic reticulum membrane required for nuclear fusion, J. Biol. Chem. *272*, 12889- 92.

Nishikawa, S., Fewell, S. W., Kato, Y., Brodsky, J. L., and Endo, T. (2001). Molecular chaperones in the yeast ER maintain the solubility of proteins for retro-translocation and degradation, J. Cell Biol. *153*, 1061-69.

Niwa, M., Sidrauski, C., Kaufman, R. J., and Walter, P. (1999). A role for presenilin-1 in nuclear accumulation of Ire1 fragments and induction of the mammalian unfolded protein response, Cell *99*, 691-702.

Oda, K., Ikehara, Y., and Omura, S. (1996). Lactacystin, an inhibitor of the proteasome, blocks the degradation of a mutant precursor of glycosylphosphatidylinositol-linked protein in a pre-Golgi compartment, Biochem. Biophys. Res. Commun. *219*, 800-05.

Okamura, K., Kimata, Y., Higashio, H., Tsuru, A., and Kohno, K. (2000). Dissociation of Kar2p/BiP from an ER sensory molecule, Ire1p, triggers the unfolded protein response in yeast, Biochem. Biophys. Res. Commun. *279*, 445-50.

Ostermann, J., Horwich, A. L., Neupert, W., and Hartl, F. U. (1989). Protein folding in mitochondria requires complex formation with hsp60 and ATP hydrolysis, Nature *341*, 125-30.

Ou, W. J., Cameron, P. H., Thomas, D. Y., and Bergeron, J. J. (1993). Association of folding intermediates of glycoproteins with calnexin during protein maturation, Nature *364*, 771-6.

Parodi, A. J. (2000). Protein glycosylation and its role in protein folding, Annu. Rev. Biochem. *69*, 69-93.

Parodi, A. J., Lederkremer, G. Z., and Mendelzon, D. H. (1983). Protein glycosylation in Trypanosoma cruzi. The mechanism of glycosylation and structure of protein-bound oligosaccharides, J. Biol. Chem. *258*, 5589-95.

Pelham, H. R. (1986). Speculations on the functions of the major heat shock and glucose-regulated proteins, Cell *46*, 959-61.

Pilon, M., Schekman, R., and Römisch, K. (1997). Sec61p mediates export of a misfolded secretory protein from the endoplasmic reticulum to the cytosol for degradation, EMBO J. *16*, 4540-48.

Plemper, R. K., Böhmler, S., Bordallo, J., Sommer, T., and Wolf, D. H. (1997). Mutant analysis links the translocon and BiP to retrograde protein transport for ER degradation, Nature *388*, 891-5.

Plemper, R. K., and Wolf, D. H. (1999). Retrograde protein translocation: ERADication of secretory proteins in health and disease, Trends Biochem. Sci. *24*, 266-70.

Pollard, M. G., Travers, K. J., and Weissman, J. S. (1998). Ero1p: a novel and ubiquitous protein with an essential role in oxidative protein folding in the endoplasmic reticulum, Mol. Cell *1*, 171-82.

Poon, W. W., Do, T. Q., Marbois, B. N., and Clarke, C. F. (1997). Sensitivity to treatment with polyunsaturated fatty acids is a general characteristic of the ubiquinone-deficient yeast coq mutants, Mol. Aspects Med. *18 Suppl*, S121-7.

Qu, D., Teckman, J. H., Omura, S., and Perlmutter, D. H. (1996). Degradation of a mutant secretory protein, alpha1-antitrypsin Z, in the endoplasmic reticulum requires proteasome activity, J. Biol. Chem. *271*, 22791-5.

Reddy, P. S., and Corley, R. B. (1998). Assembly, sorting, and exit of oligomeric proteins from the endoplasmic reticulum, Bioessays *20*, 546-54.

Rietsch, A., and Beckwith, J. (1998). The genetics of disulfide bond metabolism, Annu. Rev. Genet. *32*, 163-84.

Rietsch, A., Belin, D., Martin, N., and Beckwith, J. (1996). An in vivo pathway for disulfide bond isomerization in Escherichia coli, Proc. Natl. Acad. Sci. USA *93*, 13048-53.

Roberg, K. J., Crotwell, M., Espenshade, P., Gimeno, R., and Kaiser, C. A. (1999). LST1 is a SEC24 homologue used for selective export of the plasma membrane ATPase from the endoplasmic reticulum, J. Cell Biol. *145*, 673-688.

Robinson, A. S., and King, J. (1997). Disulphide-bonded intermediate on the folding and assembly pathway of a non-disulphide bonded protein, Nat. Struct. Biol. *4*, 450-5.

Rothman, J. E. (1989). Polypeptide chain binding proteins: catalysts of protein folding and related processes in cells, Cell *59*, 591-601.

Saibil, H. (2000). Molecular chaperones: containers and surfaces for folding, stabilising or unfolding proteins, Curr. Opin. Struct. Biol. *10*, 251-8.

Santos, M. A., García-Ramírez, J. J., and Revuelta, J. L. (1995). Riboflavin biosynthesis in Saccharomyces cerevisiae. Cloning, characterization, and

expression of the RIB5 gene encoding riboflavin synthase, J. Biol. Chem. *270*, 437-44.

Saris, N., Holkeri, H., Craven, R. A., Stirling, C. J., and Makarow, M. (1997). The Hsp70 homologue Lhs1p is involved in a novel function of the yeast endoplasmic reticulum, refolding and stabilization of heat-denatured protein aggregates, J. Cell Biol. *137*, 813-24.

Sato, N., Urano, F., Yoon Leem, J., Kim, S. H., Li, M., Donoviel, D., Bernstein, A., Lee, A. S., Ron, D., Veselits, M. L., *et al.* (2000). Upregulation of BiP and CHOP by the unfolded-protein response is independent of presenilin expression, Nat. Cell Biol. *2*, 863-70.

Sauer, R. T., Hehir, K., Stearman, R. S., Weiss, M. A., Jeitler-Nilsson, A., Suchanek, E. G., and Pabo, C. O. (1986). An engineered intersubunit disulfide enhances the stability and DNA binding of the N-terminal domain of lambda repressor, Biochemistry *25*, 5992-8.

Scheele, G., and Jacoby, R. (1983). Proteolytic processing of presecretory proteins is required for development of biological activities in pancreatic exocrine proteins, J. Biol. Chem. *258*, 2005-9.

Schena, M., Picard, D., and Yamamoto, K. R. (1991). Vectors for constitutive and inducible gene expression in yeast, Meth. Enzymol. *194*, 389-98.

Schiebel, T., and Buchner, J. (1997). The Hsp90 family - an overview. In Guidebook to molecular chaperones and protein-folding catalysts, M.-J. Gething, ed. (Oxford, Oxford University Press), pp. 147-51.

Schlenstedt, G., Harris, S., Risse, B., Lill, R., and Silver, P. A. (1995). A yeast DnaJ homologue, Scj1p, can function in the endoplasmic reticulum with Bip/Kar2p via a conserved domain that specifies interactions with hsp70s, J. Cell Biol. *129*, 979-88.

Schmid, D., Baici, A., Gehring, H., and Christen, P. (1994). Kinetics of molecular chaperone action, Science *263*, 971-3.

Schmitt, M. E., Brown, T. A., and Trumpower, B. L. (1990). A rapid and simple method for preparation of RNA from Saccharomyces cerevisiae, Nuc. Acids Res. *18*, 3091-2.

Schmitz, A., Maintz, M., Kehle, T., and Herzog, V. (1995). In vivo iodination of a misfolded proinsulin reveals co-localized signals for Bip binding and for degradation in the ER, EMBO J. *14*, 1091-98.

Schneider, K. R., Smith, R. L., and O'Shea, E. K. (1994). Phosphate-regulated inactivation of the kinase PHO80-PHO85 by the CDK inhibitor PHO81, Science *266*, 122-6.

Schultz, S. C., Dalbadie-McFarland, G., Neitzel, J. J., and Richards, J. H. (1987). Stability of wild-type and mutant RTEM-1 beta-lactamases: effect of the disulfide bond, Proteins *2*, 290-7.

Schumacher, R. J., Hansen, W. J., Freeman, B. C., Alnemri, E., Litwack, G., and Toft, D. O. (1996). Cooperative action of Hsp70, Hsp90, and DnaJ proteins in protein renaturation, Biochemistry *35*, 14889-98.

Shamu, C. E., and Walter, P. (1996). Oligomerization and phosphorylation of the Ire1p kinase during intracellular signaling from the endoplasmic reticulum to the nucleus, EMBO J. *15*, 3028-39.

Sherman, F. (1991). Getting started with yeast, Meth. Enzymol. *194*, 3-21.

Shevchik, V. E., Condemine, G., and Robert-Baudouy, J. (1994). Characterization of DsbC, a periplasmic protein of Erwinia chrysanthemi and Escherichia coli with disulfide isomerase activity, EMBO J. *13*, 2007-12.

Shi, Y., Vattem, K. M., Sood, R., An, J., Liang, J., Stramm, L., and Wek, R. C. (1998). Identification and characterization of pancreatic eukaryotic initiation factor

2 alpha-subunit kinase, PEK, involved in translational control, Mol. Cell. Biol. *18*, 7499-509.

Sidrauski, C., Cox, J. S., and Walter, P. (1996). tRNA ligase is required for regulated mRNA splicing in the unfolded protein response, Cell *87*, 405-13.

Sidrauski, C., and Walter, P. (1997). The transmembrane kinase Ire1p is a site-specific endonuclease that initiates mRNA splicing in the unfolded protein response, Cell *90*, 1031-9.

Sigler, P. B., Xu, Z., Rye, H. S., Burston, S. G., Fenton, W. A., and Horwich, A. L. (1998). Structure and function in GroEL-mediated protein folding, Annu. Rev. Biochem. *67*, 581-608.

Sikorski, R. S., and Hieter, P. (1991). A system of shuttle vectors and yeast host strains designed for efficient manipulation of DNA in Saccharomyces cerevisiae, Genetics *122*, 19-27.

Simonen, M., Jämsä, E., and Makarow, M. (1994). The role of the carrier protein and disulfide formation in the folding of beta-lactamase fusion proteins in the endoplasmic reticulum of yeast, J. Biol. Chem. *269*, 13887-92.

Simons, J. F., Ferro-Novick, S., Rose, M. D., and Helenius, A. (1995). BiP/Kar2p serves as a molecular chaperone during carboxypeptidase Y folding in yeast, J. Cell Biol. *130*, 41-9.

Skowronek, M. H., Hendershot, L. M., and Haas, I. G. (1998). The variable domain of nonassembled Ig light chains determines both their half-life and binding to the chaperone BiP, Proc. Natl. Acad. Sci. USA *95*, 1574-78.

Sommer, T., and Jentsch, S. (1993). A protein translocation defect linked to ubiquitin conjugation at the endoplasmic reticulum, Nature *365*, 176-9.

Sone, M., Akiyama, Y., and Ito, K. (1997). Differential in vivo roles played by DsbA and DsbC in the formation of protein disulfide bonds, J. Biol. Chem. *272*, 10349-52.

Stamnes, M. A., Shieh, B. H., Chuman, L., Harris, G. L., and Zuker, C. S. (1991). The cyclophilin homolog ninaA is a tissue-specific integral membrane protein required for the proper synthesis of a subset of Drosophila rhodopsins, Cell *65*, 219-27.

Stevens, F. J., and Argon, Y. (1999). Protein folding in the ER, Semin. Cell Dev. Biol. *10*, 443-54.

Stevens, T., Esmon, B., and Schekman, R. (1982). Early stages in the yeast

secretory pathway are required for transport of carboxypeptidase Y to the

vacuole, Cell *30*, 439-48.

Stryer, L. (1995). Biochemistry (New York, W. H. Freeman and Company).

Szabo, A., Langer, T., Schröder, H., Flanagan, J., Bukau, B., and Hartl, F. U.

(1994). The ATP hydrolysis dependent cycle of the Escherichia coli Hsp70

system-DnaK, DnaJ, and GrpE, Proc. Natl. Acad. Sci. USA *91*, 10345-349.

Szyperski, T., Pellecchia, M., Wall, D., Georgopoulos, C., and Wuthrich, K.

(1994). NMR structure determination of the Escherichia coli DnaJ molecular

chaperone: secondary structure and backbone fold of the N-terminal region

(residues 2-108) containing the highly conserved J domain, Proc. Natl. Acad. Sci.

USA *91*, 11343-7.

Tirasophon, W., Welihinda, A. A., and Kaufman, R. J. (1998). A stress response

pathway from the endoplasmic reticulum to the nucleus requires a novel

bifunctional protein kinase/endoribonuclease (Ire1p) in mammalian cells, Genes

Dev. *12*, 1812-24.

Tokunaga, F., Brostrom, C., Koide, T., and Arvan, P. (2000). Endoplasmic reticulum (ER)-associated degradation of misfolded N-linked glycoproteins is suppressed upon inhibition of ER mannosidase I, J. Biol. Chem. *275*, 40757-64.

Travers, K. J., Patil, C. K., Wodicka, L., Lockhart, D. J., Weissman, J. S., and Walter, P. (2000). Functional and genomic analyses reveal an essential coordination between the unfolded protein response and ER-associated degradation, Cell *101*, 249-58.

Trilla, J. A., Durán, A., and Roncero, C. (1999). Chs7p, a new protein involved in the control of protein export from the endoplasmic reticulum that is specifically engaged in the regulation of chitin synthesis in Saccharomyces cerevisiae, J. Cell. Biol. *145*, 1153-63.

Wang, X. Z., Harding, H. P., Zhang, Y., Jolicoeur, E. M., Kuroda, M., and Ron, D. (1998). Cloning of mammalian Ire1 reveals diversity in the ER stress responses, EMBO J. *17*, 5708-17.

Wang, Y., Shen, J., Arenzana, N., Tirasophon, W., Kaufman, R. J., and Prywes, R. (2000). Activation of ATF6 and an ATF6 DNA binding site by the endoplasmic reticulum stress response, J. Biol. Chem. *275*, 27013-20.

Ward, C. L., Omura, S., and Kopito, R. R. (1995). Degradation of CFTR by the ubiquitin-proteasome pathway, Cell *83*, 121-7.

Wei, J., and Hendershot, L. M. (1996). Protein folding and assembly in the endoplasmic reticulum, EXS *77*, 41-55.

Weissman, J. S., and Kim, P. S. (1991). Reexamination of the folding of BPTI: predominance of native intermediates, Science *253*, 1386-93.

Weissman, J. S., and Kim, P. S. (1992). Kinetic role of nonnative species in the folding of bovine pancreatic trypsin inhibitor, Proc. Natl. Acad. Sci. USA *89*, 9900-4.

Weissman, J. S., and Kim, P. S. (1993). Efficient catalysis of disulphide bond rearrangements by protein disulphide isomerase, Nature *365*, 185-8.

Werner, E. D., Brodsky, J. L., and McCracken, A. A. (1996). Proteasome-dependent endoplasmic reticulum-associated protein degradation: an unconventional route to a familiar fate, Proc. Natl. Acad. Sci. USA *93*, 13797-801.

Westphal, V., Darby, N. J., and Winther, J. R. (1999). Functional properties of the two redox-active sites in yeast protein disulphide isomerase in vitro and in vivo, J. Mol. Biol. *286*, 1229-39.

Wiertz, E. J., Jones, T. R., Sun, L., Bogyo, M., Geuze, H. J., and Ploegh, H. L. (1996a). The human cytomegalovirus US11 gene product dislocates MHC class I heavy chains from the endoplasmic reticulum to the cytosol, Cell *84*, 769-79.

Wiertz, E. J., Tortorella, D., Bogyo, M., Yu, J., Mothes, W., Jones, T. R., Rapoport, T. A., and Ploegh, H. L. (1996b). ER degradation of a misfolded luminal protein by the cytosolic ubiquitin-proteasome pathway, Nature *384*, 432-8.

Wiertz, E. J., Tortorella, D., Bogyo, M., Yu, J., Mothes, W., Jones, T. R., Rapoport, T. A., and Ploegh, H. L. (1996c). Sec61-mediated transfer of a membrane protein from the endoplasmic reticulum to the proteasome for destruction, Nature *384*, 432-8.

Wileman, T., Carson, G. R., Shih, F. F., Concino, M. F., and Terhorst, C. (1990). The transmembrane anchor of the T-cell antigen receptor beta chain contains a structural determinant of pre-Golgi proteolysis, Cell Regul. *1*, 907-19.

Wilkinson, B. M., Tyson, J. R., Reid, P. J., and Stirling, C. J. (2000). Distinct domains within yeast Sec61p involved in post-translational translocation and protein dislocation, J. Biol. Chem. *275*, 521-29.

Wilson, C. M., Farmery, M. R., and Bulleid, N. J. (2000). Pivotal role of calnexin and mannose trimming in regulating the endoplasmic reticulum-associated degradation of major histocompatibility complex class I heavy chain, J. Biol. Chem. *275*, 21224-32.

Wodicka, L., Dong, H., Mittmann, M., Ho, M. H., and Lockhart, D. J. (1997). Genome-wide expression monitoring in Saccharomyces cerevisiae, Nat. Biotech. *15*, 1359-67.

Wolin, S. L. (1994). From the elephant to E. coli: SRP-dependent protein targeting, Cell *77*, 787-90.

Worland, S. T., and Wang, J. C. (1989). Inducible overexpression, purification, and active site mapping of DNA topoisomerase II from the yeast Saccharomyces cerevisiae, J. Biol. Chem. *264*, 4412-6.

Wu, M., Repetto, B., Glerum, D. M., and Tzagaloff, A. (1995). Cloning and characterization of FAD1, the structural gene for flavin adenine dinucleotide synthetase of Saccharomyces cerevisiae, Mol. Cell. Biol. *15*, 264-71.

Ye, J., Rawson, R. B., Komuro, R., Chen, X., Dave, U. P., Prywes, R., Brown, M. S., and Goldstein, J. L. (2000). ER stress induces cleavage of membrane-bound ATF6 by the same proteases that process SREBPs, Mol. Cell *6*, 1355-64.

Yoshida, H., Haze, K., Yanagi, H., Yura, T., and Mori, K. (1998). Identification of the cis-acting endoplasmic reticulum stress response element responsible for transcriptional induction of mammalian glucose-regulated proteins. Involvement of basic leucine zipper transcription factors, J. Biol. Chem. *273*, 33741-9.
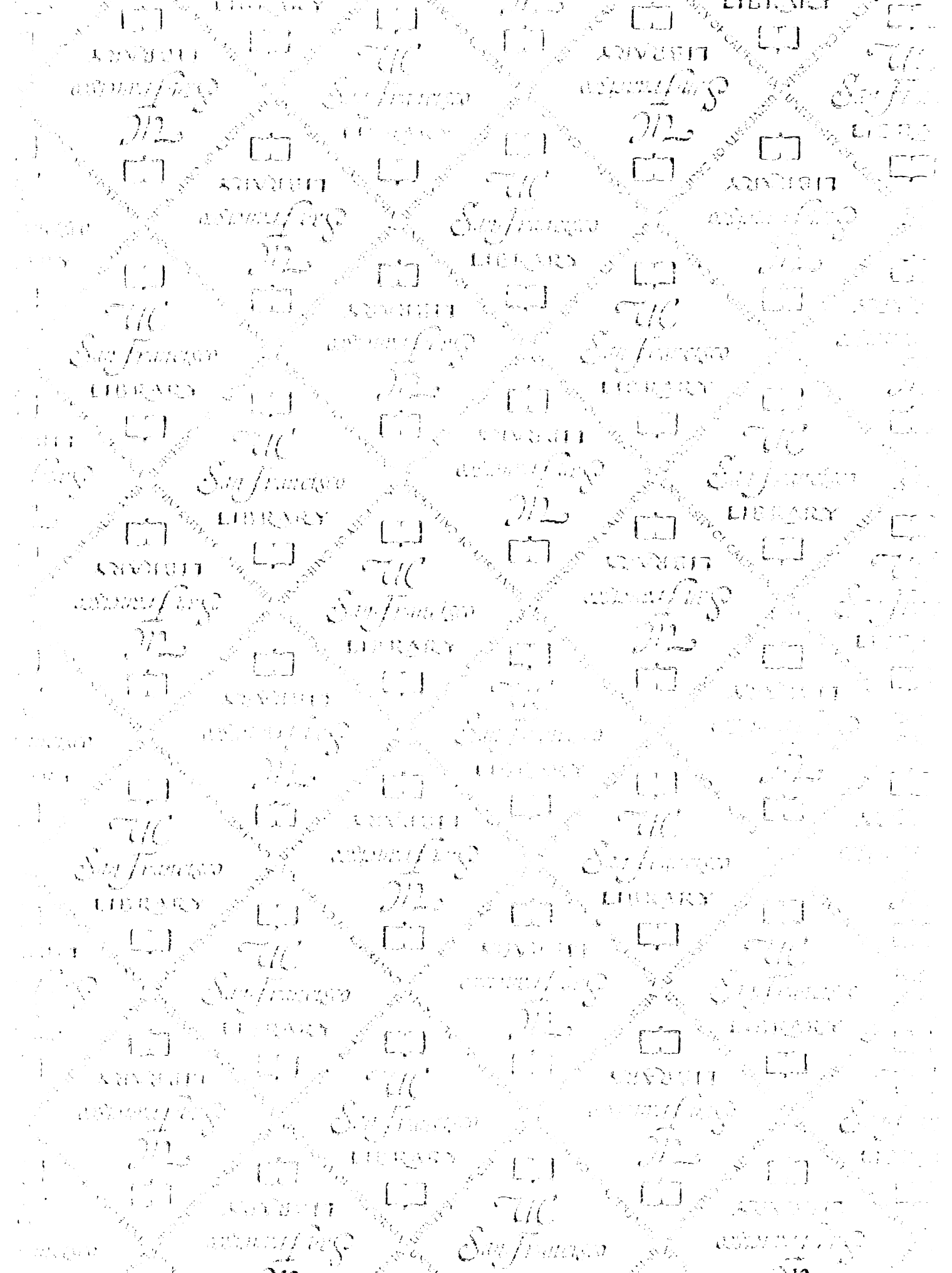
Yu, H., Kaung, G., Kobayashi, S., and Kopito, R. (1997). Cytosolic degradation of T- cell receptor alpha chains by the proteasome, J. Biol. Chem. *272*, 20800-04.

Zapun, A., Jakob, C. A., Thomas, D. Y., and Bergeron, J. J. M. (1999). Protein folding in a specialized compartment: the endoplasmic reticulum, Struct. Fold Des. *7*, R173-R182.

Zhang, J. X., Braakman, I., Matlack, K. E., and Helenius, A. (1997). Quality control in the secretory pathway: the role of calreticulin, calnexin and BiP in the retention of glycoproteins with C-terminal truncations, Mol. Biol. Cell *8*, 1943-54.

Zhou, M., and Schekman, R. (1999). The engagement of Sec61p in the ER dislocation process, Mol. Cell *4*, 925-934.

Ziegler, D. M., and Poulsen, L. L. (1977). Protein disulfide bond synthesis: a possible intracellular mechanism, Trends Biochem. Sci. *2*, 79-81.